LIÈGE université
Gembloux
Agro-Bio Tech

Study on preparation of cattle bone collagen peptides-calcium chelate and its anti-osteoporosis activity

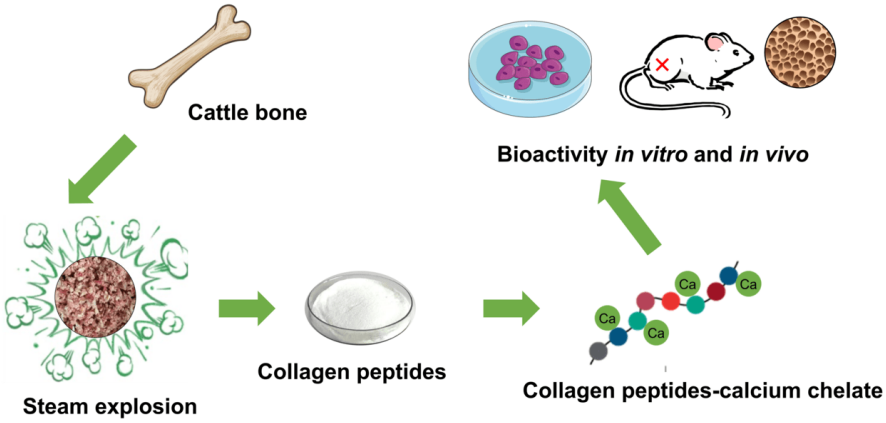

Author: Hongru Zhang
Supervisor: Prof. Aurore Richel
Co-supervisor: Prof. Chunhui Zhang
Academic year: 2022-2023

COMMUNAUTÉ FRANÇAISE DE BELGIQUE
UNIVERSITÉ DE LIÈGE – GEMBLOUX AGRO-BIO TECH

Study on preparation of cattle bone collagen peptides-calcium chelate and its anti-osteoporosis activity

Étude sur la préparation de peptides de collagène osseux bovin chélaté au calcium et son activité anti-ostéoporose

Hongru Zhang

Supervisor: Prof. Aurore RICHEL, Prof. Chunhui Zhang
Year: 2023

Abstract

Cattle is one of the most important livestock resources globally. In 2019, the global production of beef was about 62.9 million tons, and collagen-rich bovine bones, skins, and tendons yield was up to 31.4 million tons. In the EU, cattle bones have long been considered waste generated by the slaughterhouse industry and are typically disposed of in landfills or rendering plants. From economic, environmental protection, and human health perspectives, the high-value utilization of cattle bone resources is of great significance. Steam explosion has attracted attention as a method for extracting active ingredients from animal bone, due to its advantages of lower cost, lower energy usage, and environmental friendliness. Furthermore, the bioactivities of peptides-metal chelate, especially collagen peptides-calcium chelate (CPs-Ca), are poorly reported *in vitro* and *in vivo*. The objectives were: (1) to determinate the composition of cattle bone, (2) to extract collagen peptides using an eco-friendly steam explosion method, (3) to prepare collagen peptide-calcium chelate and analyze its structural characteristics and digestive stability *in vitro*, and (4) to evaluate its anti-osteoporotic activity through cell experiment (MC3T3-E1, mouse embryo osteoblast precursor cells) and rat animal experiment.

First, 143 cattle bones were collected from eight provinces in China: Inner Mongolia, Shandong, Gansu, Henan, Shaanxi, Tibet, Sichuan, and Jilin. Sample species included yak and yellow cattle. The protein content, fat content, and elemental profile of cattle bone were determined. Sampling site included marrow bone, spine, and rib. Geographical origin and species did not show significant effect on protein content. Yak bone showed higher fat content that of yellow cattle bone. There were significant differences of protein content and fat content in different sampling sites. Meanwhile, to regulate the bone products market, the geographical origin and species of yellow cattle bone and yak bone can be discriminated by the bone elemental profiles. The combined use of multi-element analysis and Linear discriminant analysis was well-suited for the distinction of the geographic origin and species (yellow cattle vs. yak), with K-cross validation accuracies of 94.5% and 99.3%, respectively.

Next, steam explosion technology was used to liquefy cattle bone for collagen peptides (CPs) extraction. The effects of experimental parameters (pressure and action time) on cattle bone liquefaction were investigated. The microstructural changes of the solid residue of the steam explosion treated bone were verified by scanning electron microscopy. Steam explosion indicated that with the increase of pressure and reaction time, the protein recovery rate and calcium/phosphorus release increased. Under 2.5 MPa-30 min, the protein recovery rate reached 62.5%. In addition, steam explosion significantly decreased the molecular weight determination of collagen peptides ($P < 0.05$). The results suggest that steam explosion can be used as a pretreatment method to liquefy cattle bone for environmentally friendly isolation of CPs.

Cattle bone collagen peptides were applied to prepare CPs-Ca, and the preparation conditions (pH 7, temperature 60 °C, time 60 min, peptides/$CaCl_2$ 5/1) were optimized by single factor test. The results of physical characteristics indicated that CPs-Ca was

obviously different from CPs. The Fourier transform-infrared spectroscopy analysis demonstrated that chelating sites were carboxyl oxygen, hydroxyl oxygen, and amino nitrogen atom of CPs. The results of X-ray diffraction spectroscopy, scanning electron microscope, atomic force microscopy showed revealed alterations in the structure after calcium chelating. When calcium ions bind with peptides, they create links that lead to the organization of a crystal structure and the aggregation of the microstructure. According to the stability analysis, it was determined that CPs-Ca remains stable when subjected to thermal processing. The digestion experiment *in vitro* indicated that exposure to the gastric digestion environment may cause CPs-Ca to undergo partial dissociation.

In addition, collagen peptides-calcium chelate prepared by ultrasound method (CPs-Ca-US) was successfully prepared and characterized, and the calcium-chelating ability reached 39.48 μg/mg. Compared with CPs-Ca prepared by hydrothermal method, the CPs-Ca-US did not show significant difference in structure characterizations. CPs-Ca-US showed a more stable property in gastric juice than former by digestion experiment *in vitro*. CPs-Ca-US could significantly promote the proliferation and mineralization of MC3T3-E1 cells (mouse embryo osteoblast precursor cells) and promote calcium absorption by interacting with calcium-sensing receptor, which regulates calcium and other metal ion homeostasis. CPs-Ca-US had a higher ability to promote the proliferation and mineralization of MC3T3-E1 cells ($P > 0.05$).

Finally, the anti-osteoporosis bioactivity of CPs-Ca was studied *in vivo* (ovariectomized rat, a kind animal mode of osteoporosis). Our results indicated that dietary CPs-Ca may be effective in mitigating osteoporosis induced by estrogen deficiency, which could be due to changes in gut microbiota observed in fecal samples. For the osteoporosis rats, CPs-Ca dietary intervention increased the bone mineral density and enhanced the microstructure and changed the bone formation-related or bone resorption-related bone turnover markers levels in serum. CPs-Ca dietary intervention increased short-chain fatty acids contents in feces. In addition, CPs-Ca treatment increased the *Bifidobacterium*, *Escherichia-Shigella*, and *Allobaculum*, while decreased *Firmicutes*, and the *Firmicutes*/*Bacteroidetes* ratio at phylum level along with some specific gut microbiota community changed at genus level. Our study provided scientific evidence that CPs-Ca can be used as a functional food to treat osteoporosis.

Keywords: Cattle bone, Collagen peptides, Collagen peptides-calcium chelate, Steam explosion, Osteoporosis, Gut microbiota.

Résumé

Les bovins sont l'une des ressources d'élevage les plus importantes dans le monde. En 2019, la production mondiale de boeuf était d'environ 62,9 millions de tonnes, et le rendement en os, peaux et tendons bovins riches en collagène s'élevait à 31,4 millions de tonnes. Dans l'UE, les os de bovins ont longtemps été considérés comme des déchets générés par l'industrie de l'abattage et sont généralement éliminés dans des décharges ou des installations de traitement. Du point de vue économique, de la protection de l'environnement et de la santé humaine, l'utilisation à haute valeur ajoutée des ressources osseuses bovines revêt une grande importance. L'explosion à la vapeur a attiré l'attention en tant que méthode d'extraction d'ingrédients actifs à partir d'os d'animaux, en raison de ses avantages de coût moindre, de consommation d'énergie moindre et d'écologie. De plus, les bioactivités des peptides-chélate métallique, en particulier du chélate de peptides de collagène-calcium (CPs-Ca), sont peu rapportées *in vitro* et *in vivo*. Les objectifs étaient : (1) de déterminer la composition de l'os de bovins, (2) d'extraire des peptides de collagène en utilisant une méthode d'explosion à la vapeur respectueuse de l'environnement, (3) de préparer un chélate de peptides de collagène-calcium et d'analyser ses caractéristiques structurales et sa stabilité digestive *in vitro*, et (4) d'évaluer son activité anti-ostéoporotique par l'expérience cellulaire (cellules ostéoblastiques de souris MC3T3-E1) et l'expérience animale sur des rats.

Tout d'abord, 143 os de bovins ont été collectés dans huit provinces en Chine : Mongolie-Intérieure, Shandong, Gansu, Henan, Shaanxi, Tibet, Sichuan et Jilin. Les espèces d'échantillons comprenaient le yak et le bétail jaune. La teneur en protéines, en matières grasses et le profil élémentaire des os de bovins ont été déterminés. Les sites d'échantillonnage comprenaient l'os de la moelle, la colonne vertébrale et la côte. L'origine géographique et l'espèce n'ont pas montré d'effet significatif sur la teneur en protéines. L'os de yak a montré une teneur en matières grasses plus élevée que l'os de bétail jaune. Il y avait des différences significatives de teneur en protéines et en matières grasses dans différents sites d'échantillonnage. En outre, pour réguler le marché des produits osseux, l'origine géographique et l'espèce de l'os de bétail jaune et de l'os de yak peuvent être différenciées par les profils élémentaires des os. L'utilisation combinée de l'analyse multi-élémentaire et de l'analyse discriminante linéaire était bien adaptée à la distinction de l'origine géographique et de l'espèce (bétail jaune vs yak), avec des précisions de validation croisée de 94,5% et 99,3%, respectivement.

Ensuite, la technologie d'explosion à la vapeur a été utilisée pour liquéfier l'os de bovin pour l'extraction des peptides de collagène (CPs). Les effets des paramètres expérimentaux (pression et temps d'action) sur la liquéfaction de l'os de bovin ont été étudiés. Les changements microstructuraux du résidu solide de l'os traité à l'explosion à la vapeur ont été vérifiés par microscopie électronique à balayage. L'explosion à la vapeur a indiqué qu'avec l'augmentation de la pression et du temps de réaction, le taux de libération des protéines et la libération de calcium/phosphore augmentaient. Sous 2,5 MPa-30 min, le taux de libération des protéines atteignait 62.5%. De plus, le prétraitement de l'explosion à la vapeur diminuait significativement la détermination

de la masse moléculaire des peptides de collagène ($P < 0,05$). Les résultats suggèrent que l'explosion à la vapeur peut être utilisée comme méthode de prétraitement pour liquéfier l'os de bovin pour l'isolement respectueux de l'environnement des CPs.

Les peptides de collagène d'os de bovin ont été utilisés pour préparer des CPs-Ca, et les conditions de préparation (pH 7, température 60 °C, temps 60 min, peptides/$CaCl_2$ 5/1) ont été optimisées par test à facteur unique. Les résultats des caractéristiques physiques ont indiqué que les CPs-Ca étaient clairement différents des CPs. L'analyse spectroscopique infrarouge à transformée de Fourier a démontré que les sites de chélation étaient l'oxygène carboxyle, l'oxygène hydroxyle et l'atome d'azote amino des CPs. Les résultats de la spectroscopie de diffraction des rayons X, de la microscopie électronique à balayage et de la microscopie à force atomique ont montré les changements structurels après la chélation avec le calcium. Les ions calcium se lient aux peptides, entraînant la formation d'une structure cristalline ordonnée et une agrégation dans la microstructure. L'analyse de la stabilité révèle que les CPs-Ca sont stables pendant le traitement thermique. L'expérience de digestion *in vitro* a indiqué que l'environnement de digestion gastrique pouvait entraîner une dissociation partielle des CPs-Ca.

De plus, le chélate de peptides de collagène-calcium préparé par la méthode des ultrasons (CPs-Ca-US) a été préparé et caractérisé avec succès, et la capacité de chélation de calcium a atteint 39,48 μg/mg. Comparé au CPs-Ca préparé par la méthode hydrothermique, le CPs-Ca-US n'a pas montré de différence significative dans les caractérisations de structure. Le CPs-Ca-US a montré une propriété plus stable dans le jus gastrique que le premier par l'expérience de digestion *in vitro*. Le CPs-Ca-US pourrait favoriser de manière significative la prolifération et la minéralisation des cellules MC3T3-E1 et favoriser l'absorption de calcium en interagissant avec le récepteur de détection du calcium, qui régule la calcémie et l'homéostasie d'autres ions métalliques. Le CPs-Ca-US avait une capacité plus élevée de favoriser la prolifération et la minéralisation des cellules MC3T3-E1 ($P > 0,05$).

Enfin, l'activité biologique anti-ostéoporose de CPs-Ca a été étudiée *in vivo* (rat castré, un modèle animal de l'ostéoporose). Nos résultats ont indiqué que l'apport alimentaire de CPs-Ca peut soulager l'ostéoporose induite par la déficience en œstrogènes, ce qui implique probablement un changement de la microbiote intestinale dans les selles. Pour les rats atteints d'ostéoporose, l'intervention alimentaire en CPs-Ca a augmenté la densité minérale osseuse, amélioré la microstructure et modifié les taux de marqueurs de renouvellement osseux liés à la formation osseuse ou à la résorption osseuse dans le sérum. L'intervention alimentaire en CPs-Ca a augmenté la teneur en acides gras à chaîne courte dans les selles. De plus, le traitement en CPs-Ca a augmenté *Bifidobacterium*, Escherichia-Shigella et *Allobaculum*, tout en réduisant Firmicutes, et le rapport *Firmicutes*/*Bacteroidetes* au niveau du phylum ainsi que certaines communautés microbiennes intestinales spécifiques ont changé au niveau du genre. Notre étude a fourni des preuves scientifiques que CPs-Ca peut être utilisé comme aliment fonctionnel pour traiter l'ostéoporose.

Mots-clés: Osselet de bétail, Peptides de collagène, Chélate de calcium de peptides de collagène, Explosion de vapeur, Ostéoporose, Microbiote intestinal.

Acknowledgments

I would like to extend my sincere thanks and appreciation to all the members who contributed to the completion of my PhD dissertation. I am grateful for the support provided by the National Natural Science Foundation of China (32072156) and the National Agricultural Science and Technology Innovation Program (CAAS-ASTIP-2020-IFST05).

In the past four years, I have been fortunate to have the support of my advisors, Prof. Aurore RICHEL and Prof. Chunhui Zhang, as well as many others. They provided me with the opportunity to undertake this fascinating and challenging work. If it were not for them giving me the chance to conduct research, I would not have discovered the joys as well as the frustrations that come with it. They guided me through this dissertation with their advice, ideas, knowledge, and helpful discussions, and gave me enough freedom to explore my own ideas. It was kind of them to provide me with opportunities to attend various scientific conferences, meetings, and workshops. I am indebted to them for their professional, social, and moral support throughout my PhD.

I am grateful to all the staff at the Laboratory of Biomass and Green Technologies, Gembloux Agro-Bio Tech, University of Liege. Their warm guidance and assistance helped me better orient myself in various aspects of my work and life in Europe.

I am also thankful to all the members of Laboratory of Chinese Food Processing and Equipment Research Team, Institute of Food Science and Technology, Chinese Academy of Agricultural Sciences, especially Liwei Qi, Xia Li, Yujie Guo, Dong Han, Shuyi Qian, Mengliang Ye, Qingshan Shen, Xiaojie Qin, and Jingfan Wang for providing me with a convenient and friendly research and living environment. I really benefited from the different occasions.

Special thanks to my family members and my girlfriend Xiaodan Wang, who enabled me to accomplish this task through their moral support, love, and prayers.

Hongru Zhang
15/02/2023 in Gembloux, Belgium

Tables of Contents

List of Figures

List of Tables

List of Abbreviations

CPs	Collagen peptides
CPs-Ca	Collagen peptides-calcium peptides
OP	Osteoporosis
CPs-Ca-HT	Collagen peptides-calcium peptides (hydrothermal)
CPs-Ca-US	Collagen peptides-calcium peptides (ultrasound)
ICP-MS	Inductively Coupled Plasma Mass Spectrometry
HCA	Hierarchical cluster analysis
LDA	Linear discriminant analysis
FT-IR	Fourier transform-infrared spectroscopy
XRD	X-ray diffraction
TGA	Thermal gravimetric analysis
SEM	Scanning electron microscope
AFM	Atomic force microscopy
MC3T3-E1 Cells	Mouse embryo osteoblast precursor cells
CaSR	Calcium-sensing receptor
Ala	Alanine
Arg	Arginine
Asp	Aspartic acid
Cys	Cystine
Glu	Glutamic acid
Gly	Glycine
His	Histidine
Ile	Isoleucine
Leu	Leucine
Lys	Lysine
Met	Methionine
Phe	Phenylalanine
Ser	Serine
Thr	Threonine
Tyr	Tyrosine
BMD	Bone mineral density
Val	Valine
BTMs	Bone turnover markers
BAP	Bone alkaline phosphatase
OCN	Osteocalcin

PINP	Procollagen type-I Npeptide
TRACP	Tartrate-resistant acid phosphatase
S.CTX	Serum C-terminal telopeptide of type-I collagen
SCFAs	Short-chain fatty acids
RANKL	Receptor activator of nuclear factor-κb ligand
BMD	Bone mineral density
BV/TV	Bone volume fraction
Cw·T	Bone cortical thickness
Tb·Th	Trabecular thickness
Tb·Sp	Trabecular separation
Tb·N	Trabecular number

1

Chapter I. General introduction

1.1. Context

Collagen was first known as the component of tissues that produced glue when boiled, derived from the Greek words of "glue" and "to produce". The word "collagen" was coined in the 19th century to describe the constituent of connective tissues that yields gelatin when boiled, which is considered as the biological glue to hold cells in place. Collagen is the main extracellular matrix (ECM) molecule that self-assembles into cross-striated fibers, supports cell growth, and contributes to connective tissue's mechanical resilience (Sorushanova et al., 2019). Collagen is mainly composed of glycine, proline, and hydroxyproline (primary structure) in a triplex helix, including three α chains (León-López et al., 2019). Each alpha chain contains 1014 amino acids approximately with a molecular weight of around 100 KDa. The amino acid repeating sequence [Gly–X–Y]n is a periodic structure (Figure 1-1). In the collagen family, type I collagen is the most widespread with the highest content, accounting for about 90% of the total collagen in animals. Type I collagen molecule is rod-shaped and consists of two α1 chains and one α2 chain. This substance is primarily derived from animal by-products, including bones, skin, horns, hooves, feet, and internal organs (Figure 1-2).

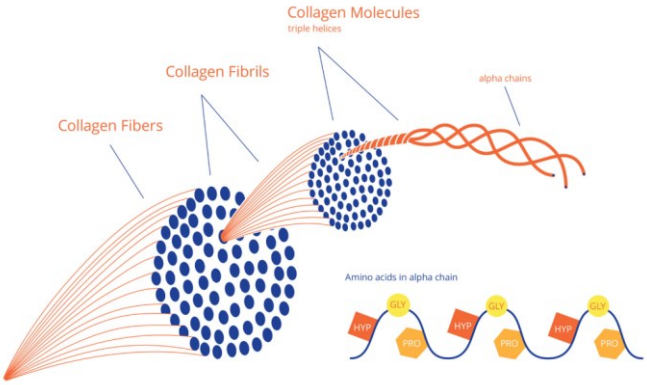

Figure 1-1: The organization of collagen fibrils into fiber bundles. (Nijhuis et al., 2019).

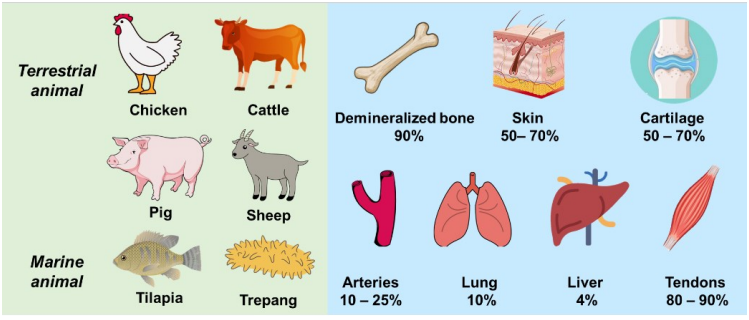

Figure 1-2: Approximate content of collagen in different tissues, and the animal resources.

Collagen peptides (CPs) are collagen hydrolysates. Commonly, bioactive peptides include oligopeptides (2–20 amino acids) and polypeptides (more than 20 amino acids) (Karami & Akbari-adergani, 2019). Collagen peptides have been confirmed to have multiple biological activities including antihypertensive (Ding et al., 2015), antioxidant (Wang et al., 2013), immune activity (Soriano-Romaní et al., 2022), metal chelating activity (Caetano-Silva et al., 2021), skin health (Proksch et al., 2014), and so on (Figure 1-3). Vivo animal models and human clinical trials have confirmed some bioactivities of collagen peptides. Approximately 80% of collagen products are utilized for purposes related to health management (48%) and the food and beverage industry (32%), such as meat products, dairy and beverage products, baked food, food packaging and preservation, edible collagen coatings (Cao et al., 2021; Damodaran & Wang, 2017; Harper et al., 2012; Nguyen et al., 2018; Yu et al., 2017).

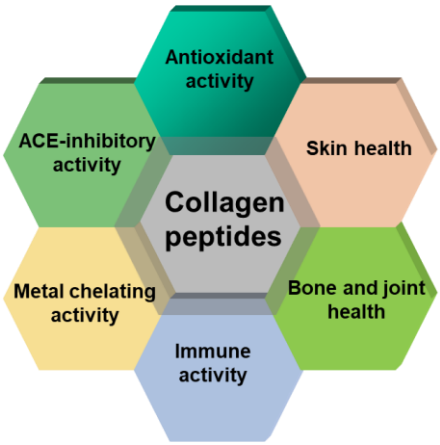

Figure 1-3: Biological activities of collagen peptides.

Accumulating evidence suggests that collagen hydrolysates/peptides play a positive role in the treatment of osteoporosis, joint disease, and osteoarthritis (Bello & Oesser, 2006). Ye et al., (2020) indicated that yak bone collagen peptides could recover osteoporosis by regulating the amino acid metabolism and lipid metabolism (especially unsaturated fatty acid). Porcine bone collagen peptides could promote MC3T3-E1 (mouse embryo osteoblast precursor cells) cell proliferation by activating PI3K/Akt pathway (Zhu et al., 2020). Watanabe-Kamiyama et al., (2010) demonstrated that the dietary intervention of low molecular weight collagen hydrolysate to ovariectomized osteoporosis rats improved the organic substance content of the left femur. The abundant Pro and Hyp in collagen hydrolyzates may increase on osteoblast proliferation by inducing insulin-like growth factor 1 (IGF1) secretion and activating calcium-sensing receptors.

However, there are some problems that need to be resolved. The preparation method with low cost, environmentally friendly, and high efficiency is urgently needed. Especially, the beneficial effects of collagen peptides on bone, joint and skin health have attracted an increasing attention globally. At the same time, the modification activities of CPs by Ca^{2+} have been reported to improve calcium bioavailability. The

structural features of CPs suggest that they have abundant carboxyl group and amino group in the chains, which means that the chains are capable of binding certain metal ions. The modification of CPs by metal ions has attracted attention for a long time. In calcium-binding peptides, oxygen atom of the carboxyl group and nitrogen atom of the amino group participate in peptide calcium chelation reaction.

In recent years, numerous studies have demonstrated progress in the management of osteoporosis using collagen peptides. Collagen peptides from fish scales promoted the proliferation of osteoblasts and inhibited the proliferation of mature osteoclasts (Hu, et al., 2016). Val-Ser-Glu-Glu from duck egg white reversed bone loss through Wnt/β-catenin signaling pathway in ovariectomized rats (Guo et al., 2019). A previous study isolated calcium-chelating peptides from tilapia bone collagen hydrolysate, which could enhance calcium absorption activity in intestinal Caco-2 cells (Liao et al., 2020). Current research was mainly focused on the isolation of calcium-binding peptides, structural analysis, transportation across Caco-2 cells, and bioactivity on osteoblasts. (X. Wang et al., 2020) indicated calcium could be chelated through carboxyl oxygen and amino nitrogen atoms of collagen peptides. W. Wu et al., (2019) indicated that collagen peptide-calcium chelate could improve calcium transport in Caco-2 cell monolayer and reverse the inhibition of calcium absorption by phosphate and phytate. (K. Zhang et al., 2018) indicated that peptide-calcium chelate could improve the intestinal calcium absorption, calcium bioavailability, and serum calcium. The study of collagen peptides-calcium chelate (CPs-Ca) on osteoporosis treatment is limited. Except vitro experiment, the vivo experiment for anti-osteoporosis should be considered. Based on the above-mentioned problems, study is needed to investigate the bioactivities of CPs-Ca and expand the applications for bone care.

1.2. Objectives

The general objectives of the study were to determinate the compositions of cattle bone from different regions of China, to apply steam explosion on collagen peptides extraction from cattle bone and investigate the structural characteristics and anti-osteoporosis properties of CPs-Ca *in vivo*, thus laying the foundation for the application of CPs-Ca as a kind of calcium supplement for anti-osteoporosis.

Four specific objectives are as follows:

(1) To determinate the composition of cattle bone in different regions of China

The composition of cattle bone and the activity of collagen peptides are influenced by geographical origin and species. Differences in the quality of cattle bones can result in discrepancies in pricing, incidents of food fraud, and cases of adulteration and mislabeling. In Chapter II, cattle bones were collected to determine protein, fat, and mineral contents from eight provinces, two species, and three sampling sites in China. Meanwhile, we established the discrimination model for the discrimination of geographical origins and species, based on multi-elemental fingerprints.

(2) To reveal the effect of steam explosion on collagen peptides extraction from cattle bone

Many methods can be used to produce bioactive peptides, the most common of

which are chemical hydrolysis (acid and alkali hydrolysis), enzymatic hydrolysis and fermentation. These methods lead to large volumes of solvent use, high cost, and low efficiency. the steam explosion method has potential advantages including lower cost, lower energy, and environment friendly. Steam explosion could soften raw material by using high temperature and mechanical damage due to momentary steam release. It provides mechanical destructuration by a combination of two steps: vapocracking and explosive decompression. Our previous study used steam explosion to extract chondroitin sulfate from chicken cartilage (Shen et al., 2019). However, cattle bone (femur) is harder and stronger than chicken cartilage, which create obstacles to collagen peptides extraction. In Chapter III, the steam explosion method was applied to extract collagen peptides from cattle bone.

(3) To prepare cattle bone CPs-Ca and analysis its structural characterization and stability

The preparation method of peptides-calcium chelate is usually hydrothermal method. At a microscopic level, ultrasound treatment generates strong forces by inducing shock waves that lead to chemical transformations in the substance. Thus, we predicted ultrasound might increase the calcium chelating ability of peptides due to inhibit the aggregate of peptides in solution. To the best of our knowledge, there are few reports about the application of the ultrasound method in collagen peptides-calcium chelate preparation. In Chapter IV and Chapter V, we used the hydrothermal and ultrasound methods to prepare CPs-Ca and compared their structural properties and activities in MC3T3-E1 cells.

(4) To investigate the anti-osteoporosis activity of CPs-Ca in ovariectomized rats

Previous research on the anti-osteoporosis effect of CPs-Ca was mostly based on the cell experiment on MC3T3-E1 Cells. Whether the CPs-Ca can relieve osteoporosis in animal models? Are there some connections among CPs-Ca, bone turnover markers (BTMs), and gut microbiota? In Chapter VI, a twelve-week administering trial by CPs-Ca was designed on ovariectomized rats, and BTMs, micro-CT, and gut microbiota analysis were performed to explore and discuss the connections among CPs-Ca, anti-osteoporosis bioactivity, and gut microbiota.

1.3. Research roadmap and outline

1.3.1. Research roadmap

The research roadmap is presented in Figure 1-4.

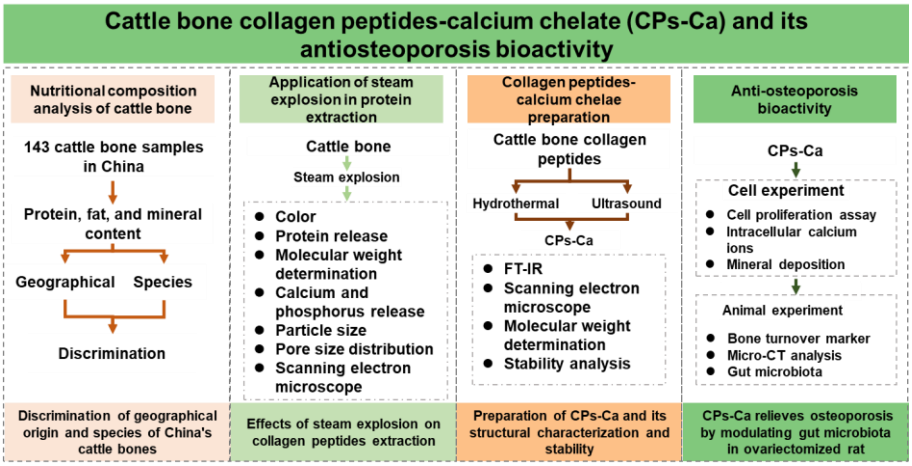

Figure 1-4: Thesis research roadmap.

1.3.2. Research Outline

The protein content and fat content of 143 cattle bones from China were determined. The geographical origin and species of China's cattle bones were discriminated by inductively coupled plasma mass spectrometry.

The steam explosion was performed to extract collagen peptides from cattle bone. The protein recovery rate, molecular weight distribution and amino acid composition were determined to evaluate the effects of steam explosion on the extraction.

The hydrothermal and ultrasound methods were used to prepare CPs. The preparation conditions of hydrothermal method included peptides/$CaCl_2$ (W/W), temperature, time, and pH. The preparation conditions of ultrasound method included peptides/$CaCl_2$ (W/W), power, time, and pH. The molecular mass distribution, Fourier transform-infrared spectroscopy (FT-IR), X-ray diffraction (XRD), thermal gravimetric analysis (TGA), and stability were determined to evaluate the characterizations of CPs.

Cell experiment (MC3T3-E1 cells, mouse embryo osteoblast precursor cells) and animal experiment (ovariectomized rat) was conducted to evaluate the bioactivity of CPs-Ca against osteoporosis. In cell experiment, cell proliferation rate, intracellular calcium ions, and mineral deposition were determined. In animal experiment, histopathological structure of the small intestine, bone turnover markers, the microstructure of the femur, gut microbiota, and short chain fatty acids were determined.

1.4. State of the review of the scientific literature

1.4.1. Preparation of collagen peptides

In the food field, the extraction of CPs from animal by-products is the main

production method, which is effective for large-scale production in industry and for meeting the growing demand of CPs. Collagen peptides extraction procedures mainly contain three steps: (1) pre-treatment of raw material, (2) collagen extraction, and (3) collagen hydrolysis (Figure 1-5).

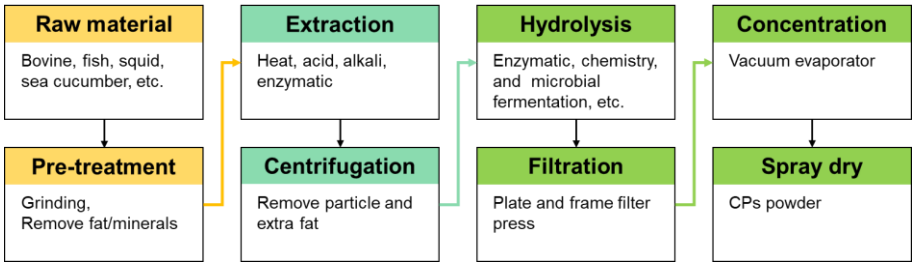

Figure 1-5: Production process of collagen peptides.

In the pre-treatment process, collagen (or gelatin) is enriched by removing non-collagenous substances. According to the characteristics of raw, the pre-treatment process includes swelling, degreasing, and demineralization. To extract collagen from raw material, acid, alkali, enzymes, and organic solvent are usually used to remove non-collagen components, while cutting off the collagen cross-linking. Raw materials are most treated with NaOH to remove non-collagenous proteins. After pre-treatment, to increase hydrolysis susceptibility and purity of collagen, further collagen extraction is required. The most commonly extraction method is based on the high solubility of collagen in acidic solution and alkaline solution. In the first two steps of pre-treatment and collagen extraction, acid/alkaline hydrolysis with a high concentration of HCl/NaOH, cysteine, or guanidine is required. In the third step, by using physical, chemical, or biological methods, collagen can be hydrolyzed into collagen peptides (collagen hydrolysates) with low molecular weight and high hydrophilicity. Using different preparation methods, the obtained collagen peptides vary in purity, physicochemical properties, and functional activity. Among them, the enzymatic hydrolysis method is the most used, mild, and easy to manage, and the prepared peptides have high safety and low-molecular-weight. (Hong et al., 2019).

1.4.1.1. Enzymatic hydrolysis

Enzymatic hydrolysis is the common method of producing bioactive peptides from parent protein (Sun et al., 2016), because there are no toxic chemicals and residual organic solvents in the final products. A series of process conditions could control the reaction efficiency including pH, temperature, time, substrate concentration, enzyme activity, etc. (Zambrowicz et al., 2013). The used enzymatic in peptides production is protease normally, and it can be divided into terminal peptidase and endopeptidase. Terminal peptidase includes carboxypeptidase and aminopeptidase, which could hydrolyze the polypeptide chain one by one from the free carboxyl terminal or free amino terminal, respectively. Endopeptidase can cut off the polypeptide chain of large molecular weight from the middle to form a smaller molecular weight prion and peptide.

The common proteolytic enzymes involve pepsin, trypsin, cathepsin, papain and

subtilis protease, which are used under the respective optimal conditions. Multiple enzymes can be used simultaneously or sequentially in the preparation of bioactive peptides. It is worth noting that the sequence of enzymatic hydrolysis is an important production process (Singh et al., 2014). Although the bioactive peptides prepared by enzymatic hydrolysis are considered as GRAS (Generally Recognized as Safe) (Ulug et al., 2021), enzymatic hydrolysis has some disadvantages including high cost, specificity of the cleavage sites, and precise hydrolysis conditions. Especially, animal collagen has a complex triple helix structure, which limits enzyme-substrate interaction. Additionally, the endogenous proteases (pepsin, trypsin, chymotrypsin or cathepsin) of animal also cleavage protein to peptides. This biochemical process is called autolysis (Matsumura et al., 1993; Song et al., 2016). Autolysis usually occurs in marine by-products, due to the high content of endogenous enzymes. This is a simple and economical method to prepare bioactivity peptides from animal. Considering the structural complexity of by-product materials, it is challenging to optimum enzymatic hydrolysis due to limited interaction between enzyme and substrate. Meanwhile, it is difficult to control and predict the reaction product (Marciniak et al., 2018).

1.4.1.2. Chemical hydrolysis

Chemical hydrolysis of proteins is widely applied due to its simple and low cost. The common chemical hydrolysis methods in the preparation process of active peptide contain Acidic hydrolysis and Alkaline hydrolysis. For a long time, acidic hydrolysis has been considered as an effective method to prepare bioactivity peptides. Inorganic acids (hydrochloric acid,) and organic acids (acetic acid, citric acid, lactic acid, formic acid) can be used in acid hydrolysis. Formic acid could improve the yield of small collagen hydrolysates from spent hens, due to the high permeability of formic acid in raw (Hong et al., 2018). However, tryptophan is destroyed during the reaction of acidic hydrolysis, while sulfur-containing amino acids (e.g., cysteine, methionine) are partially destroyed. Alkaline hydrolysis is often used to digest a variety of proteins to analyses amino acid compositions, and it does not destroy tryptophan. However, chemical hydrolysis has many limitations, such as the different control of process. strong chemicals and solvents could destroy the chemical structure of bioactivity peptide resulting in the decline of bioactivity and low functionalities. Additionally, the equipment is easily corroded by acid and alkali reagents, resulting in economic burden, while acid and alkali reagents lead a high salt content in the final product.

1.4.1.3. Fermentation hydrolysis

The fermentation hydrolysis method is to prepare peptides using microbial fermentation with a process of degrading protein into polypeptides or free amino acids. This process is mainly due to the proteases produced by microbial fermentation. At the same time, the produced enzymes other than proteases could degrade carbohydrates and lipids. The common microorganisms include Bacillus subtilis, Actinomyces, Aspergillus niger, Aspergillus oryzae, Saccharomyces cerevisiae, etc. Fermentation hydrolysis is a promising method to produce bioactive peptides, but the efficiency needs to be further improved (Hu et al., 2020). Wang et al., (2020) prepared CPs with calcium chelating activity by *Lactobacillus* strain.

Considering sustainability, some novel extraction methods have been developed to replace traditional methods, such as ultrasound, high voltage pulsed electric field, hot-pressure, microwave (Marciniak et al., 2018). Meanwhile, the target peptides could be synthesized by chemical synthesis, which is mainly used in short peptide synthesis. For chemical synthesis, amino acids are condensed by chemical shrinkage agents to produce the target bioactive peptides with high specificity. However, limitations are obvious, due to the high cost and using toxic reagents. Therefore, to obtain CPs by chemical synthesis, there are still problems to be solved, including large-scale production in industry, control of preparation conditions, and reduction of production costs. Therefore, if animal bone is used to acquire CPs, the industry must consider the environmental issue and the safety of the raw materials. In addition, process simplification and reduction of chemical use are highly recommended for large-scale production.

1.4.1.4 Steam explosion technology

Steam explosion (SE, QBS-80 SE, Gentle Bioenergy Co. Ltd., Hebi, Henan province, China) treatment as a kind of thermal liquefaction method, is characterized high-pressure and high-temperature (110 ℃–260 ℃, 0.04 MPa–4.59 MPa). This pre-treatment technology is applied to lignocellulosic biomass such as cellulose, hemicellulose, and lignin. It is based on pressurization and forcing of steam into the fibrous tissues and cells of biomass, followed by instantaneous pressure release. SE provides huge explosion power to disrupt the compact structure of raw material, while avoids a long-time treatment with high temperature and pressure (Jacquet et al., 2015). In a study by Jacquet et al., (2011), the effects of various steam explosion treatments on the thermal degradation of a bleached cellulose were compared. The results showed that the thermal stability of the samples decreased as the intensity of the treatment increased. Previous study indicated that the combine of steam explosion and papain can be applied to process chicken cartilage to extract chondroitin sulfate with high recovery rate of 92.15% (Shen et al., 2019). When subjected to steam explosion (1.5 MPa for 120 seconds), chicken feather powder underwent keratinolysis and more than 90% of it was degraded into soluble peptides within 3 hours. Additionally, approximately 90% of the peptides produced were smaller than 3 kDa, owing to the synergistic effect of the steam explosion treatment (Qin et al., 2022). Steam explosion treatment induced chemical modifications in lignin structure such β-O-4 and spirodienone substructure degradations, increased of free COOH and phenolic OH bonds, decrease of aliphatic OH ferulate and p-coumarate bonds and changes in G/H/S units proportions (Maniet et al., 2017). Therefore, based on these known reports, we propose steam explosion technology, as a potential treatment to liquefy cattle bone for CPs extraction.

1.4.2. Osteoporosis review

Osteoporosis (OP) is a kind of systemic bone metabolism disease, characterized by the loss of bone mass and strength, leading to an increased risk of fracture (Raisz & Rodan, 2003). Osteoporosis can lead to a significant decrease in an individual's quality of life, and women are more likely to suffer from osteoporosis than men. Recent estimates suggest that over 200 million people worldwide are afflicted with

osteoporosis. Based on statistics from the International Osteoporosis Foundation, one in three women over the age of 50 and one in five men globally will experience fractures resulting from osteoporosis during their lifetimes. (Guo et al., 2021). While osteoporosis was previously viewed as an unavoidable aspect of aging, it is now widely acknowledged that the condition can be effectively prevented and treated. (Khosla & Hofbauer, 2017). The bone mass loss is caused by an imbalance between bone resorption and bone formation processes. There are three major pathogenetic reasons for the reduction of bone mass: (1) Increased osteoclastic activity without increased osteoblastic activity (high turnover); (2) Normal osteoclastic but decreased osteoblastic activity (low turnover); (3) Decreased osteoclastic and osteoblastic activity ("atrophic" or "adynamic" bone) (Bartl et al., 2009). Osteoclasts break down or resorb the existing bone, whereas osteoblasts guide the synthesis of new matrix to fill the resorption cavities (Figure 1-6). In healthy individuals, bone metabolism is balanced, and is maintained through a balance between bone resorption and bone formation. The disruption of balance by endocrine disorders, calcium malabsorption, nutritional, hormone regulation, aging and numerous pathological processes could result in osteoporosis (Brown, 2017). Osteoporosis is categorized into primary and secondary, based on the pathogenesis. Primary OP can be classified into type I (postmenopausal) OP and type II (age-related) OP. Secondary osteoporosis has a clearly definable etiologic mechanism, which is not as common as primary OP, due to the underlying disease or medication. Many risk factors lead to osteoporosis fractures including modifiable and nonmodifiable risk factors in Figure 1-7. Pharmacological and non-pharmacological interventions are two approaches that can be used to prevent and/or treat osteoporosis (Guo et al., 2021). Pharmacological treatments can be classified into three main categories: to prevent bone loss (anti-resorption drugs), to stimulate bone formation (anabolic drugs), and those that have a dual effect (such as bisphosphonates, estrogen, denosumab, teriparatide, and strontium ranelate). However, these medications can have some adverse effects, including injection site reactions, hypercalcemia, and orthostatic hypotension. (Khosla & Hofbauer, 2017). The bone mineral density (BMD) in the proximal femur and lumbar spine detected by dual-energy X-ray absorptiometry (XRD) is a conventional standard test for osteoporosis classification.

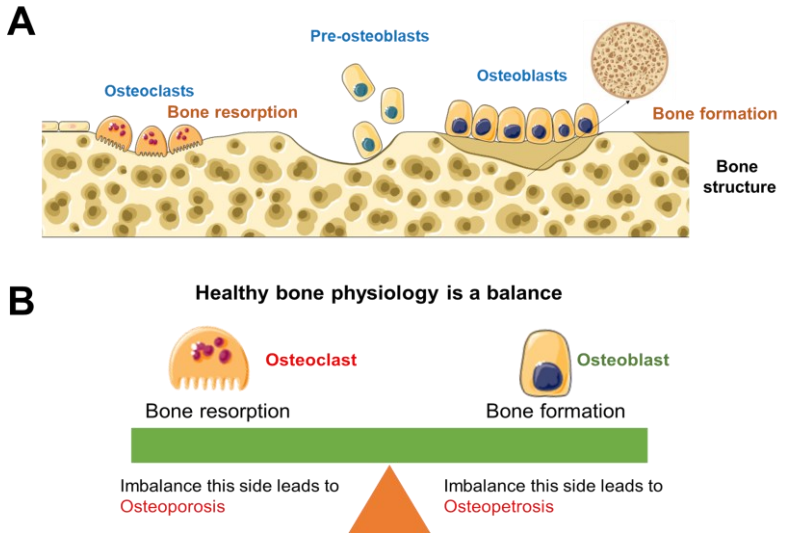

Figure 1-6: (A) Illustration of bone remodeling process, (B) Bone balance.

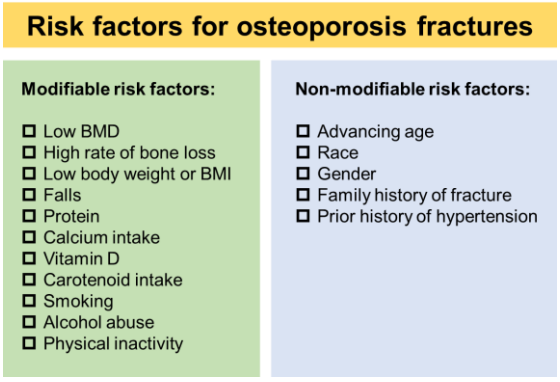

Figure 1-7: Risk factors for osteoporosis fractures

The incidence of osteoporosis increases with age; approximately 30% to 40% of adults over the age of 60 have this disease (Steelman & Zeitler, 2001). As shown in Figure 1-8A, in the past 70 years, the degree of aging population has gradually deepened. Bone loss is a natural part of the aging process and typically occurs at an average rate of 0.5-1% per year starting in midlife. In women, the average age of menopause is around 51 years old. As a result, bone loss tends to accelerate in women after menopause due to a decrease in estrogen levels. (Treloar, 1981). The decrease in estrogen levels at menopause could cause an increase in cytokine-mediated bone resorption. It also affects bone cell number and bone turnover through the immune system (D'Amelio & Sassi, 2018). Estrogen could regulate bone remodeling by modulating the production of cytokines and growth factors from bone marrow and

bone cells (Li & Wang, 2018). Meanwhile, calcium requirement rises due to the increase in obligatory calcium loss and a small reduction in calcium absorption at the menopause (Nordin et al., 1998). Increases in the elderly population worldwide will cause a dramatic rise in osteoporotic fractures (Melton III et al., 2004).

Roughly half the volume of the extracellular material of bone consists of protein and the other half of calcium phosphate crystals. The formation of bone relies on the intake of nutrients from the diet to provide the necessary materials to produce the extracellular matrix, which makes up more than 95% of the bone's composition and plays a crucial role in its structural and mechanical characteristics. Therefore, maintaining a healthy diet that includes adequate amounts of calcium and protein is essential for promoting optimal bone health. International osteoporosis foundation (IOF) demonstrated that the healthy diet with enough calcium and protein could prevent osteoporosis. As shown in Figure 1-8A, many people in Asia, Africa, South America, and China consume less than 600 mg/day of calcium, below the recommended 800 mg/day (Balk et al., 2017). Dietary intake is the main effective source to improve calcium storage in bone. Calcium has long been recognized as important and required nutrients for bone health and maintenance.

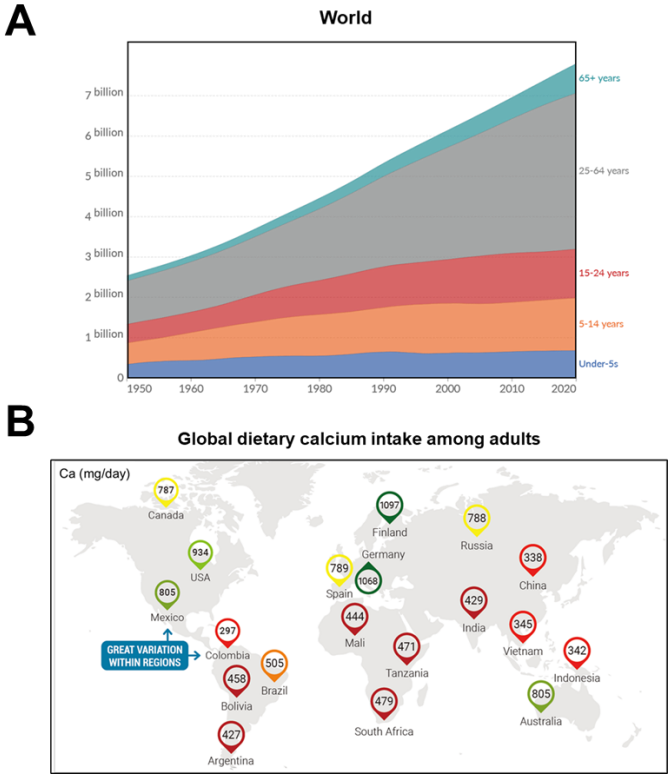

Figure 1-8: (A) Population by broad age group in world. (B) Global dietary calcium intake among adults.

1.4.3. The bioactivities of CPs-Ca on osteoporosis

1.4.3.1. Calcium absorption

Adequate calcium intake is important for preventing and treating osteoporosis. Meanwhile, dietary absorption is the major method to improve calcium absorption. The oxalate and phytic acid present in the intestinal environment, which originate from food, can hinder the absorption of ionized calcium by causing the formation of insoluble calcium deposits. Oxalate and phytic acid are natural compounds that are commonly present in seeds, nuts, legumes, whole grains, and other parts of various plants. However, they are often referred to as anti-nutritional factors due to their potential to reduce the bioavailability of certain nutrients in the body (Gemede, 2014). Excessive intake of ionized calcium may cause gastrointestinal side effects, such as constipation, gas, flatulence, and bloating. Therefore, it is very important to enhance calcium absorption by overcoming the disadvantageous factors in the digestive system. At present, the market calcium supplements mainly include inorganic calcium, organic acid calcium, and amino acid calcium complex. The small peptides have the advantages of low energy consumption and less saturated carriers in adsorption. Collagen-calcium chelate has attracted considerable interest as a potential dietary calcium supplement to improve calcium absorption and bioavailability. Many peptides with calcium-chelate ability have been isolated and identified from various foods, such as Auxis thazard, Pacific cod, sheep bone, and whey protein (Chen et al., 2019; S.-L. Huang et al., 2015; Zhang et al., 2019).

1.4.3.2. Gut microbiota

Gut microbiota (GM) has been recognized to play a key role in the mechanisms and biology of human health and disease. It has become a recent topic of interest in the role of many diseases, such as bone health. In recent years, the importance of the GM for both health has been intensively concerned. Gut microbiota could regulate bone mass via the effects on the immune system, which in turn regulates osteoclastogenesis (Ohlsson & Sjögren, 2015). The composition of the GM is modulated by many environmental factors including diet and antibiotic treatments. Gut microbiota-derived metabolites short-chain fatty acids (SCFAs) can improve bone mineral density (BMD) by the reduction of osteoclast differentiation and the inhibition bone resorption (Lucas et al., 2018). SCFAs in the intestine mainly come from the metabolites of intestinal bacteria. There are many microorganisms parasitic in the human gut, which co-exist with our body and participate in many important physiological processes. SCFAs are formed principally from polysaccharide, oligosaccharide, protein, peptide, and glycoprotein precursors by anaerobic micro-organisms (Macfarlane & Macfarlane, 2003). SCFAs are an important energy supply of intestinal mucosa cells, especially butyric acid, which is the favorite of colon and cecum mucosa cells. SCFAs could reduce histone deacetylase activity in colon cells and immune cells. So SCFAs promote intestinal cell growth and increase the intestinal absorption areas to enhance calcium absorption (Wang et al., 2022). Osteoprotegerin (OPG) is the decoy receptor for the crucial osteoclast differentiation factor receptor activator of nuclear factor kappa-B ligand (RANKL), which indirectly leads to bone formation by reducing osteoclast activity. One study found the increased expression

of OPG and reduced RANKL production in MG-63 osteoblastic cells after 3 days of exposure to lower concentrations of butyrate (1–8 mM) by increasing histone H3 acetylation (Chang et al., 2018). In addition, butyrate-mediated induction of TREG cells can prevent osteoclast formation by Treg secreted anti-osteoclastogenic cytokines, such as interleukin 10, and through a CTLA4/CD80/86 cell-cell contact-dependant mechanism (Zaiss et al., 2019).

Alterations in the microbiome or metabolites affect bone growth and health. McCabe et al., (2015) demonstrated that gut microbiota could modulate bone mass by decreasing intestinal inflammation and changing intestinal calcium absorption in mice. Several studies indicated that food-derived peptides could modulated gut microbiota, such as collagen peptides (Guo et al., 2021; Wang et al., 2020), whey peptides (Y. Li et al., 2016), and soy bioactive peptides (Ashaolu, 2020). Gut microbiota can improve bone health by increasing calcium absorption and modulating the production of some bone growth factors, such as gut serotonin, a molecule that has been suggested as a bone mass regulator (Y. Chen et al., 2017; D'Amelio & Sassi, 2018; Quach & Britton, 2017; Weaver, 2015). Therefore, based on the activity of CPs-Ca *in vitro* (MC3T3-E1, mouse osteoblast cells) and its limited study for osteoporosis (W. Wu et al., 2020), it is necessary to investigate the effect of CPs-Ca on osteoporosis *in vivo* (animal explosion), involving gut microbiota.

1.4.4. Conclusions

CPs extraction including the traditional methods and potential methods, CPs activities *in vitro* and *in vivo* including the bone cell activity and the influencing on gut microbiota, the overview of osteoporosis and the effect of CPs-Ca on osteoporosis, were systematically discussed. To achieve the environmentally friendly extraction of CPs, the raw material of cattle bone could be treated by steam explosion. CPs-Ca could be a dietary calcium supplement for bone health, but its bioactivity is poorly studied *in vivo*. Therefore, the characteristics of CPs-Ca and its bioactivity need to be further studied through animal experiment.

2

Chapter II. Determination of the composition of cattle bone in different regions of China

Adapt from:

Zhang, H., Liu, W., Shen, Q., Zhao, L., Zhang, C., & Richel, A. (2021). Discrimination of geographical origin and species of China's cattle bones based on multi-element analyses by inductively coupled plasma mass spectrometry. Food Chemistry, 356, 129619. https://doi.org/10.1016/j.foodchem.2021.129619

Abstract:

In this study, protein content, fat content, and 50 element contents of a total of 143 cattle bone samples from eight producing regions in China, were determined. The protein content in cattle bones was 16.67 to 24.45 g/100 g, and the fat content of cattle bone was 7.9–29.97 g/100 g. Element contents were used as chemical indicators to discriminate species and geographical origins of cattle bone samples by multivariate data analysis, including hierarchical cluster analysis (HCA) and linear discriminant analysis (LDA). The K-fold cross validation accuracy for species and geographical origin discrimination was 99.3% and 94.5%, respectively. This study reveals that multi-element analysis accompanied by LDA is an effective technique to ensure the information reliability of cattle bone samples, and this strategy may be a potential tool for standardizing market.

Keywords: Geographical origin, Species, Cattle bone, Multi-element, ICP-MS, Discrimination

2.1. Introduction

Animal bones, as a co-product of animal slaughter, more than 12 million tons of that are produced annually in China (USDA, 2018). It is a sustainable alternative source for protein industry because of low cost, high yields, high collagen content (Eastridge, 2006). Yak holds product of geographical indication (PGI) status, and yak farming is supported by the local government to enhance farmer's economic income (Spink & Moyer, 2011). Yak bone is one of the major components of Tibetan medicine (traditional Chinese medicine), with extra bioactive peptides that promote bone growth and prevent osteoporosis (Ye et al., 2019). The protein content and biological activity of nutrients found in cattle bones vary depending on their geographical origin and species. These differences may be attributed to the variations in the breeding environment. And the price of yak bone is approximately 2-fold higher than that of other available cattle bones in the Chinese market, which contributes to the yak bone prone to food fraud, adulteration, and mislabeling. Adulteration and misbranding of food have economic implications and a potential public health risk. Therefore, it is necessary for the geographical origin and species discrimination of the yak bone by a reliable method, which is of great importance for standardizing the market.

In Europe, the indication of the geographical origin is normalized in Commission Implementing Regulation (EU) No. 1420/2013 (17 December 2013). The Chinese government has promulgated the PGI for enhancing the economic and social benefits of agricultural products. The governments and producers also attempt to discriminate the geographical origin of agricultural products for reducing fraud and mislabeling. Cattle is one of the most widely distributed and stockpiled animals in the world (Baghurst et al., 2001), and the dietary intake, region, climate, species, and other factors can affect the concentration of mineral elements in the different tissues of the animal organism. The animal bone, as the main mineral element storage position, probably can be employed for the regions and species discrimination via the various elemental contents.

Over the last decade, multi-element analysis has been applied widely for authenticating wines, olive oil, honey, milk, coffee, tea, cereal crops and meat (Behkami et al., 2017; Epova et al., 2020; Karabagias et al., 2017; Ortea & Gallardo, 2015), but this method is scarcely used for authentication in livestock bone. Multi-element analysis is as an effective technique to assess authenticity and traceability in food products. Inductively coupled plasma mass spectrometry (ICP-MS) has been widely applied to multi-element analysis in food samples, because of the high sensitivity along with a wide linear dynamic range, low detection limits, and high precision (Markiewicz et al., 2017; Tokalioglu, 2012; Tokalıoğlu et al., 2018).

The objective of this study was to conduct a comprehensive assessment of the composition (protein, fat, and mineral content) of cattle bone and differentiate the geographical origin and species. A total of 50 element contents of 143 cattle bones collected in China were determined by ICP-MS. The geographical origins and species of cattle bone samples were analyzed by establishing the discrimination model through linear discriminant analysis (LDA).

2.2 Materials and methods

2.2.1. Materials

Nitric acid and H_2O_2 were purchased from Sinopharm Chemical Reagent Co., Ltd. (Shanghai, China). Unless otherwise stated, all chemicals and reagents were of analytical grade. All the other element standards used in this study were obtained from National Standards Center (Beijing, China).

2.2.2. Sample collection and preparation

The study procedures were approved by the Animal Care and Use Committee of the Institute of Food Science and Technology, Chinese Academy of Agricultural Sciences and performed in accordance with animal welfare and ethics (IFST-2019-43). Male cattle of 2 to 3 years old (yellow cattle) and 4 to 5 years old (yak) were processed by conventional procedures in commercial slaughterhouses. Sample locations included Inner Mongolia (IM), Shandong (Sd), Gansu (Gs), Henan (Hn), Shaanxi (Sx), Tibet (Tb), Sichuan (Sc) and Jilin (Jl) in China. To ensure the reliability of the data, samples were collected from three sampling sites, which increased the accuracy of study. Sample species included yellow cattle and yak, and sampling sites included marrow bone, spine, and rib. To ensure proper representation of samples, six authentic local cattle were collected randomly from each region. The detailed sample information was shown in Figure 2-1 and Table 2-1. The bone samples were evaluated in the present investigation, which were taken 24 h post-slaughter. The meat, tendons and other impurities from the bone samples were removed thoroughly by hand. Bone samples were rinsed with distilled water for 3 times and then air-dried in the fume hood for 12 h. Samples were crushed and blended in a laboratory blender (FW 100, Tianjin Taisite Instrument Co., LTD, China) with a diameter of bone particles of 0.5–1.0 mm and stored with vacuum packing in individual bags of 10 g at -23 °C until analysis.

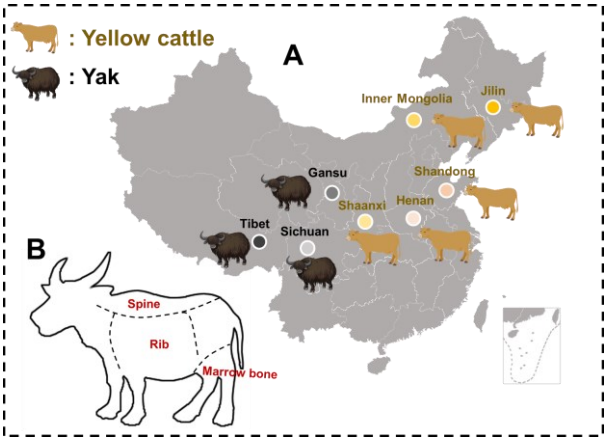

Figure 2-1: (A) The distribution of geographical origins and species of cattle bone samples in China. (B) The sampling sites within cattle carcasses.

Table 2-1: The information of cattle bone samples.

Geographical origin	Species	Sampling site (n)		
		Marrow bone	Spine	Rib
Inner Mongolia (IM)	Yellow cattle	6	6	6
Shandong (Sd)	Yellow cattle	6	6	6
Gansu (Gs)	Yak	5	6	6
Henan (Hn)	Yellow cattle	6	6	6
Shaanxi (Sx)	Yellow cattle	6	6	6
Tibet (Tb)	Yak	6	6	6
Sichuan (Sc)	Yak	6	6	6
Jilin (Jl)	Yellow cattle	6	6	6

n: Number.

2.2.3. Protein and fat content

To determine the protein content, the AOAC method 976.05 was used, and measurements were taken using a Kjeltec 2300 Analyzer (Foss Tecator, Hoganas, Sweden). The conversion factor from nitrogen to protein was 6.25. For analysis of the fat content, the AOAC method 960.39 was employed.

2.2.4. Microwave digestion

The method of microwave digestion for bone samples was carried out according to Mi's method (Mi et al., 2019) with a minor modification. 150 mg bone samples (wet weight) were digested with 8 mL HNO_3 (65%, v/v; Beijing Institute of Chemical Reagents, Beijing, China) and 2 mL of H_2O_2 (30%, v/v; Beijing Institute of Chemical Reagents, Beijing, China) by microwave program in a Mars Lp5 microwave system (CEM, Matthews, USA). Overall digested solutions were transferred into 100 mL centrifuge tubes and diluted to approximately 100 mL with distilled deionized water (Milli-Q Millipore 18.2 MX/cm).

2.2.5. Inductively coupled plasma mass spectrometry determination

The content of mineral elements was measured by ICP-MS (Agilent 7500 Series ICP-MS, Agilent Technologies, Santa Clara, CA, USA). The method of ICP-MS analysis for bone samples was carried out according to Mi's method (Mi et al., 2019). Analysis of each sample was done in triplicate and quantified by using external standards analysis. The Environmental Calibration Standard (Part number 5183-4688) and the Multi-Element Calibration Standard (Part number 8500-6944) supplied by Agilent company (Palo Alto, CA, USA) were used as the standard solution and the determination coefficient of the standard curve was higher than 0.99. Internal Standard Multi-Element Mix #4 (Part Number 5190-8593) containing ^{72}Ge, ^{115}In, and ^{209}Bi supplied by Agilent Technologies (Palo Alto, CA, USA) were used to ensure the stability of the instrument. Samples were remeasured whenever the relative standard deviation (RSD) of internal standards was higher than 10%.

2.2.6. Statistical Analysis

Data from all measurements were expressed as the mean ± standard deviation (SD). The multi-element data were then exported to R (R Core Team, 2016) for multivariate statistical analysis including analysis of variance (ANOVA), hierarchical clustering (HCA), and LDA. ANOVA was applied to 50 minerals detected, to study which data variables of each parameter group are significant for the geographical origins and species discrimination of cattle bone. The significance level was set at $P < 0.05$. To measure the similarity between samples, HCA, an unsupervised classification method, was applied to the multi-element data. Prior to heatmap analysis, data were subjected further standardization and centralization for each element and HCA was carried out based on Pearson correlation. LDA is a supervised pattern recognition method widely used for geographical origins or species discrimination in foodstuffs, such as sugarcane spirits, honey, red wine (Karabagias et al., 2017; Lima et al., 2020). LDA was applied to reduce dimensionality and to visualize the dataset. To avoid overfitting and under-fitting, K-fold cross validation was applied to validate the discrimination model using the multi-element data fully. In detail, the original data were equally divided into K groups, and the data of each subset was made as a verification set, respectively, and the data of the rest K-1 data were used as a training set. In this study, K (K=10) models were obtained. The dividing of the dataset was executed through random sampling while considering the balance of class distributions within each division. The average classification accuracy of these K models was used as the performance index of the discrimination model. The above-mentioned statistical methods were performed using the statistical programming language R (R Core Team, 2016) including the packages of *mass*, *pheatmap*, and *ggplot2*.

2.3. Results and discussions

2.3.1. Protein and fat content

Table 2-2: Protein content between different geographical origins cattle bone samples.

Geographical	Sampling site		
	Marrow bone	Spine	Rib
Jilin (yellow cattle)	17.25±1.12	20.41±1.14	22.99±1.59
Mongolia (yellow cattle)	17.23±2.71	22.24±1.55	24.45±1.41
Shandong (yellow cattle)	17.66±0.55	20.77±1.09	21.93±0.65
Shaanxi (yellow cattle)	16.67±1.33	20.01±1.20	21.97±0.50
Henan (yellow cattle)	19.17±2.25	21.68±1.12	22.69±1.25
Gansu (yak)	17.58±1.74	20.80±0.76	21.90±0.98
Sichuan (yak)	18.39±0.86	22.51±0.66	24.10±0.75
Tibet (yak)	21.95±0.65	17.91±1.25	24.85±0.87

To get the maximum economic benefit, the slaughtered cattle are generally male at 2–5 years old (yellow cattle: 2–3 years old, yak: 4–5 years old) in China. Because female cattle need to reproduce, and the muscle of cattle have a high quality at the above slaughtered age. The available cattle bones were mainly male and have similar slaughter age in the market. As shown in Table 2-2, the protein content in cattle bones varied from 16.67 to 24.85 g/100 g. The protein content of the Shaanxi cattle bone was lower than that of the other samples. Overall analysis, no significant difference was observed in samples of different geographical origins, except for Tibet and Shaanxi samples. There were significant differences in different sampling sites ($P < 0.05$), and the protein content of ribs is significantly higher than that of spine and rib ($P < 0.05$).

Table 2-3: Fat content between different geographical origins cattle bone samples.

Geographical	Sampling site		
	Marrow bone	Spine	Rib
Jilin (yellow cattle)	19.84±1.12	16.53±1.14	9.89±1.59
Inner Mongolia (yellow cattle)	26.89±2.71	13.61±1.55	7.9±1.41
Shandong (yellow cattle)	24.04±0.55	16.4±1.09	12.38±0.65
Shaanxi (yellow cattle)	19.33±1.33	16.65±1.20	10.65±0.50
Henan (yellow cattle)	26.78±2.25	13.14±1.12	8.15±1.25
Gansu (yak)	29.09±1.74	13.01±0.76	15.64±0.98
Sichuan (yak)	29.97±0.86	13.8±0.66	8.6±0.75
Tibet (yak)	18.17±0.65	27.66±1.25	13.61±0.87

As shown in Table 2-3, the fat content of cattle bone ranged from 7.9 to 29.97 g/100 g, and it varied in different geographical origins and sampling sites. In terms of yak bone, the Tibet samples showed low fat content. In yellow cattle bones, Jilin and Shaanxi bones showed low fat content. There were significant differences in fat content among different sampling sites ($P < 0.05$). The fat content of marrow bone was significantly higher than that of spine and rib ($P < 0.05$).

2.3.2. Multi-element composition

A total of 50 element contents were simultaneously measured in the cattle bone samples. The mineral levels in animal bones reflected the eating habits and environmental characteristics of the organism (Trueman & Tuross, 2002). ANOVA was applied for the data between different geographical origins. It has been shown that 45 of 50 elements (except for ^{39}K, ^{63}Cu, ^{107}Ag, ^{193}Ir, ^{232}Th) in the cattle bone are significantly different (Table 2-4). It showed the element contents: 124.2–184.2 g/kg of ^{43}Ca, 127.0–183.3 g/kg of ^{44}Ca, 47.3–80.0 g/kg of ^{31}P, 3.6–5.1 g/kg of ^{23}Na, 2.2%–3.3 g/kg of ^{24}Mg, and 0.6–0.9 g/kg of ^{39}K in cattle bones. In addition, compared with other trace elements, the nine elements, ^{27}Al (4.3–13.9 mg/kg), ^{45}Sc (0.1–1.0 mg/kg), ^{52}Cr (0.3–2.5 mg/kg), ^{56}Fe (24.7–91.2 mg/kg), ^{66}Zn (37.9–50.4 mg/kg), ^{85}Rb (0.4–1.3 mg/kg), ^{88}Sr (93.6–214.7 mg/kg), ^{137}Ba (52.7–178.0 mg/kg) and ^{175}Lu (0.2–1.9

mg/kg), with the mean content ＞ 0.5 mg/kg, are in high content. In terms of constant minerals (^{23}Na, ^{24}Mg, ^{31}P, ^{39}K, ^{43}Ca, ^{44}Ca), the total content of Jl and Sx samples was higher than that of other geographical origins, and Sc samples showed the lowest contents among all samples. Moreover, the toxic elements of ^{208}Pb, ^{111}Cd, and ^{75}As were detected in the cattle bone samples, and the contents of ^{208}Pb (0.4–1.8 μg/kg), ^{111}Cd (0.4–7.3 μg/kg), and ^{75}As (4.1–42.9 μg/kg) were far below the limits (100 μg/kg, 50 μg/kg, 500 μg/kg, respectively) reported by the European Commission (2008).

ANOVA was also applied for the data between species. Compared with the yellow cattle bones, except for ^{27}Al, ^{39}K, ^{51}V, ^{52}Cr, ^{55}Mn, ^{59}Co, ^{60}Ni, ^{63}Cu, ^{85}Rb, ^{95}Mo, ^{107}Ag, ^{111}Cd, ^{121}Sb, ^{125}Te, ^{139}La, ^{193}Ir, ^{195}Pt, ^{197}Au, ^{232}Th, other elements contents showed significant differences ($P < 0.05$) in the yak bone samples. The quantitative contents of all the elements were shown in Table 2-5. Figure 2-2 showed the beeswarm plots of the most significant elements of ^{147}Sm, ^{157}Gd, ^{163}Dy, ^{165}Ho, ^{166}Er, and ^{172}Yb. The contents of above elements of yak bone samples were higher than those of yellow cattle bone samples. The difference may be attributed to yak live in cold living conditions and high-altitude regions where beef cattle or dairy cows hardly live (Nie et al., 2020). Due to the difference of soil, water, and forage in a living environment, elements in different species of cattle bones can vary (Jia et al., 2017).

Table 2-4: Statistical data of different minerals between different geographical origins cattle bone samples.

Element	Inner Mongolia	Shandong	Gansu	Henan	Shaanxi	Tibet	Sichuan	Jilin	P-value
^{23}Na (g/kg)	4.8	3.9	4.1	3.8	5.1	3.6	3.9	4.6	1.84E-04
^{24}Mg (g/kg)	2.9	2.7	2.2	2.4	3.3	2.2	2.4	3.0	3.71E-04
^{27}Al (mg/kg)	11.0	13.9	10.2	4.3	7.3	7.6	4.6	7.9	4.96E-06
^{31}P (g/kg)	77.6	68.1	66.1	61.8	79.9	47.3	80.0	70.0	< 2E-16
^{39}K (g/kg)	0.6	0.7	0.9	0.8	0.7	0.6	0.8	0.7	1.05E-01
^{43}Ca (g/kg)	151.2	133.5	139.5	137.4	184.2	149.6	124.2	178.4	2.72E-03
^{44}Ca (g/kg)	150.3	132.1	138.8	135.4	183.3	147.4	127.0	176.4	3.24E-03
^{45}Sc (mg/kg)	1.0	0.6	0.6	0.3	0.8	0.5	0.1	0.5	2.95E-08
^{51}V (μg/kg)	9.7	52.6	3.7	21.0	50.3	7.4	61.5	28.2	7.68E-08
^{52}Cr (mg/kg)	1.0	0.6	1.1	2.5	0.5	0.8	1.8	0.3	1.85E-04
^{55}Mn (μg/kg)	223.7	297.5	256.5	576.9	357.8	414.4	276.4	244.5	2.82E-04
^{56}Fe (mg/kg)	28.6	44.7	91.2	58.7	50.8	64.0	72.5	24.7	1.49E-03
^{59}Co (μg/kg)	8.0	9.3	6.6	10.2	8.1	11.1	6.0	6.2	1.60E-03
^{60}Ni (μg/kg)	255.6	ND	322.1	26.1	18.7	ND	10.6	ND	< 2E-16
^{63}Cu (μg/kg)	118.0	141.2	112.0	196.5	200.5	75.7	230.1	135.4	4.60E-01
^{66}Zn (mg/kg)	41.9	44.2	50.4	37.9	49.3	49.8	49.7	48.2	7.43E-03
^{75}As (μg/kg)	3.6	6.7	13.0	3.8	15.0	42.9	2.6	4.1	< 2E-16
^{78}Se (μg/kg)	87.1	64.8	84.7	60.6	82.9	57.9	4.3	65.0	< 2E-16

^{85}Rb (mg/kg)	0.4	0.9	0.4	1.3	0.5	0.6	0.8	0.6	2.00E-08
^{88}Sr (mg/kg)	132.7	120.8	108.1	108.9	106.8	119.3	93.6	214.7	6.01E-08
^{95}Mo (μg/kg)	313.1	57.4	82.5	41.5	95.1	172.9	65.7	110.8	5.06E-08
^{105}Pd (μg/kg)	16.2	12.5	15.3	16.8	14.3	16.5	4.0	16.1	2.54E-14
^{107}Ag (μg/kg)	1.4	1.0	1.8	2.3	1.2	1.4	6.3	1.3	4.33E-01
^{111}Cd (μg/kg)	0.6	6.7	1.0	4.5	3.3	7.3	0.4	5.4	1.77E-13
^{118}Sn (μg/kg)	145.9	ND	149.3	205.0	ND	201.3	57.6	ND	< 2E-16
^{121}Sb (μg/kg)	61.4	5.1	69.7	1.7	8.8	4.5	0.3	6.4	< 2E-16
^{125}Te (μg/kg)	1.7	0.4	1.2	4.2	4.8	3.3	0.4	1.7	5.07E-08
^{133}Cs (μg/kg)	2.0	2.7	2.1	4.5	3.2	16.4	2.5	2.5	7.06E-08
^{137}Ba (mg/kg)	52.7	76.2	178.0	116.5	84.2	163.5	105.5	96.8	5.11E-12
^{139}La (μg/kg)	5.6	18.5	16.6	14.3	20.6	14.4	3.9	7.8	3.44E-06
^{140}Ce (μg/kg)	ND	9.3	2.3	ND	7.8	ND	ND	6.5	< 2E-16
^{141}Pr (μg/kg)	0.7	1.4	3.0	0.5	1.5	3.5	1.1	0.9	4.77E-07
^{146}Nd (μg/kg)	2.6	6.3	13.6	1.1	4.3	13.6	3.6	3.7	2.22E-14
^{147}Sm (μg/kg)	0.5	1.2	4.0	0.6	1.2	4.1	1.4	1.0	< 2E-16
^{153}Eu (μg/kg)	1.8	3.6	6.5	4.8	3.7	8.1	3.5	4.3	1.68E-14
^{157}Gd (μg/kg)	1.0	1.4	6.1	1.0	1.5	6.6	1.5	1.1	< 2E-16
^{163}Dy (μg/kg)	0.7	1.1	4.6	0.7	0.8	5.0	0.8	0.7	< 2E-16
^{165}Ho (μg/kg)	0.2	0.2	0.9	0.3	0.4	1.1	0.5	0.1	1.12E-12
^{166}Er (μg/kg)	0.5	0.6	2.1	0.4	0.6	2.3	0.7	0.4	< 2E-16
^{169}Tm (μg/kg)	0.2	0.1	0.4	0.2	0.3	0.5	0.2	ND	9.79E-05
^{172}Yb (μg/kg)	0.3	0.5	1.5	0.4	0.7	1.9	0.5	0.5	< 2E-16

^{175}Lu (mg/kg)	1.0	1.0	0.7	1.6	1.6	1.9	0.2	1.2	< 2E-16
^{178}Hf (μg/kg)	2.0	13.9	1.8	3.4	2.0	3.1	2.7	1.0	< 2E-16
^{193}Ir (μg/kg)	1.5	1.6	1.4	1.3	1.6	1.4	1.2	1.0	9.20E-01
^{195}Pt (μg/kg)	3.4	3.7	3.3	2.1	4.4	2.2	4.4	2.7	1.58E-06
^{197}Au (μg/kg)	0.3	0.9	0.4	0.8	0.3	0.9	0.5	0.1	2.88E-03
^{205}Tl (μg/kg)	0.2	0.4	0.2	0.1	0.4	0.2	0.1	0.3	6.45E-03
^{208}Pb (μg/kg)	0.7	0.7	0.9	0.4	0.9	1.8	0.5	0.6	< 2E-16
^{232}Th (μg/kg)	35.9	42.5	33.9	52.0	51.7	57.9	44.1	27.3	9.42E-01
^{238}U (μg/kg)	3.0	2.2	2.1	1.8	2.9	8.9	2.5	2.0	< 2E-16

ND: Not detected

Table 2-5: Statistical data of different minerals between different species bone samples.

Minerals	Yak	Yellow cattle	P-value
^{23}Na (g/kg)	3.9 ± 0.7	4.3 ± 1.3	3.78E-03
^{24}Mg (g/kg)	2.3 ± 0.6	2.8 ± 0.9	8.76E-05
^{27}Al (mg/kg)	7.4 ± 5.9	9.2 ± 8.2	1.88E-01
^{31}P (g/kg)	64.4 ± 15.4	71.5 ± 9.9	1.16E-03
^{39}K (g/kg)	0.8 ± 0.4	18.4 ± 44.9	1.64E-01
^{43}Ca (g/kg)	137.7 ± 36.5	151.4 ± 57.7	3.37E-02
^{44}Ca (g/kg)	137.7 ± 35.0	132.0 ± 77.3	4.48E-02
^{45}Sc (mg/kg)	0.4 ± 0.4	0.5 ± 0.5	5.30E-03
^{51}V (μg/kg)	24.6 ± 59.9	156.1 ± 585.4	2.59E-01
^{52}Cr (mg/kg)	1.2 ± 1.5	0.9 ± 1.6	3.77E-01
^{55}Mn (μg/kg)	316.9 ± 247.6	293.2 ± 271.1	6.08E-01
^{56}Fe (mg/kg)	75.6 ± 73.0	36.5 ± 29.1	1.23E-04
^{59}Co (μg/kg)	7.9 ± 4.6	21.0 ± 50.5	5.67E-01
^{60}Ni (μg/kg)	106.9 ± 179.7	98.3 ± 187.6	6.07E-02
^{63}Cu (μg/kg)	139.0 ± 144.8	177.7 ± 262.8	2.46E-01
^{66}Zn (mg/kg)	50.0 ± 9.3	44.2 ± 12.8	5.65E-03
^{75}As (μg/kg)	19.6 ± 18.9	6.6 ± 6.5	7.65E-09
^{78}Se (μg/kg)	48.3 ± 41.5	174.4 ± 269.4	1.58E-05
^{85}Rb (mg/kg)	0.6 ± 0.3	8.8 ± 24.1	5.20E-02
^{88}Sr (mg/kg)	107.0 ± 36.7	116.1 ± 86.1	8.97E-03
^{95}Mo (μg/kg)	107.5 ± 59.3	104.9 ± 180.7	5.51E-01
^{105}Pd (μg/kg)	11.9 ± 7.6	13.3 ± 6.6	1.50E-03
^{107}Ag (μg/kg)	3.0 ± 9.5	1.7 ± 4.4	1.91E-01
^{111}Cd (μg/kg)	2.9 ± 3.4	3.7 ± 4.1	9.71E-02
^{118}Sn (μg/kg)	135.8 ± 79.1	69.1 ± 87.2	2.35E-05
^{121}Sb (μg/kg)	24.0 ± 38.8	16.9 ± 27.5	1.92E-01
^{125}Te (μg/kg)	1.7 ± 2.2	2.3 ± 3.1	7.48E-02
^{133}Cs (μg/kg)	7.1 ± 13.5	2.9 ± 1.8	5.14E-03
^{137}Ba (mg/kg)	148.4 ± 64.6	80.0 ± 54.3	1.59E-09
^{139}La (μg/kg)	11.5 ± 9.1	12.9 ± 13.2	3.80E-01
^{140}Ce (μg/kg)	0.7 ± 2.9	4.5 ± 6.3	5.71E-08
^{141}Pr (μg/kg)	2.5 ± 2.8	1.5 ± 2.1	6.42E-06
^{146}Nd (μg/kg)	10.2 ± 9.3	4.9 ± 6.2	4.29E-09
^{147}Sm (μg/kg)	3.2 ± 2.0	1.2 ± 1.4	< 2E-16
^{153}Eu (μg/kg)	6.0 ± 2.9	3.5 ± 2.3	2.51E-07

^{157}Gd (μg/kg)	4.7 ± 3.4	1.5 ± 1.3	< 2E-16
^{163}Dy (μg/kg)	3.5 ± 2.6	1.0 ± 1.0	< 2E-16
^{165}Ho (μg/kg)	0.8 ± 0.6	0.4 ± 0.7	2.40E-12
^{166}Er (μg/kg)	1.7 ± 1.1	0.7 ± 0.7	< 2E-16
^{169}Tm (μg/kg)	0.4 ± 0.4	0.2 ± 0.5	3.29E-04
^{172}Yb (μg/kg)	1.3 ± 0.9	0.6 ± 0.6	3.98E-12
^{175}Lu (mg/kg)	0.9 ± 0.8	1.1 ± 0.6	6.47E-04
^{178}Hf (μg/kg)	2.6 ± 2.3	4.4 ± 6.1	4.02E-02
^{193}Ir (μg/kg)	1.3 ± 2.0	1.3 ± 0.9	8.39E-01
^{195}Pt (μg/kg)	3.3 ± 1.4	3.5 ± 1.8	9.15E-01
^{197}Au (μg/kg)	0.6 ± 1.1	0.6 ± 0.8	1.81E-01
^{205}Tl (μg/kg)	0.2 ± 0.3	0.4 ± 0.6	2.52E-02
^{208}Pb (μg/kg)	1.1 ± 0.7	0.6 ± 0.3	1.12E-06
^{232}Th (μg/kg)	45.5 ± 77.0	51.4 ± 94.5	7.83E-01
^{238}U (μg/kg)	4.5 ± 3.5	3.2 ± 3.1	4.78E-07

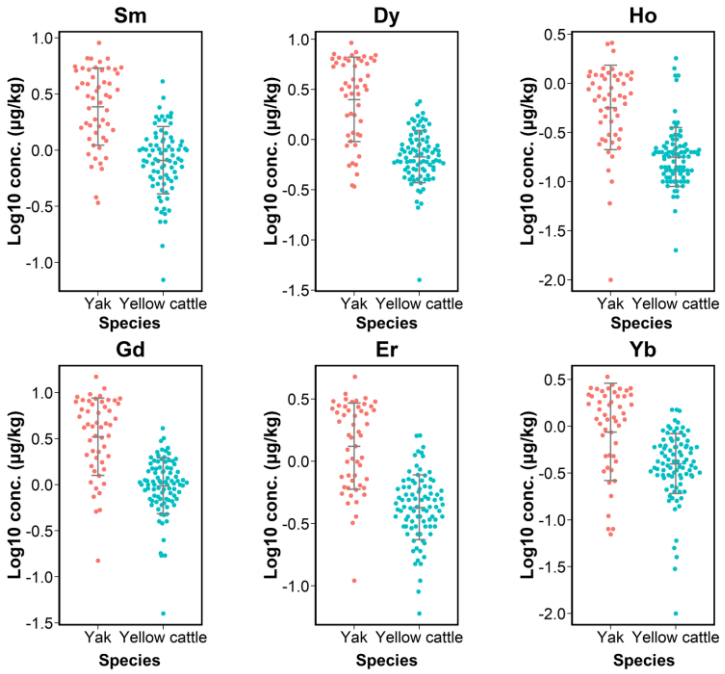

Figure 2-2: Beeswarm plots with concentration profiles of elements most relevant for species discrimination. Each dot constitutes one cattle bone sample, and the bands are indicating mean and sd (standard deviation).

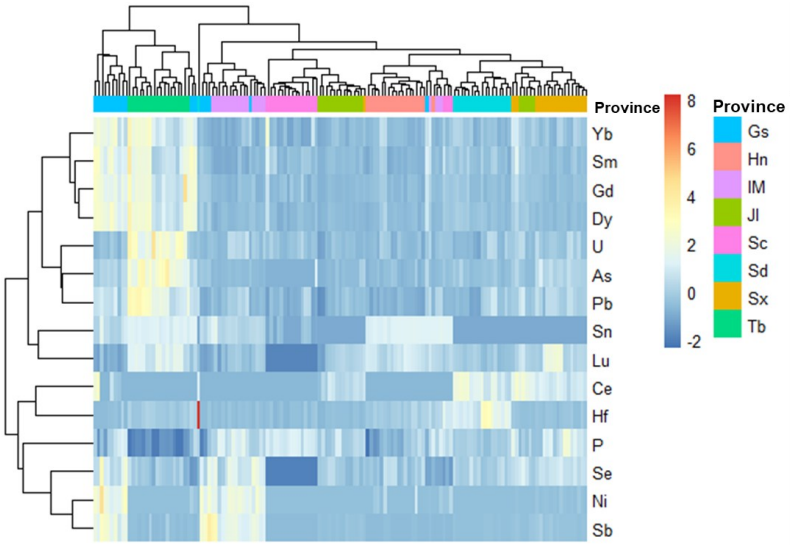

Figure 2-3 Cluster heat map showing the element concentrations in cattle bone samples from different geographical origins. Color scale displays the range of concentrations from low (blue) to high (red). Gs: Gansu, Hn: Henan, IM: Inner Mongolia, Jl: Jilin, Sc: Sichuan, Sd: Shandong, Sx: Shaanxi.

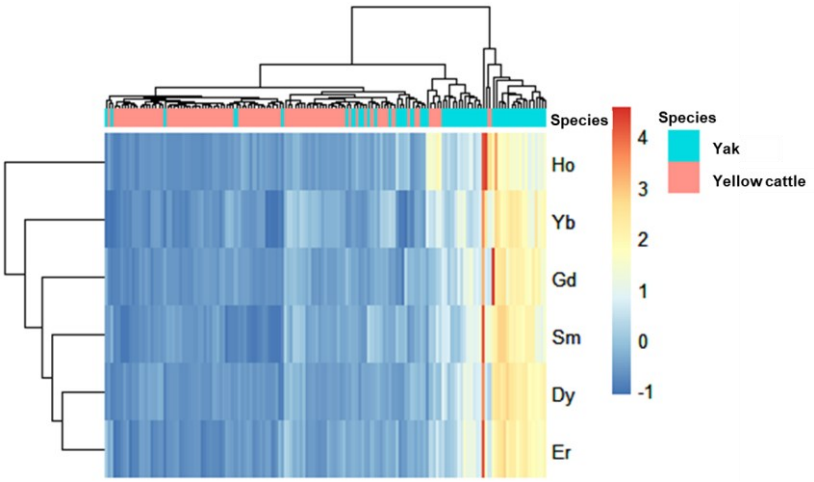

Figure 2-4: Cluster heat map showing the element concentrations in cattle bone samples from different species. Color scale displays the range of concentrations from low (blue) to high (red). Gs: Gansu, Hn: Henan, IM: Inner Mongolia, Jl: Jilin, Sc: Sichuan, Sd: Shandong, Sx: Shaanxi.

HCA of the samples was performed to distinguish cattle bone species (yellow cattle

vs. yak) and geographical origins based on the elemental data. In the cluster analysis, the key elements with highest significance and relevance for the different region were used in Figure 2-3. The dendrogram of cattle bone samples (horizontal) showed fully separated clusters for Tb, and Hn samples. The major Sx samples locate in an own cluster in the right part. In addition, most samples from the Gs situate on the left edge, while a small amount of Gs sample and IM samples were grouped into one category. Most of the IM samples gather into a cluster structures, while few samples disperse in the Sd samples. Samples of Jl origin were nearly divided into two separate cluster structures. Cattle bone samples of different origins were divided into two clusters based on the dendrogram cut. One cluster included Gs and Tb samples, and the main reason may be the same species and closer geographical origin discrimination. The samples from other geographical origins aggregate into a cluster. Indications for key elements relevant for geographical origin distinction can be extracted from the concentration profile. It displayed high concentrations of ^{172}Yb, ^{147}Sm, ^{157}Gd, ^{60}Ni, and ^{121}Sb in Gs samples. Cattle bones from Tb were associated with larger amounts of ^{172}Yb, ^{147}Sm, ^{147}Sm, ^{238}U, ^{75}As, and ^{208}Pb. The elements of ^{175}Lu and ^{78}Se were lower in the Sc samples. These results implied that element information can be suitably utilized to classify geographical origin. In addition, HCA was also carried out to evaluate a possible influence between two species. As shown in Figure 2-4, although presenting the overlap, the dendrogram of samples could be separated to two clusters. Results revealed a great influence of species on the element composition of cattle bone samples.

2.3.3. Species discrimination

LDA is a classical statistical approach for dimensionality reduction and classification while retaining the highest possible variance (Yan et al., 2015). Since cattle bones samples showed different elemental compositions between yellow cattle and yak, the data of 31 elements with significant differences ($P < 0.05$) were subjected to the LDA for species discrimination. The LDA plot (Figure 2-5) showed yellow cattle and yak bone samples were clustered separately, suggesting this method exhibited a good discrimination function. The yellow cattle bone samples were concentrated in the upper section (DF1 score > 0), and the yak bone samples were concentrated in the under section (DF1 score < 0). In the simple cross validation, the data were divided into the training set and test set (8: 2), and the simple cross validation accuracy was 97.7%. Table 2-6 showed the confusion matrix of cross validation for classification of species in detail. The results indicated that the two cattle species can be effectively identified using a combination of multi-element and LDA.

Although isoelectric focusing (IEF) and DNA tests as the acknowledged methods for species differentiation (Magdas et al., 2019), the multi-element was also applied in the discrimination of species in agricultural field. The elemental profile completely separated (100% in both initial and cross-validation procedure) the cheese samples of sheep and cow cheese. The mineral elements of Ca and Mg were discovered to be effective discriminators for goats and cow cheeses (Fantuz et al., 2016). The multi-element analysis was applied to species discrimination between Taihe black-boned

silky fowl (a rare chicken breed that is native to China) and crossbred muscle samples with a high discriminatory power (Mi et al., 2019). Similar results were obtained in this study.

Table 2-6: Confusion matrix for classification of the species of origin with the build LDA model.

		Predictable class (Species)	
		Yak	Yellow cattle
Actual class	Yak	14	1
	Yellow cattle	0	28
Prediction accuracy		97.7%	

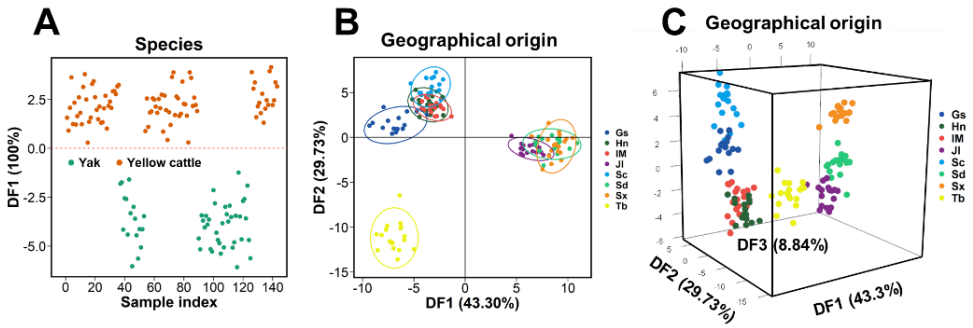

Figure 2-5 (A) The LDA score plot based on the mineral data from cattle bone samples collected from different species. The green dots represent the samples from yaks, and the red-brown dots represent the samples from yellow cattle. (B) The LDA score plots (the first two discrimination functions) based on the mineral data from cattle bone samples collected from different geographical origins. (C) The LDA score plots (the first three discrimination functions) based on the mineral data from cattle bone samples collected from different geographical origins. Gs: Gansu, Hn: Henan, IM: Inner Mongolia, Jl: Jilin, Sc: Sichuan, Sd: Shandong, Sx: Shaanxi.

2.3.4. Geographical origin discrimination

Many factors (e.g., rocks, soils, fertilization strategies, and cultivars) can largely affect the elements composition of agricultural products (Barbosa et al., 2014; Drivelos & Georgiou, 2012). Since cattle bone cultivated in different geographical origins showed different element compositions. Therefore, to get visual differences of cattle bones samples among the various geographical origins in China, the data of 45 elements with significant differences ($P < 0.05$) were subjected to the LDA. The first two discriminant functions (DF) that in sum explain was 72.44% of the total variance, which was slightly lower than that of the LDA using 50 elements. Thus, all the elements were chosen for the future LDA. Figure 2-5B presented the LDA plot

including scores plots and the corresponding loadings by the first two DFs that in sum explain 73.03% of the total variance. Tb cattle bone samples were fully separated from all other samples. In contrast, the other regions' samples overlapped with at least one region. The first DF separated Gs samples from all the samples, while the second DF discriminated Tb samples. Figure 2-5C presented the LDA plot between different geographical origins by the first three DF that in sum explain 81.87% of the total variance. The discrimination power was obviously better than that of using two DF. As shown, Tb, Gs, Sc, and Sx samples were separated from other samples. In contrast, IM samples overlapped with some of the Hn ones, which indicated the great similarity between IM samples and one part of Hn samples. The Sd samples and Jl samples had a slight overlap. A possible reason could be the close distance from Sd to Jl. The simple cross validation accuracy was 96.6 % (Table 2-7), and it showed the confusion matrix of cross validation for classification of geographical origin.

Table 2-7: Confusion matrix for classification of the region of origin with the build LDA model.

		Predictable class (Geographical origin)							
		Gs	Hn	IM	Jl	Sc	Sd	Sx	Tibet
Actual class	Gs	5	0	0	0	0	0	0	1
	Hn	0	5	0	0	0	0	0	0
	IM	0	0	2	0	0	0	0	0
	Jl	0	0	0	1	0	0	0	0
	Sc	0	1	0	0	1	0	0	0
	Sd	0	0	0	0	0	5	0	0
	Sx	0	0	0	0	0	0	4	0
	Tibet	0	0	0	0	0	0	0	4
Prediction accuracy		96.6%							

Gs: Gansu, Hn: Henan, IM: Inner Mongolia, Jl: Jilin, Sc: Sichuan, Sd: Shandong, Sx: Shaanxi.

Furthermore, we also built the discrimination models for geographical origin in the same species (yak and yellow cattle), because the species difference had great influence on the element component of cattle bone samples. Figure 2-7A and Figure 2-7B present the LDA plots, which respectively describe the clustering of different geographical origins in the same species (yellow cattle and yak). Figure 2-7A showed the Hn, Sx, and IM samples were distinguished from each other according to 50 mineral elements. Unlike the results of Figure 2-7C, the Hn and IM samples were fully separated without overlap. The first two DFs that in sum explained 86.7% of the total variance. Figure 2-7B showed that the Gs, Sc, and Tb samples were separated effectively, and the sum explanation of first two DFs (100%).

These results suggested that the multi-element data could be applied for geographical origins of cattle bone samples. Present studies have shown similar

results. Differences in elements contents were observed for the geographical origins of raw beef (Zhao et al., 2013), cheese (Magdas et al., 2019), pork (Kim et al., 2017). As explained by Kim & Thornton, (1993), the content and availability of elements in soils were influenced by different factors, such as humidity, pH, and clay-humus complex. The elemental composition of vegetation reflects the difference of element in soils where plants are growing, which also determines the multi-element composition of the animals consuming that vegetation (Kelly et al., 2005).

In this study, to fully employ the multi-element data for discriminate the geographical origin of cattle bone, we also built the discrimination models of three sampling sites, separately, since the sampling site had a great influence on the elemental profile of samples. There were reports indicating that the differences in mineral contents were observed for the different cuts of Taihe black-boned silky fowl muscles (Mi et al., 2019), broiler chicken (Sager et al., 2018), raw beef (Cabrera et al., 2010). Figure 2-6 showed the LDA plot between three sampling sites with a sum explanation of 100%. Figure 2-7 (C-E) showed the LDA plots built in three sampling sites (Marrow bone, Spine, and Rib) with the sum explanation of 79.06%, 78.17%, and 79.71%, respectively. Figure 2-7C showed that the distribution of Jl and Sd overlap due to closer geographic location and plain topography, suggesting the cattle bones samples with similar mineral composition. Hn samples slightly overlapped with some of the IM ones, which are consistent with the accuracy of 80%. Figure 2-7D and Figure 2-7E showed the samples could distinctly discriminate between eight geographical origins. These results based on multi-element analysis and LDA suggested this method had a potential application for geographical origin discrimination.

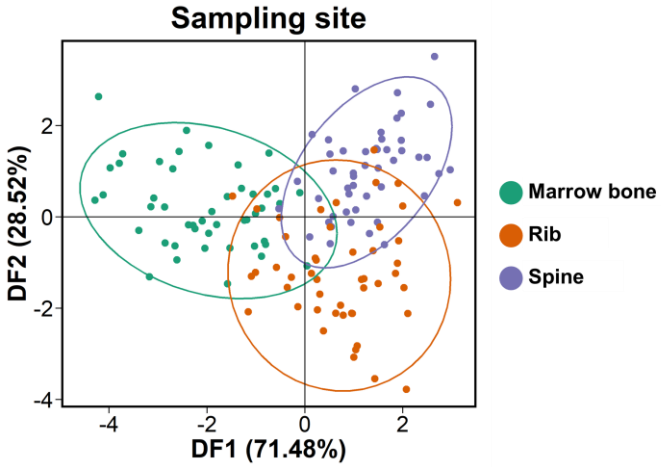

Figure 2-6 LDA score plot based on the mineral data from cattle bone samples collected from different sampling site.

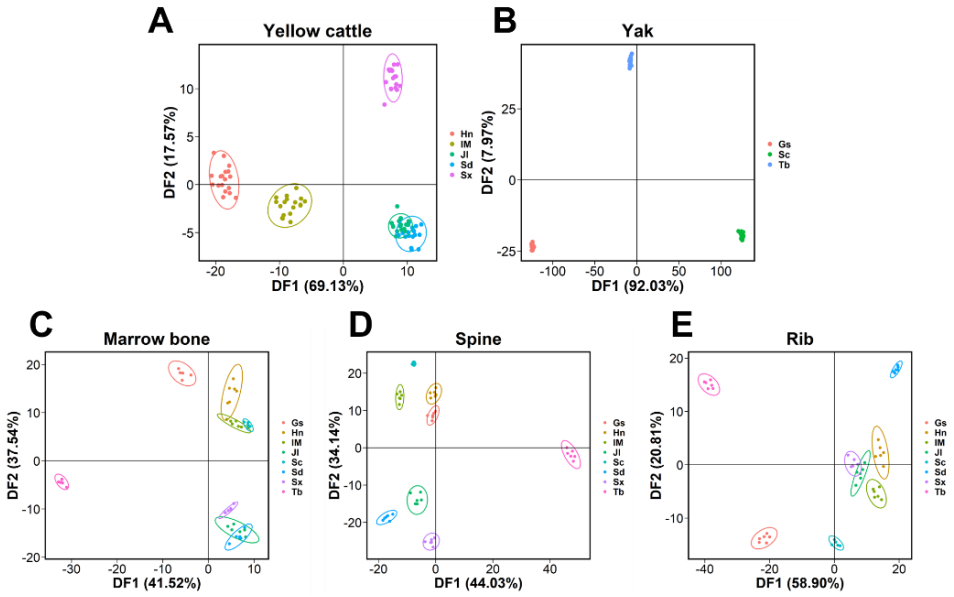

Figure 2-7 (A-B) The LDA score plots based on the mineral data from cattle bone samples of yellow cattle and yak, respectively. (C-E) The LDA score plots based on the mineral data from cattle bone samples of marrow bone, spine, rib, respectively. Gs: Gansu, Hn: Henan, IM: Inner Mongolia, Jl: Jilin, Sc: Sichuan, Sd: Shandong, Sx: Shaanxi.

2.3.5. Discrimination models validation

The simple cross validation accuracies for species and geographical origin were 97.7% (Table 2-6) and 96.6% (Table 2-7), respectively. The simple cross-validation used the same data for parameter tuning as for assessing the model performance, with a risk of notable overfitting and bias of the samples. The limitation of experimental data might affect the accuracies of discrimination mode. To evaluate the performance of the obtained discrimination models, proper validation is of great importance. Therefore, K-fold cross validation was applied in this work for making full use of the original data.

Table 2-8 showed the accuracy of K-fold cross-validation for species and geographical origin discriminations are 99.3% and 94.5%, respectively. The K-fold cross-validation accuracy of species increased to 99.3%, suggesting the discrimination models possess a good species identification ability. The K-fold cross-validation accuracy of geographical origin decreased to 94.5%. This may be due to the number limitation of samples in the test set of the simple crossover model. It demonstrated that cattle bone samples from different regions can be separated based on LDA.

Table 2-8: The results of K-cross validation results of regions and species by LDA model.

Discrimination model	K-cross validation result	Average accuracy
Geographical origin	92.9%, 93.3%, 87.5%, 93.3%, 92.3%, 100%, 100%, 100%, 85.7%, 100%	94.5%
Species	100%, 100%, 100%, 100%, 100%, 100%, 93.3%, 100%, 100%, 100%	99.3%

2.4. Conclusions

Geographical origin and species did not show significant effect on protein content of cattle bone and sampling site showed significant effect. The fat content of yak bone was higher than that of yellow cattle bone. The sampling site showed significant effect on protein and fat content of cattle bone. We established the discrimination mode by the bone elemental profiles to discriminate the geographical origin and species of cattle bone. The combined use of multi-element analysis and LDA was suited for the distinction of the geographic origin and species (yellow cattle vs. yak), with K-cross validation accuracies of 94.5% and 99.3%, respectively. This work can make a crucial contribution to detect false product declarations and standardize the bone products market.

3

Chapter III. Study of the effect of steam explosion on collagen peptides extraction from cattle bone

Adapt from:

Zhang, H., Liu, H., Qi, L., Xv, X., Li, X., Guo, Y., Jia, W., Zhang, C., & Richel, A. (2021). Application of steam explosion treatment on the collagen peptides extraction from cattle bone. *Innovative Food Science and Emerging Technologies*. (Accept)

Abstract: In this study, steam explosion (SE) treatment was applied to extract collagen peptides from cattle bone. The SE treatment conditions included steam pressure: 1.5 MPa (200.43 ℃), 2.0 MPa (213.85 ℃), and 2.5 MPa (224.99 ℃), and reaction time: 10 min, 20 min, and 30 min. With the increase of pressure and reaction time, the protein recovery rate improved, and reached to 62.5% at 2.5 MPa–30 min. SE significantly decreased the molecular weight of collagen peptides ($P < 0.05$) with increasing pressure and reaction time. However, at 2.5 MPa, SE darkened the sample color resulting in dark yellow. Particle size analysis and SEM images indicated that SE decreased the particle size and destroyed microstructure of cattle bone powder. FT-IR analysis showed that SE induced distinct characteristic peaks of hydroxyapatite in cattle bone powder. Amino acid analysis indicated SE could not change the amino acid composition of collagen peptides. The findings put forward data support and a scientific basis for the application and development of SE technology to collagen peptides extraction and high-value utilization of cattle bone.

Keywords: Cattle bone, Steam explosion, Collagen peptides, Extraction

3.1. Introduction

Cattle production is a very important livestock sector worldwide. In 2019, the global beef output is about 62.9 million tons, and the output of collagen-rich cattle bone, skin, and tendon was as high as 31.4 million tons (Song et al., 2021). However, in beef process, most of bones cannot be fully utilized, and cause a huge waste of bone resources and environmental pollution. In EU, cattle bones have been usually considered as slaughterhouse waste and are disposed of in landfills or sent to rendering plant. After refining, a portion of this waste is often reused as meat and bone meal for animal feed, fertilizer, and bulk pet food ingredients. This low utilization rate leads to the waste of livestock bone resources.

Due to its high collagen content, Cattle bone was considered a great source of bioactive peptides. A series of studies have identified that collagen peptides have multiple biological activities, such as skin health, antioxidant, antidiabetic, and bone health (Fu et al., 2019). Food-derived bioactive peptides have great potential in the development of functional foods and nutraceuticals to prevent and manage many chronic diseases (Ulug et al., 2021). The use of bone resources to obtain nutritionally fortified products has broad prospects. Collagen peptides derived from bones have been identified as a potential source of novel calcium supplements due to their ability to chelate calcium. Sources of bone usually include pig bone, sheep bone, and cattle bone (Wang et al., 2020; Wu et al., 2019; Zhang et al., 2021). It is gradually arousing people's interest to effectively utilize bone-derived collagen peptides.

The most common methods for extracting bioactive peptides are chemical hydrolysis (acid and alkali hydrolysis), enzymatic hydrolysis and fermentation (Ulug et al., 2021). High hydrostatic pressure (Marciniak et al., 2018), subcritical water hydrolysis (Rivas-Vela et al., 2021), and ultrasound assisted hydrolysis (Kadam et al., 2015) have also been extensively researched. These methods require large volumes of solvent, high temperatures, and high energy costs (Sui et al., 2019). Due to the high toughness and stiffness of bone, it is difficult to extract collagen peptides from cattle bone (Bonadio et al., 2013). Therefore, it is of great significance to develop an efficient and energy-saving method for extracting collagen peptides from bone.

Steam explosion is a technology for biomass treatment, that is usually applied at 160–240 ℃ and 0.69–4.46 MPa for several seconds to a few minutes, with saturated steam followed by an explosive decompression (Lama-Muñoz et al., 2019). Steam explosion is a thermophysico-chemical process which provides mechanical destructuration by a combination of two steps: vapocracking and explosive decompression (Maniet et al., 2017). Compared with others treatment methods, the SE method has potential advantages including lower cost, lower energy, and environmental friendliness (Cantarella et al., 2004; Conde-Mejía et al., 2012). Except for the application of SE on plant biomaterials (lignocellulosic biomass, aspen wood, and corn strove) (Jacquet et al., 2015), SE is also applied in animal by-product for increasing the bioactivity of nutrient content (Qin et al., 2021; Shen et al., 2019). Zhang et al., (2014) demonstrated that SE is an effective method to improve the bio-utilization of feather meal. Shen et al., (2019) indicated that SE can be used to isolate chondroitin sulfate from chicken cartilage, with the recovery and total yield of 92.15% and 18.55%, respectively. Cui et al., (2021) prepared tuna bone powder by SE

treatment at steam pressure 0.6 MPa and reaction time 5 min. However, studies about the effects of SE on peptides extraction form animal bone were limited. Thus, we predicted that SE treatment might destroy the dense structure of cattle bones by physical and chemical action, which can be beneficial to extract collagen peptides.

In this study, we aimed to establish a new method to extract collagen peptides from cattle bone. It has the advantage of without using chemical reagent. To achieve this, cattle bone was subjected to steam explosion apparatus at different pressures and reaction time. The effects of steam explosion on the protein recovery rate, molecular weight of peptides, and the change of sample color were evaluated. The microstructure of cattle bone (after SE) was evaluated via scanning electron microscope. Then, FT-IR spectra of cattle bone powder, amino acid composition, calcium-binding ability, and osteoblast proliferative activity of collagen peptides were investigated. This study provided a novel technology for the high-value utilization of cattle bone.

3.2. Materials and Methods

3.2.1. Materials

Cattle bone (femurs from 2 years old cattle) was purchased from the Tibet Academy of Agricultural and Animal Husbandry Sciences (Tibet, China). The impurities and marrow of bone were removed manually. Then, cattle bone was crushed into pieces (about 1 cm) by a crusher (PE-180S, Hangzhou xuzhong machinery equipment Co, Ltd., China). The components of raw cattle bone were shown protein content (253.2 g/kg), calcium content (219 g/kg), and phosphorus content (94 g/kg). The commercial collagen peptides were provided by Hulunbuir Muyuankangtai Biotechnology Co. LTD, (Inner Mongolia province, China). Acetonitrile (chromatographic grade) was purchased from Thermo Fisher Scientific (Waltham, USA) for molecular mass distribution. Potassium bromide was purchased from Sinopharm Chemical Reagent Co. Ltd. (Shanghai, China) for Fourier Transform infrared spectroscopy analysis. Murine osteoblast MC3T3-E1 cells, α-MEM medium, and fetal bovine serum were purchased from Procell Life Science & Technology Co., Ltd for measuring the osteoblast proliferative activity of collagen peptides. Other used reagents (analytical grade) were purchased from Sinopharm Chemical Reagent Co., Ltd. (Shanghai, China). The deionized water was prepared by a Milli-Q purification 50 system (Millipore, Bedford, MA).

3.2.2. Steam explosion pretreatment on cattle bone

Steam explosion treatment was performed by the SE apparatus (QBS-80 SE, Gentle Bioenergy Co. Ltd., Hebi, Henan province, China). Briefly, 100 g of bone sample was added to the sample chamber (400 mL). The SE treatment conditions included pressure and reaction time. The schematic diagram of SE treatment to liquefy cattle bone was shown in Figure 3-1A. The pressures were 1.5, 2.0, and 2.5 MPa, and the reaction times were 10, 15, 20, 25, and 30 min. The pressurization time (from 0 to intentional pressure) was about 2-3 min. After the violent SE reaction, a sieve (< 25 μm) was used to screen the samples for removing bulky samples. Fat was removed by centrifuging (8000 rpm, 15 min). After that, all supernatants were collected and

lyophilized (–38 ℃ for 7 days) to determine protein, mineral contents, amino acid composition, and bioactivities. All sediments were collected and lyophilized at (–38 ℃ for 3 days) to analysis particle size and scanning electron microscope.

3.2.3. Protein content

To determine the protein content, the AOAC method 976.05 was used, and measurements were taken using a Kjeltec 2300 Analyzer (Foss Tecator, Hoganas, Sweden). The conversion factor from nitrogen to protein was 6.25.

3.2.4. Color

To evaluate the sample color difference, the software ImageJ (National Institutes of Health) was used to quantize the chroma values, and each color is represented by a color point (L*, a*, b*). CIE Lab color coordinates (L* = lightness, a* = redness, b* = yellowness). ImageJ is widely used in analyzing the color characteristics of a sample. It is a useful tool for color analysis in various fields, such as food science, agriculture, and material science (do Amaral et al., 2019).

3.2.5. Protein recovery rate

The protein content was determined by the Kjeldahl method of AOAC 976.05-1977 (1996), using a Kjeltec 2300 Analyser (Foss Tecator AB, Hoganas, Sweden). The flesh and marrow were separated from raw bone manually. Then, raw bone was crushed into pieces (about 1 cm) by using the bone grinding machine (PG-300, Xingyang Tianjin food machinery factory, Zhengzhou, China). The raw bone pieces were and stored at –20 ℃ for protein content determination. The extraction (the lyophilized powder) was weighed and assayed for protein determination. Briefly, 0.5 g sample was subjected to nitrogen bottle. Then, 0.4 g copper sulfate, 6 g potassium sulfate, and 20 mL sulfuric acid were added to the above nitrogen bottle. After that, sample was digested by using the Kjeldahl Digestion Furnace (DK, Beijing Ecotek Technology Company Limited, China). Finally, the digested sample was subjected to Kjeltec Analyser for protein content determination. The protein conversion factor was 6.25. The protein recovery rate was calculated as follows:

$$\text{Protein recovery rate (\%)} = \frac{\text{Pro (extraction)} \times \text{W1}}{\text{Pro (raw)} \times \text{W2}} \times 100$$

Where Pro (extraction) represents the protein content of extraction (mg/g), Pro (raw) represents the protein content of raw bone (mg/g), W1 represents the weight of extraction (g), and W2 represents the weight of raw bone (g).

3.2.6. Molecular weight determination

The molecular weight of samples was determined by using an HPLC apparatus (Agilent 1260, Agilent Technologies, Walnut Creek, CA, USA) equipped with DAWN HELEOS-II (Wyatt Technology Corporation, America) and Optilabr EX (Wyatt Technology Corporation, USA) detectors coupled with a TSK gel G4000PWxl column (7.8 × 300 mm, TOSOH, Tokyo, Japan) (Zhang et al., 2022). The mobile phase was of 45% of acetonitrile, 0.1% of trifluoroacetic acid, and 54.9% of ultrapure

water. Samples were dissolved in mobile phase (1 mg/mL). The standards were Gly-Sar (146 Da), Gly-Gly-Tyr-Arg (451 Da), bacitracin (1422 Da), aprotinin (6511 Da), and cytochrome C (12327 Da).

3.2.7. Calcium and phosphorus release rate

Calcium and phosphorus contents of samples were determined by flame spectrophotometry method (Qin et al., 2021). Sample was weighted and digested with HNO3 using a microwave digestion instrument. Then, the digestion was transfer to a bottle and diluted to 100 mL with deionized water. The diluted solution was further diluted 10 times before analyzing by an atomic absorption spectrophotometer (AA-3300F). The calcium and phosphorus release rates were determined by the following formula:

$$\text{Calcium release rate (\%)} = \frac{\text{Ca (extraction)} \times \text{W1}}{\text{Ca (raw)} \times \text{W2}} \times 100$$

$$\text{Phosphorus release rate (\%)} = \frac{\text{P (extraction)} \times \text{W1}}{\text{P (raw)} \times \text{W2}} \times 100$$

Where Ca (extraction) represents the calcium content of extraction (mg/g); Ca (raw) represents the calcium content of raw bone (mg/g); P (extraction) represents the phosphorus content of extraction (mg/g); P (raw) represents the phosphorus content of raw bone (mg/g); W1 represents the weight of extraction (g); and W2 represents the weight of raw bone (g).

3.2.8. Particle size

The particle size distribution of bone powder produced by SE was determined by particle size analyzer (Helos-kr, Sympatec GmbH, Germany) (Qin et al., 2021). The results were analyzed by the HELOS system. The particle size was represented by volume median diameter (VMD).

3.2.9. Scanning electron microscope

The SEM images were obtained to display the microstructure of samples by a scanning electron microscope (Zeiss Merlin Compact, Germany) (Wang et al., 2020). The sample plate was uniformly covered with 5 mg of the samples, sprayed with a gold plating film before detection. Micrographs were obtained at 10 kV of accelerating voltage.

3.2.10. Amino acid content

Amino acid content was determined by using an amino acids automatic analyzer (L-8900, Hitachi LTD, Japan), according to (Zhang et al., 2021). In brief, the sample was placed in hydrolysis tube. Then 10 mL of 6 M HCl was added to tube. To remove air, the tube was filled with N_2 for 1.5 min, and the tube was sealed with caps and placed at 110 ℃ for 24 h for sufficient hydrolysis. Finally, the hydrolysate was filtrated by a 0.45 μm filter membrane before amino acid analysis.

3.2.11. Fourier transform infrared spectroscopy (FT-IR)

The chemical structure of cattle bone (raw bone and after SE) was analyzed using an FT-R spectrometer (Tensor-27, Bruker Company, Germany), according to (Malison et al., 2021). Briefly, approximately 10 mg of sample was mixed with potassium bromide (1:100, w/w) and manually extruded into a transparent sheet. Then, it was scanned against a blank potassium bromide background with the absorption spectrum of FT-IR in a range from 4000 to 400 cm.

3.2.12. Statistical analysis

Data from all measurements were expressed in triplicate as the mean ± SD (standard deviation). Analysis of variance (ANOVA) and Duncan's test were performed using the statistical programming language R (R Core Team, 2016). ggplot2, agricolae, and dplyr packages were used to visualize data. $P < 0.05$ was considered as statistically significant.

3.3. Results and discussion

3.3.1. Color

With the increase of pressure (from 1.5 to 2.5 MPa) and reaction time (from 10 to 30 min), the color of the samples showed some apparent differences (Figure 3-1B). At the pressure of 2.5 MPa, the color of the supernatant obviously changed to brownish yellow. To further evaluate the color change, we evaluated the L*, a*, and b* value of samples. Samples treated with 2.5 MPa showed the higher a* value and b* value compared to samples treated with 1.5 MPa and 2.0 MPa (in Figure 3-1D&E). There were differences between samples treated with 1.5 MPa and 2.0 MPa (at the same reaction time) in a* value and b* value, but the differences were not significant. In conditions of 1.5 MPa and 2.0 MPa, the reaction time did not show rule influence on a* value and b* value. As shown in Figure 3-1C, samples treated with 2.5 MPa showed lower L* values compared to samples treated with 1.5 MPa and 2.0 MPa. There were no significant differences observed between the samples treated with 1.5 MPa and 2.0 MPa. At the pressure of 1.5 MPa and 2.0 MPa, the reaction time did not significantly influence the L* value of sample. At 2.5 MPa, the L* value significantly decreased ($P < 0.05$) with increasing reaction time. A previous study found similar results that SE treated wool inducing a dark-yellow color of supernatant (Tonin et al., 2006). Wang et al., (2021) indicated that after the SE treatment, the color of brassica seed was dark. The Maillard reaction induced by SE might lead to brown-colored melanoidins (Serpen & Gökmen, 2009). At severe conditions, collagen could be easily undergo hydrolyzed, breaking down into peptides or individual amino acids. Therefore, at 2.5 MPa, the Maillard reaction was more likely to occur, leading to a darker color. The formation of oxidation products could be the possible reason for the decrease in lightness observed in the SE treated samples (Guo et al., 2015; Kong et al., 2022). The polysaccharides found in bone (glycosaminoglycans and hyaluronic acid) could be broken down into monosaccharides and oligosaccharides through physical and chemical reactions. These hydrolyzed products might contribute to the

formation of a dark brown material through caramelization when subjected to extreme temperatures. Food Color is an essential quality attribute in the food and bioprocess industries, which influences consumer's choice and preferences. In addition, color measurement is an objective parameter to evaluate the quality change in food processing, storage, and distribution.

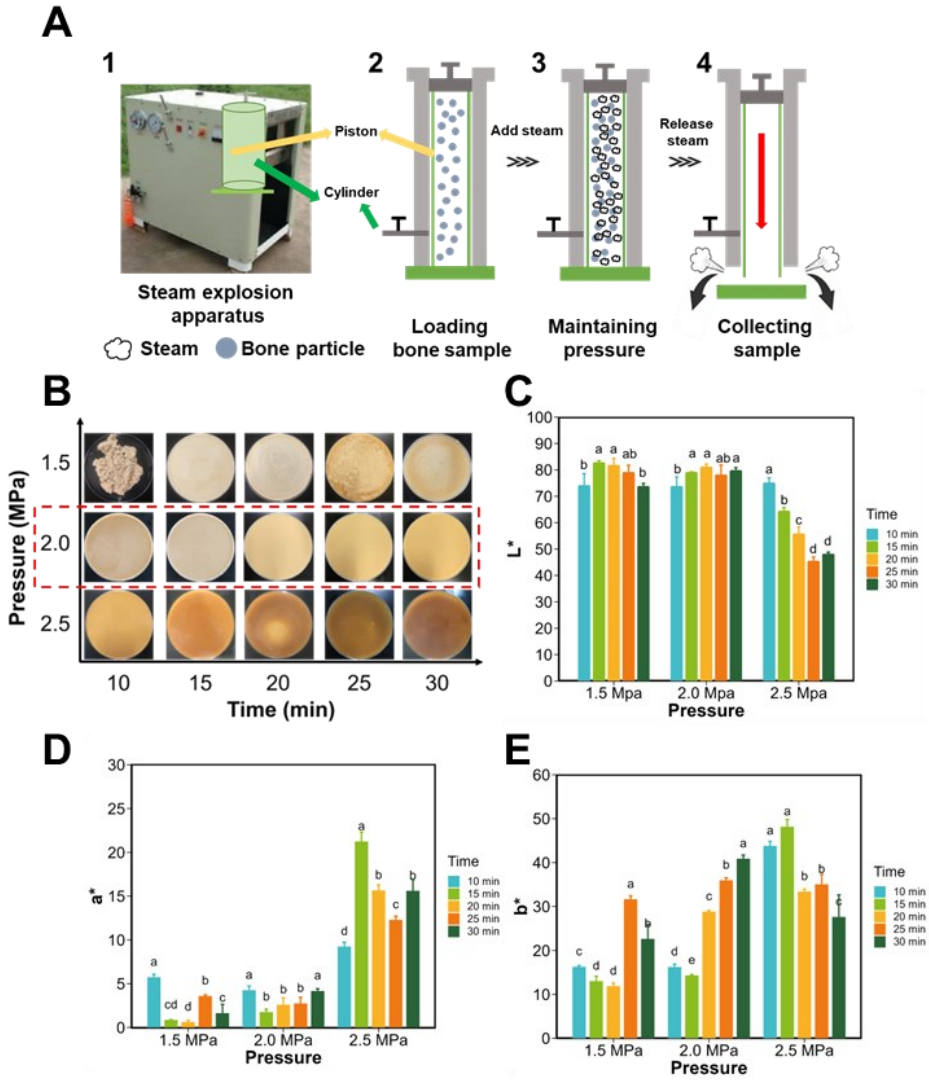

Figure 3-1: (A) Schematic representation of liquefying cattle bone by steam explosion treatment, (B) Liquefaction mixture of cattle bone, (C-E) L*, a*, and b* value of liquefied cattle bone. Duncan's test was used to evaluate the significant differences between different groups. The different letters mean a significant difference between the two groups.

3.3.2. Calcium and phosphorus release rate

Bone is a complex cellular tissue that contains, by weight, approximately 70% mineral and 30% organic constituent (Vannucci et al., 2018). Calcium and phosphorus are the most abundant minerals in bone. To extract high-purity peptides, desalination is an important step in the processing of peptides preparation. Therefore, the calcium and phosphorus release rates are essential for the application of SE. As shown in Figure 3-2, with the increase of pressure and reaction time, calcium and phosphorus release rates improved significantly ($P < 0.05$). At 2.0 MPa and 2.5 MPa, no significant difference was observed in the calcium release rate between 25 min and 30 min. Compared with 2.0 MPa, the calcium release rate of 2.5 MPa showed an improvement. However, the difference did not reach a statistically significant level. The phosphorus release regulation was similar with that of calcium release. However, the phosphorus release rate between 25 min and 30 min showed significant difference ($P < 0.05$) at 1.5 MPa, 2.0 MPa, and 2.5 MPa. At 2.5 MPa–30 min, calcium and phosphorus release rates reached up to the maximum 0.258% and 0.259%, respectively. Calcium and phosphorus mainly existed in the stable structure of hydroxyapatite, which was embedded in collagen matrix, and was extremely hard to damage (Olszta et al., 2007). During the SE process, cattle bone was subjected to high-pressure saturated steam, and the structure of biomass was destroyed and decomposed by mechanical shear caused by steam heating accompanied by sudden release of pressure. SE destructed the network structure formed by the organic matter, resulting in the inorganic matter release. The apparent solubility of hydroxyapatite increased with increasing temperature in the wet-chemical synthesis route of Ca(OH)2 and H3PO4 (Prakash et al., 2006). At the action of high temperature and mechanical destruction, calcium and phosphorus were released from bone. The results were in agreement with a previous study that SE promoted the release of minerals from cattle bones (Qin et al., 2021). Meanwhile, the mineral release rate was low, and did not negatively impact protein purity. The protein purity was from 88.6 g/100g to 90.2 g/100 g.

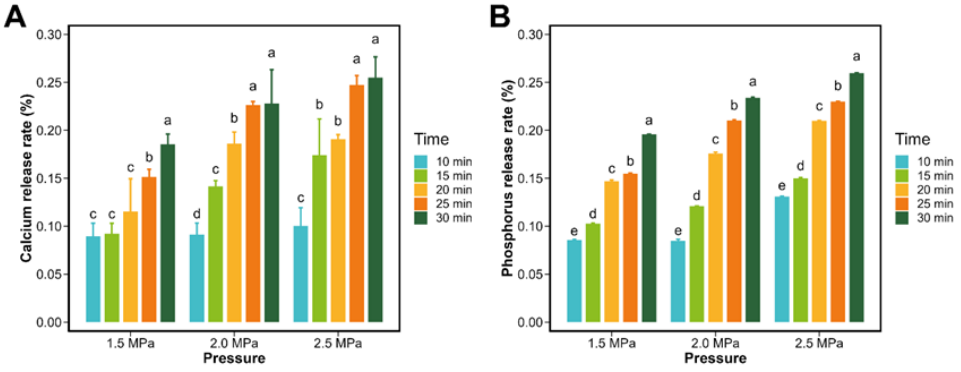

Figure 3-2: Mineral release rate under different steam explosion treatments. (A) Calcium release rate, (B) Phosphorus release rate. Duncan's test was used to evaluate the significant differences between different groups. The different letters mean a significant difference between the two groups.

3.3.3. Protein recovery rate

To evaluate the effects of SE on the extraction efficiency, the protein recovery rate was analyzed. As shown in Figure 3-3A, the protein recovery rate gradually improved with the increase of pressure and reaction time. However, at short reaction times (10–20 min), the protein recovery rates were found to be low (< 45%) and there was no significant difference observed between the treatments. The protein recovery rate showed a significant improvement when the reaction time was extended to 30 min, compared with the shorter reaction times. The protein recovery rate reached up to 60.5% and 62.5% at 2.0 MPa–30 min and 2.5 MPa–30 min, respectively. A previous study indicated a similar result that SE could enhance the protein release from cattle bone (Zhang et al., 2020). SE treatment might disrupt the bone structure formed by the tight association of protein and hydroxyapatite, open the superhelix structure of collagen, and thus produce more soluble protein. Dong et al., (2019) extracted protein from chicken bone by ultrasound-assisted enzymatic hydrolysis with a highest yield of 56.49 ± 0.67%. Hou et al., (2011) prepared protein hydrolysates from Alaska pollock frame by enzymatic hydrolysis with the nitrogen recovery of 76.89%. The result of our study did not show superior protein recovery rate. The main reason might be the sample loss due to sample sputtering. Protein recovery rate could increase if collection equipment was effectively improved. Interestingly, the advantage of SE was that it is not necessary to use any chemical reagents and enzymes to extract peptides.

3.3.4. Molecular mass distribution

Ingestion of collagen peptides has been demonstrated to exert multiple biological activities. Low molecular weight peptides are preferred over larger peptides and parent proteins due to the better bioavailability. Therefore, the molecular weight is an essential parameter to evaluate the bioactivity of peptides, reflecting the hydrolysis of proteins (Chen & Chi, 2012). As shown in Figure 3-3B–D, with increasing reaction time, the relative content of peptides < 1000 Da went up, while the relative content of peptides > 5000 Da declined. At 2.0 MPa, the relative content of the peptides (< 1000 Da) increased from 27.0% to 39.5%. At 2.5 MPa, it increased from 38.5% to 48.7%. With the increase of SE pressure, the molecular weight of peptides also presented the decreased trend. The relative content of < 1000 Da of 2.5 MPa–30 min significantly increased compared with those of 1.5 MPa–30 min and 2.0 MPa–30 min. The relative content of the peptides (< 1000 Da) was more than 40% when the SE condition over 2.5 MPa–10 min. At 2.5 MPa–25 min, the relative content of peptides < 1000 Da reached to the maximum 50.5%. The main reason might be that SE could break peptide bonds resulting in a considerable amount of peptides and free amino acids to be dissolved in water (Tonin et al., 2006). Hot pressure destabilized the hydrogen bonds and other interactions that stabilized the triple helix of collagen, leading to the release of peptides from protein (Yue et al., 2017). During the SE process, in addition to the mechanical disruption to cattle bones caused by the instantaneous release of steam, the incidental hot pressure (associated with SE) could also cause protein degradation. Based on the above research results, considering the low protein recovery rate (< 47.3%) at 1.5 MPa and the produced unpleasant color of brownish yellow at 2.5 MPa, the SE pressure condition was chosen as 2.0 MPa for the follow-up studies.

It is well known that 90% of the organic component of bone is collagen type I (Ferraro et al., 2017; Oxlund et al., 1996; Termine et al., 1981). Collagen has the strict glycine -X-Y repeating amino acid sequence, where X and Y can be almost any amino acid, but are frequently proline and hydroxyproline, respectively (Long et al., 1993). Collagen has the characteristic amino acid sequence that the presence of glycine as every third residue along the polypeptide chain and a high proportion of glycine (Doyle et al., 1975). The glycine content of collagen was about 30%. In our study, the glycine content was 28.5%, which was similar with the previous studies. The protein purity of the extraction was from 88.6 g/100 g to 90.2 g/100 g. The relative content of < 1000 Da of the extraction was 50.5% at 2.0 MPa–25 min. Meanwhile, we compared the amino acid composition of 2.0 MPa–30 min with that of commercially available collagen peptides and no significant difference was observed (Figure 3-6B). Therefore, we believe that the extracted peptides can be considered as collagen peptides.

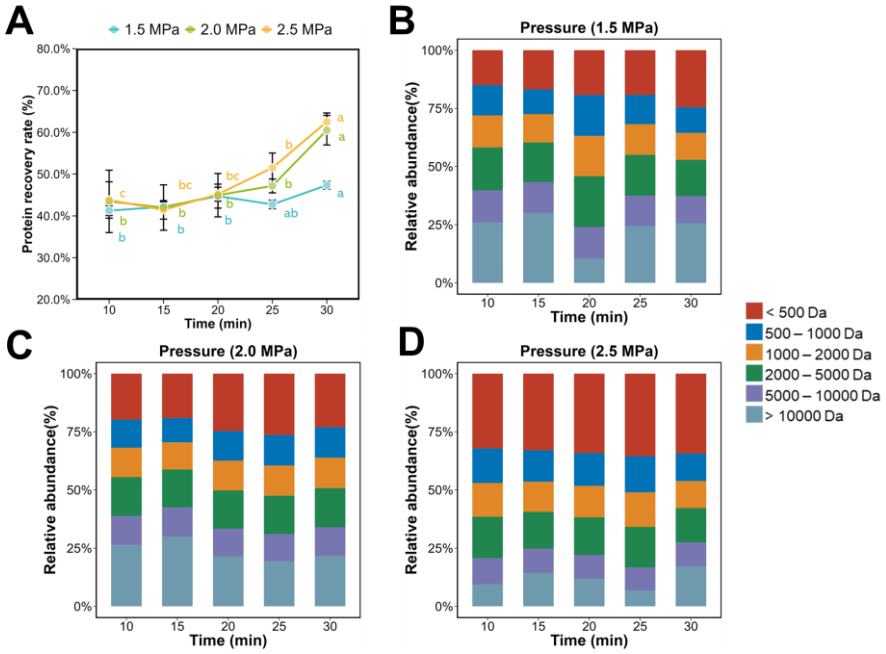

Figure 3-3 (A) Protein recovery rate under different steam explosion treatments, (B) Molecular mass distribution of collagen peptides under 1.5 MPa, (C) Molecular mass distribution of collagen peptides under 2.0 MPa, (D) Molecular mass distribution of collagen peptides under 2.5 MPa. Duncan's test was used to evaluate the significant differences between different groups. Letters of the same color represent the same pressure condition. The different letters mean a significant difference between the two groups.

3.3.5. Particle size and microstructure

The particle size reflected the degree of bone destruction by SE and thus affected protein recovery rate. As shown in Figure 3-4A, the particle size decreased significantly with the prolongation of SE time ($P < 0.05$). At 2.0 MPa–30 min

treatment, the particle size reduced to 7.45 µm. No significant difference was observed in particle size between 2.0 MPa–20 min and 2.0 MPa–30 min. The previous study found a similar result that the application of SE obviously reduced the particle size of tuna bones, leading to a narrow range of size distribution (Wan et al., 2022). In bone matrix, the mineral phase provides the stiffness, and the collagen fibers provide the ductility and ability to absorb energy (Viguet-Carrin et al., 2006). In SE process, high temperature steam induced collagen modification and disrupt the dense and ordered network, making bones brittle. At pressure, the steam penetrated the voids of the bone. At the moment of pressure release, most of the steam in the biomass would quickly expand, and ultimately the internal structure of the biomass was disrupted by a mechanical shearing force (Zhao et al., 2012). The increased pressure and reaction time led more steam to penetrate the voids of the bone, and the huge pressure differential produced mechanical destruction, which caused the formation of particles.

To investigate the effects of SE on the bone microstructure, the bone sample (after SE) were chosen randomly to observe the microstructure by SEM in Figure 3-4B. The results indicated the microporous structure of bone changed significantly. The microstructure of raw bone showed small aperture and circular structured shape. After the SE treatment, the microstructure presented obvious changes. With the extension of reaction time, the microstructure suffered varying degrees of damage. At the 10 min treatment, part of the structure was destroyed forming the large-size pores, while several native pores remained. At the 20 min and 30 min treatments, the damage intensified to bone, and the large-size pores replaced native pores. The compact structure of bone was destroyed and cracked after SE, which was dependent on the huge shear force destroyed by SE, resulting in the mechanical fracture of bone. This mechanical destruction could be due to various factors such as the pressure differential and raw material properties. A previous study found similar results that at the weak SE treatment of 0.5 MPa–30 s and 1.0 MPa–30 s, the internal structure of okara was relatively complete. As SE time increased to (1.5–2.0 MPa for 30–120 s), the inside structure was gradually destroyed to some small particles (Li et al., 2019). The similar structure destroyed by SE was found in corn stover (Zhao & Chen, 2013), radix astragali (Sui & Chen, 2014), and rapeseed (Wang et al., 2021).

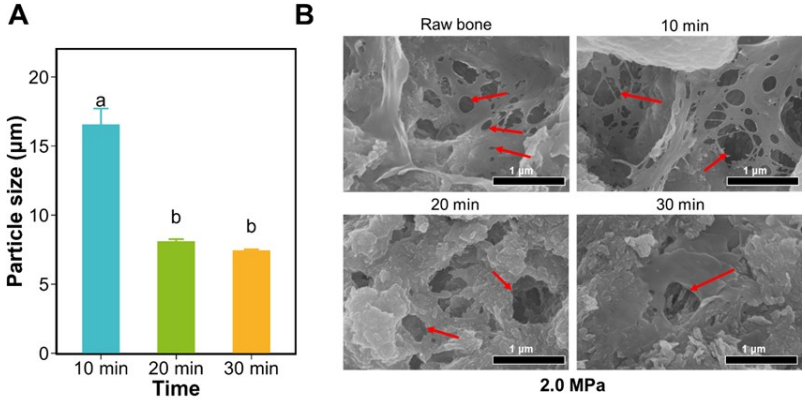

Figure 3-4 (A) Particle size of cattle bone powder treated by steam explosion, (B) Scanning

electron microscope images of cattle bone powder treated by steam explosion. Duncan's test was used to evaluate the significant differences between different groups. The different letters mean a significant difference between the two groups.

3.3.6. Fourier Transform infrared spectroscopy analysis (FT-IR)

As shown in Figure 3-5, there were distinct differences between the spectrum of raw bone and the treated bones (2.0 MPa–10 min, 2.0 MPa–20 min, and 2.0 MPa–30 min). No significant difference was observed in spectra among 2.0 MPa–10 min, 2.0 MPa–20 min, and 2.0 MPa–30 min. Take 2.0 MPa–30 min as an example, the bands of amide I and amide II were presented at 1545.33 and 1656.44 cm^{-1}, respectively, which were the characteristic peaks of collagen. The peak at 1656.44 cm^{-1} was associated with the stretching vibration peak of the C=O group, which was related to the secondary structure changes of the protein. The peak at 1545.33 cm^{-1} was associated with absorption peaks of N-H bending vibrations and C-N stretching vibrations, which represented the presence of hydrogen bonding structures in the triple helix structure of bone collagen. Peaks at 2853.94 cm^{-1} and 2925.21 cm^{-1} were assigned to the absorption of C–H bond, which indicated the presence of organic material. The bands at 1033.67 cm^{-1}, 961.97 cm^{-1}, 603.56 cm^{-1}, and 564.01 cm^{-1} were the characteristic peaks of hydroxyapatite (HAP) (Bonadio et al., 2013). The band observed at 564.01 cm^{-1} indicated the n4 symmetric P–O stretching vibration of a PO4 group. The band observed at 1033.67 cm^{-1} corresponded to the stretching mode of PO4 vibration (Cui et al., 2021). There was no significant difference in the peak positions of HAP among raw bone and treated bones, which indicated SE had no significant effects on the chemical structure of HAP. The peak at 961.97 cm^{-1} was not clear in the spectrum of the raw bone, but was clearly observed in samples treated by SE. Compared with raw bone, the peaks of 600.05 cm^{-1}, and 560.19 cm^{-1} were more obvious in 2.0 MPa–10 min, 2.0 MPa–20 min, and 2.0 MPa–30 min. The main reason might be the cross-linking structure of collagen and HAP in the raw bone, which was destroyed by SE, leading the HAP purity increased. A previous study reported the similar result that the treated bone (thermal decomposition, subcritical water, and alkaline hydrothermal processes) showed obvious HAP peaks (from 500 to 1100 cm^{-1}), and no obvious peaks in the raw cattle bone (Barakat et al., 2009). The FT-IR spectrum suggested that SE can effectively destroy the structure of bone and cause organic matter loss from cattle bone. SE could be used as a method to extract HAP and collagen peptides from livestock and poultry bones.

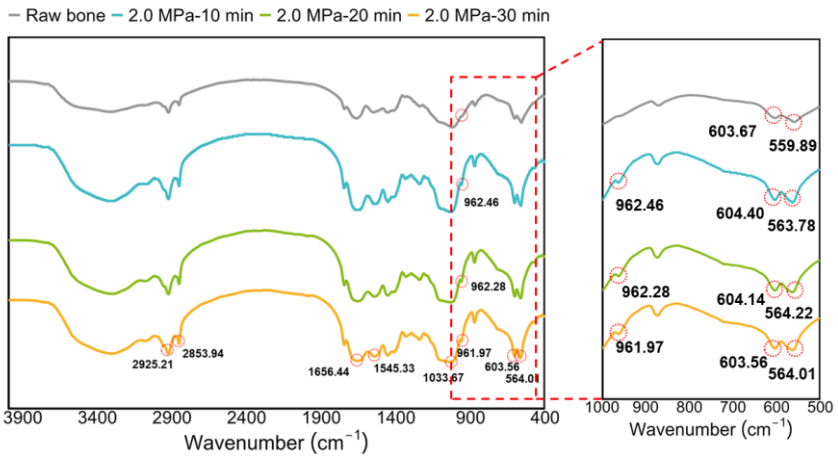

Figure 3-5 FT-IR spectrum of cattle bone powder (after steam explosion).

3.3.7. Amino acid composition

To elucidate the effects of SE treatment on peptides characteristics, the amino acid composition was analyzed (Figure 3-6A). As the result showed, the contents of main amino acids were similar among different samples. There was no significant difference among the samples of 2.0 MPa–10 min, 2.0 MPa–20 min, 2.0 MPa–30 min. The dominant amino acid of all the samples were Gly, Glu, and Ala, followed by Arg and Asp. Take the sample of 2.0 MPa–30 min as an example, Glu is the most important component for the flavor formation, which gives a specific umami taste in the formation of sodium salt. Ala is a type of amino acid that plays a role in gelatin viscosity (Cui et al., 2021). The proline in the collagen peptide sequence might also contribute to the bioactivity of peptides (Andrushchenko et al., 2006). The glycine content of extracted peptides was 28.5%. Meanwhile, the amino acid composition between 2.0 MPa–30 min and commercial collagen peptides did not show obvious difference. Taken together, SE method could be a potential treatment method to extract collagen peptides, with no effects on amino acid composition.

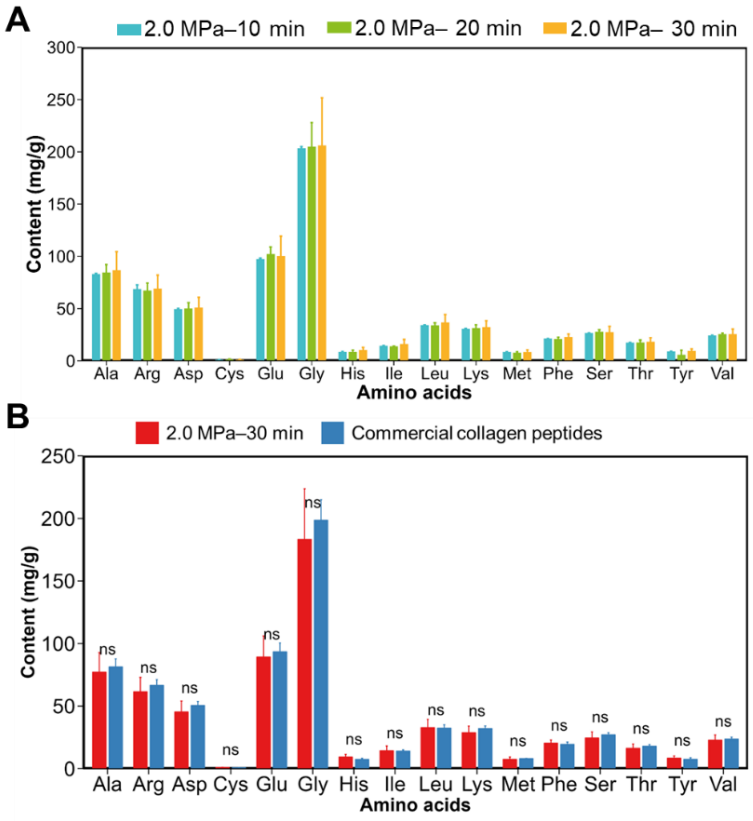

Figure 3-6 (A) Amino acids content of three kinds of collagen peptides produced by steam explosion, (B) Amino acids content of two kinds of collagen peptides from steam explosion method and commercial product.

3.4. Conclusions

This study investigated the application of SE method to extract collagen peptides from cattle bone. With the increase of pressure and reaction time, the protein recovery rate improved, and reached to 62.5% at 2.5 MPa–30 min. SE method significantly decreased the molecular weight determination of collagen peptides ($P < 0.05$). At 2.5 MPa–25 min, the relative content of peptides < 1000 Da reached up to the maximum of 50.5%. Particle size analysis and SEM images indicated that SE decreased the particle size of cattle bone powder and destroyed microstructure resulting in large size pores. FT-IR analysis showed that SE induced distinct characteristic peaks of hydroxyapatite in cattle bone powder. Amino acid analysis indicated SE could not change the amino acid composition of collagen peptides.

4

Chapter IV. Preparation of cattle bone collagen peptides-calcium chelate and its structural characterization and stability

Adapt from:

Zhang, H., Zhao, L., Shen, Q., Qi, L., & Richel, A. (2021). Preparation of cattle bone collagen peptides-calcium chelate and its structural characterization and stability. LWT- Food Science and Technology, 144(12), 111264. https://doi.org/10.1016/j.lwt.2021.111264

Abstract: In this study, cattle bone collagen peptides (CPs) were applied to prepare peptides-calcium chelate (CPs-Ca), and the physicochemical, structural properties, and stability of the CPs-Ca were characterized. The optimized preparation conditions were determined by single factor test, and the maximum calcium-chelating capacity was 42.70 ± 1.09 μg/mg. Physicochemical analysis indicated that CPs-Ca was a new substance compared with CPs. Structural analysis demonstrated that calcium ions chelated CPs via the sites of carboxyl oxygen, hydroxyl oxygen and amino nitrogen atom. Morphology analysis showed that CPs-Ca aggregated to large particles due to the crosslinking of calcium ions. According to the stability analysis, CPs-Ca was stable in thermal processing and gastrointestinal digestion. The acid environment was the major factor of CPs-Ca dissociation. The findings put forward a scientific basis for preparing a novel calcium supplement and high-value utilization of cattle bone.

Keywords: cattle bone collagen peptides, peptides-calcium chelate, physicochemical properties, structural characterizations, stability

4.1. Introduction

Calcium, one of the most abundant inorganic elements in human body, accounts for 1.5%–2.2% of the body weight. It is mainly distributed in the bone (about 99%) and plays a vital role in a wide range of physiological activities, such as neurotransmission, immune response, and cellular proliferation (Barboza et al., 2015; Peacock, 2010). Calcium deficiency could cause many diseases, such as osteoporosis, intestine cancer, and hypertension (Osborne et al., 2009). Currently, the calcium recommended daily allowance (RDA) ranges from 700 to 1200 mg (Hou, Liu, Guo, Li, & He, 2017). However, recent data collected from 74 countries revealed that many countries in Asia, Africa, and South America had low calcium intake less than 700 mg/day (Balk et al., 2017). Meanwhile, human body can enhance calcium storage in bone by the only source of dietary intake. Dietary intake has long been the most effective way to increase calcium levels in humans. Therefore, adequate oral calcium intake is profoundly important to remain health benefits.

Calcium carbonate is an extensive calcium supplement in the market, which is absorbed in the form of ionized calcium. However, ionized calcium is hard to be absorbed due to the formation of insoluble calcium deposition, resulted from some dietary factors (such as oxalate and phytic acid) in a basic intestine environment, which leads to low calcium absorption and utilization (Vavrusova & Skibsted, 2014). Furthermore, excessive intake of calcium carbonate may cause gastrointestinal side effects, such as constipation, gas, flatulence, and bloating (Straub & D., 2007). Therefore, it is very important to enhance calcium absorption by overcoming the disadvantageous factors in the digestive system. Peptides-calcium chelate has been considered as a potential dietary calcium supplement, due to its advantage in promoting calcium absorption. Recent paper reported that calcium can chelate peptides to reinforce intestinal calcium absorption by preventing calcium precipitation in the intestinal tract (Sun et al., 2020). Chelated calcium could overcome two of the major limitations of ionized calcium: (1) biological toxicity at high levels, (2) low absorption and bioavailability at low concentrations (Felix, Bronner, Danielle, & Pansu, 1999). Some peptides derived from tilapia bone collagen, desalted duck egg white, crucian skin collagen, have been used to preparing peptides-calcium chelate for improving calcium absorption (Hou et al., 2017; Liao et al., 2020; L. Zhao et al., 2014). Cattle, one of the major livestock species, is most widely scattered in the world. However, cattle bones are normally abandoned in industrial processing due to the low value of utilization, resulting in a waste of biological resources and environmental pollution. Our previous study had confirmed that cattle collagen peptides have the biological activities of anti-osteoporosis, osteoblast proliferation, inhibiting bone loss (J. Wang et al., 2020; Ye, Zhang, Jia, et al., 2020a). which revealed that cattle bones could be a good source of natural functional active ingredient. Therefore, cattle bone collagen peptides aroused our interest as a potential peptides source for achieving highly efficient calcium absorption. Recent studies have explored the utilization of peptides derived from livestock bone to prepare calcium supplement, such as pig bone and sheep bone (Wang et al., 2020; Wu et al., 2019). The pig bone collagen peptides-calcium chelate was prepared with a calcium chelating rate of 78.38%. The results of Caco-2 cell monolayer model experiment indicated that the chelate could markedly

enhance calcium transport and overcome the negative influence of phosphate and phytate. However, studies on the preparation and structural characterization of peptides-calcium chelate derived from cattle bone have hardly been reported. It combines the advantages of bioactive cattle bone peptides and chelated calcium ions and would be a natural food for enhancing calcium absorption and anti-osteoporosis.

In this study, the cattle bone collagen peptides-calcium chelate (CPs-Ca) were prepared and the conditions were optimized. The physicochemical properties and structural characterization of chelate were investigated. The stability of chelate was evaluated via simulated gastrointestinal digestion *in vitro*. The findings would be beneficial for high-value utilization of collagen peptides derived from cattle bone as a potential calcium supplement with bioactive.

4.2. Materials and methods

4.2.1. Materials

Cattle bone collagen peptides were kindly provided by Hulunbuir Muyuankangtai Biotechnology Co. LTD, (Inner Mongolia province, China). The standard mixture of amino acids was purchased from Sigma (St. Louis, Mo., USA). Calcium chloride was purchased from Sinopharm Chemical Reagent Co., Ltd. Unless otherwise indicated, all the other chemical reagents were analytical grade.

4.2.2. Preparation experiment of CPs-Ca

CPs-Ca was prepared according to the method of (Wu et al., 2019) with a minor modification. In brief, CPs were dissolved in ultrapure water with the final concentration of 50 mg/mL, and then $CaCl_2$ was added with different mass ratios (peptides/$CaCl_2$, W/W) of 2/1–6/1. The above solutions were stirred at different temperatures (40–80℃). Following the calcium chelation reaction, the absolute ethanol (5 times volume of the solution) was added to the solution to remove free Ca^{2+}. Subsequently, the mixture was centrifuged at 8000 × g for 10 min and the precipitation was collected, then lyophilized at -38℃ for 12 h. The collagen peptides and collagen peptides-calcium chelate were marked as CPs and CPs-Ca, respectively.

4.2.3 UHPLC-Q-EXACTIVE MS analysis

The collagen peptides were isolated and fragmented by an ultra-high-performance liquid chromatography (UPLC) instrument coupled with an Eclipse Plus C18 100 mm × 4.6mm，5μm. Separated peptides were identified by using a mass spectrometer (Thermo Scientific，USA). The data for the peptides sequence were obtained via the MS/MS spectra and Swiss-Prot database search, which was obtained by using a MaxQuant (version 1.5.2.8, Max Planck, Germany).

4.2.4. Moisture content and water activity

The moisture content of sample was measured by heat drying method. Briefly, the samples (1 g) were dried in laboratory oven at 103 ℃, and the post-drying weights of samples were determined when the data were within ± 3 mg. The water activities of

CPs and CPs-Ca were obtained by using a water activity meter (AquaLab, Series 4TE, USA).

$$\text{Moisture content} = 1 - \frac{\text{post-drying weight}}{\text{initial weight}}$$

4.2.5. Hydrate particle size

Samples were dissolved in ultrapure water at a final concentration of 1 mg/mL. The hydrate particle size distribution of sample was determined by dynamic light scattering (DLS) at 25 °C, using a Zetasizer NanoZS90 instrument (Malvern, UK).

4.2.6. Shear stress and shear viscosity

CPs and CPs-Ca were configured in ultrapure water with the same concentration of 10% (w/w). Then, sample solutions were dripped onto the sample plate test plate, respectively. The rheological properties of samples were obtained by using a rheometer (Discovery DHR-1, TA, USA).

4.2.7. Amino acids analysis

Total amino acid (TAA) data were detected by an L-8900 Amino Acids Automatic Analyzer (Hitachi LTD, Japan) according to the method of with a minor modification. In brief, the CP and CPs-Ca samples were transferred into hydrolysis tubes. Then 10 mL of 6 M HCl was added to each tube and mixed fully. After being filled with N_2 for 1 min to remove air, the tubes were sealed with caps and placed at 110 °C for 24 h. Then the above prepared solution was filtrated through a 0.45 μm filter membrane for subsequent amino acid analysis.

4.2.8. Molecular weight determination

The molecular weight of samples was evaluated by gel permeation chromatography following the method of (Shen et al., 2019) with some modifications. The mobile phase included 0.1% of trifluoroacetic acid, 45% of acetonitrile, and 54.9% of ultrapure water. CPs and CPs-Ca samples were solubilized in the mobile phase at a final concentration of 1 mg/mL. The injection volume of sample was set as 200 μL. The velocity of constant gradient elution was 0.5 mL/min. The standards were Gly-Sar (146 Da), Gly-Gly-Tyr-Arg (451 Da), bacitracin (1422 Da), aprotinin (6511 Da), and cytochrome C (12327 Da). The date of molecular weight of samples were evaluated under the same conditions.

4.2.9. Fourier transform-infrared spectroscopy (FT-IR), X-ray diffraction (XRD)

The FT-IR spectroscopies of CPs-Ca and CPs were observed with an FT-IR spectrometer (Tensor-27, Bruker Company, Germany). Briefly, dried sample together with KBr was extruded into a transparent sheet for the subsequent measurement in a range of 4000 − 500 cm^{-1}.

The XRD spectroscopies of CPs and CPs-Ca were determined by an X-ray diffract meter (Shimadzu, XRD-6000, Japan). The detailed experimental conditions were as

followed: scanning step size 0.02°; scanning speed 2°/min; scanning method: continuous.

4.2.10. Thermal gravimetric analysis (TGA)

The thermal properties of CPs and CPs-Ca were evaluated by a TGA (Pyris Diamond TG/DTA, PerkinElmer, USA) from 25 to 250 ℃ at 10 ℃/min in the air.

4.2.11. Scanning electron microscope (SEM) and atomic force microscopy (AFM)

The SEM Figures were applied to demonstrate the microstructure of CPs and CPs-Ca by a scanning electron microscope (Zeiss Merlin Compact, Germany). In brief, the samples (5 mg) of CPs and CPs-Ca were uniformly applied to the sample plate, sprayed with a gold plating film. Micrographs were obtained at 10 kV of accelerating voltage.

The AFM Figures of CPs-Ca and CPs were characterized by using an atomic force microscopy (Park NX 10). The liquid samples (10 mg/ml aqueous solution of CPs and CPs-Ca) were diffused on the mica surface, and the scanning images (5 μm × 5 μm) were obtained by the tapping mode at 15 kV.

4.2.12. Stability analysis

The stability of CPs-Ca against simulated gastrointestinal digestion was evaluated according to the method of (Wu et al., 2019) with a minor modification. The CPs-Ca sample was dissolved in ultrapure water to a final concentration of 10 mg /mL, and the solution was heated for 1 h at various temperatures (50–80℃) with a consistent pH 7. The stability against gastrointestinal pH were conducted by treating 10 mg/mL of CPs-Ca solution in gastric pH (2.0) and intestinal pH (7.5) for 1 h, respectively. The stability against vitro gastrointestinal digestion was evaluated by treating 10 mg/mL of CPs-Ca solution in artificial simulation of gastric juice (pH 2.0) and intestinal juice (pH 7.5) for 1 h in a water bath at 37 ℃, respectively. The reaction was terminated by heating at 100 ℃ for 10 min. The stability of CPs-Ca was expressed as calcium retention rate in chelate after digestion.

$$\text{Calcium retention rate (\%)} = \frac{\text{Calcium content in treatment group}}{\text{Calcium content in control group}} \times 100$$

4.2.13. Statistical analysis

Data from all measurements were expressed in triplicate as the mean ± SD (standard deviation). T-test, and Duncan test was performed using the statistical programming language R (R Core Team, 2016). $P < 0.05$ was considered statistically significant.

4.3. Results and discussions

4.3.1. Identification of peptides sequence of CPs

Currently, the isolation and purification of bioactive peptides derived from

agricultural products have been received considerable interest. Meanwhile, bioinformatics has been applied to conduct bioactive peptides research, and is regarded as an effective method to evaluate new peptides (Sánchez-Rivera, Martínez-Maqueda, Cruz-Huerta, Miralles, & Recio, 2014). In this study, in order to identify the sequences of peptides, the CPs were applied to a high-resolution mass spectrometer. As shown in Table 4-1, there are 94 peptides are found in the collagen peptides. It's worth noting low molecular weight peptides (MW ≤ 1000) are the main component (64 peptides). The low molecular weight peptides could favor calcium-binding peptides (Hou et al., 2015). Among these peptides, the peptides sequences of Gly-X-Y (X and Y are usually proline and hydroxyproline) are found frequently, which is considered as the characteristic sequences of collagen. As Table 4-1 shows, the collagen peptides containing Glu (E) and Asp (D) are found in 42 peptides including AGE, SGE, TGE, ASGE, PAGE, GARGE, GQRGE, GPAGE, GEAGAQ, GKDGEAGAQ, GEGGPQGPRG, GPAGERGAPGPA, GADGAPGKDGVRG, SGLDGAKGDAGPAGPK, GDRGETGPAGPAGPIGPV, GPAGPQGPRGDKGETGEQGDRG, etc. It is consistent with previous study that the acidic amino acids of Glu and Asp are beneficial for calcium ions chelating with peptides (Sun et al., 2017), due to the oxygen atoms of carboxyl group. In the amino acid content analysis, the Asp and Glu are the main amino acid, which is in agreement with the result of peptides sequence. Hou et al., (2018) indicated the chelating site of calcium ions could possibly include the amino groups of Gln, Ile and Arg. In the result of peptides sequence, Gln, Ile and Arg are frequent, and there are 24, 16, and 52 peptides containing the 3 amino acids, respectively. These results indicate that CPs are an ideal source for preparing peptides-calcium chelate.

Table 4-1 The sequence description of cattle bone collagen peptides

No.	Sequence	Length	Mass (Da)	Source of peptide
1	GKRG	4	417.26	Collagen_alpha-1(I)_chain
2	GHRG	4	426.22	Collagen_alpha-1(I)_chain
3	GQRG	4	417.22	Collagen_alpha-1(I)_chain
4	GARG	4	360.20	Collagen_alpha-1(I)_chain
5	GKEGSKGPRGE	11	367.86	Collagen_alpha-1(I)_chain
6	AAGR	4	374.21	Collagen_alpha-1(I)_chain
7	GDTGAK	6	548.27	Collagen_alpha-1(I)_chain
8	GARGE	5	245.12	Collagen_alpha-1(I)_chain
9	GQRGE	5	547.25	Collagen_alpha-1(I)_chain
10	GKDGEAGAQ	9	416.69	Collagen_alpha-1(I)_chain
11	AGE	3	276.12	Collagen_alpha-1(I)_chain
12	AGAQ	4	346.17	Collagen_alpha-1(I)_chain
13	ASGE	4	363.15	Collagen_alpha-1(I)_chain
14	SGE	3	292.11	Collagen_alpha-1(I)_chain
15	GDRGDAGPK	9	436.71	Collagen_alpha-1(I)_chain
16	TGE	3	306.13	Collagen_alpha-1(I)_chain
17	GANGDRGE	8	388.66	Collagen_alpha-2(I)_chain
18	SGASGE	6	507.20	Collagen_alpha-1(I)_chain
19	GPAGER	6	293.65	Collagen_alpha-1(I)_chain
20	PAGE	4	373.17	Collagen_alpha-1(I)_chain
21	GEAGAQ	6	532.24	Collagen_alpha-1(I)_chain
22	AGPS	4	331.16	Collagen_alpha-1(I)_chain
23	GKEGSKGPRGETGPA	15	714.37	Collagen_alpha-1(I)_chain
24	GPQGPR	6	306.17	Collagen_alpha-1(I)_chain
25	GPRGSEGPQ	9	442.71	Collagen_alpha-1(I)_chain
26	KGNSGEPGAPGS	12	529.74	Collagen_alpha-1(I)_chain
27	AGPT	4	345.18	Collagen_alpha-1(I)_chain

28	GPAGE	5	430.19	Collagen_alpha-1(I)_chain
29	VGPR	4	214.63	Collagen_alpha-2(I)_chain
30	TGPAG	5	402.20	Collagen_alpha-1(I)_chain
31	ATGPAG	6	473.24	Collagen_alpha-2(I)_chain
32	AGPAGPR	7	313.17	Collagen_alpha-2(I)_chain
33	IAGQ	4	388.22	Collagen_alpha-1(I)_chain
34	MGPR	4	460.23	Collagen_alpha-1(I)_chain
35	GPSGPQG	7	599.28	Collagen_alpha-1(I)_chain
36	GEGGPQGPR	9	427.71	Collagen_alpha-1(I)_chain
37	DGAKGDAGPAGPK	13	380.86	Collagen_alpha-1(I)_chain
38	GEGGPQGPRGS	11	499.74	Collagen_alpha-1(I)_chain
39	GAVGPR	6	278.66	Collagen_alpha-2(I)_chain
40	GEGGPQGPRG	10	456.22	Collagen_alpha-1(I)_chain
41	VAQ	3	317.18	Collagen_alpha-1(I)_chain
42	GPAGPTGAR	9	392.21	Collagen_alpha-1(I)_chain
43	GEPGKQGPSGASGE	14	629.29	Collagen_alpha-1(I)_chain
44	GPRGDQGPVGR	11	365.86	Collagen_alpha-2(I)_chain
45	GADGAPGKDGVRG	13	578.79	Collagen_alpha-1(I)_chain
46	GPAGPQGPRGDKGETGEQGDRG	22	531.50	Collagen_alpha-1(I)_chain
47	PAGPAGPR	8	361.70	Collagen_alpha-2(I)_chain
48	GADGVAGPK	9	386.20	Collagen_alpha-1(I)_chain
49	VGPQ	4	400.22	Collagen_alpha-2(I)_chain
50	GPAGPT	6	499.25	Collagen_alpha-1(I)_chain
51	GKSGDRGETGPAGPA	15	678.83	Collagen_alpha-1(I)_chain
52	GPQGPRGSEGPQG	13	612.29	Collagen_alpha-1(I)_chain
53	GGPQGPRGSEGPQG	14	640.80	Collagen_alpha-1(I)_chain
54	GPAGPAGPRG	10	418.72	Collagen_alpha-2(I)_chain
55	GPAGPAGPR	9	390.21	Collagen_alpha-2(I)_chain
56	GPMGPR	6	307.66	Collagen_alpha-1(I)_chain
57	GEGGPQGPRGSEGPQG	16	733.83	Collagen_alpha-1(I)_chain
58	GPAGERGAPGPA	12	518.76	Collagen_alpha-1(I)_chain

59	GPVGPVGKH	9	283.16	Collagen_alpha-2(I)_chain
60	SGPMGPR	7	351.17	Collagen_alpha-1(I)_chain
61	AGPSGPAGPTGAR	13	548.28	Collagen_alpha-1(I)_chain
62	GPSGPAGKDGRIGQPG	16	484.25	Collagen_alpha-2(I)_chain
63	GFQ	3	351.17	Collagen_alpha-1(I)_chain
64	AVGPRGPSGPQG	12	540.28	Collagen_alpha-2(I)_chain
65	GPRGPAGPSGPA	12	510.76	Collagen_alpha-2(I)_chain
66	SGLDGAKGDAGPAGPK	16	466.57	Collagen_alpha-1(I)_chain
67	GAVGPRGPSGPQG	13	568.79	Collagen_alpha-2(I)_chain
68	AGPAGPAGPAGPR	13	538.29	Collagen_alpha-2(I)_chain
69	AGPAGPAGPAGPRG	14	566.80	Collagen_alpha-2(I)_chain
70	VGPAGPRGPA	10	439.75	Collagen_alpha-2(I)_chain
71	AGPAGPAGPA	10	765.39	Collagen_alpha-2(I)_chain
72	GPPGAPGAP	9	720.37	Collagen_alpha-1(I)_chain
73	SGAAGPTGPIGSR	13	564.29	Collagen_alpha-2(I)_chain
74	GPIGSA	6	501.27	Collagen_alpha-2(I)_chain
75	GARGSDGSVGPVGPA	15	642.32	Collagen_alpha-2(I)_chain
76	GPIGPVGAR	9	412.24	Collagen_alpha-1(I)_chain
77	FSGLDGAK	8	397.71	Collagen_alpha-1(I)_chain
78	GPVGPTGPVG	10	837.45	Collagen_alpha-2(I)_chain
79	GPVGPV	6	525.30	Collagen_alpha-2(I)_chain
80	GKSGDRGETGPAGPAGPIGPV	21	938.98	Collagen_alpha-1(I)_chain
81	GPVGPTGPVGAA	12	979.52	Collagen_alpha-2(I)_chain
82	GPIGPVG	7	596.34	Collagen_alpha-1(I)_chain
83	GPIGPVGA	8	667.38	Collagen_alpha-1(I)_chain
84	GPAGPIGPVG	10	821.45	Collagen_alpha-1(I)_chain
85	SGDRGETGPAGPAGPIGPV	19	846.42	Collagen_alpha-1(I)_chain
86	GDRGETGPAGPAGPIGPV	18	802.90	Collagen_alpha-1(I)_chain
87	VGPAGPNGFAGPA	13	1112.54	Collagen_alpha-2(I)_chain
88	DRGETGPAGPAGPIGPV	17	774.39	Collagen_alpha-1(I)_chain
89	FSGL	4	423.22	Collagen_alpha-1(I)_chain

90	GPAGPIGPV	9	764.43	Collagen_alpha-1(I)_chain
91	AGPAGPIGPV	10	835.47	Collagen_alpha-1(I)_chain
92	TGPAGPAGPIGPV	13	1090.59	Collagen_alpha-1(I)_chain
93	ISVPGPM	7	350.69	Collagen_alpha-1(I)_chain
94	FGFDGDFYR	9	562.25	Collagen_alpha-2(I)_chain

4.3.2. Effect of different process conditions on calcium-chelating capacity of CPs

Bone collagen peptides have been reported to be a potential source for preparing peptides-calcium chelate, such as sheep bone, pig bone, and tilapia bone collagen peptides (Liao et al., 2020; Wang et al., 2020). The different process conditions may affect the calcium-chelating capacity. In the study, the effects of temperature (℃), time (min), peptides/$CaCl_2$ (W/W) on the calcium-chelating capacity of CPs-Ca were explored. Except for the experimental variables, the process conditions were as follows: pH 7, temperature 60 ℃, time 60 min, peptides/$CaCl_2$ (W/W) 5/1. As shown in Figure 4-1A, with the increasing pH between 5–9, the calcium-chelating capacity first increases ($P < 0.05$) and then remains unchanged ($P > 0.05$). When the pH value is 7, the calcium-chelating capacity reaches to 42.7 μg/mg, resulted from the decrease of H+ concentration, thus improving the coordination between Ca^{2+} with COOH− and NH3+ (Wu et al., 2019). As Figure 4-1B shows, when the chelating time is experimented at 20–60 min, there are no significant difference. As time prolonged to 100 min, the calcium-chelating capacity decreases significantly to 37.6 mg/g, which indicates the chelation reaction is rapid and affected by reaction time. As shown in Figure 4-1C, with the rise of temperature, the calcium-chelating capacity first raises and then decreases. When the temperature is 60 ℃, the calcium-chelating capacity reaches to the maximum of 41.44 μg/mg. As the temperature increases to 80 ℃, the calcium-chelating capacity notably decreases to 38.39 μg/mg compared with that of 60 ℃ ($P < 0.05$). It may be due to the uneasy formation of chelate bonds in the excessive temperature, which is consistent with the study of (Wang et al., 2020). In Figure 4-1D, the calcium-chelating capacity increases from 34.9 to 48.67 μg/mg significantly, when the peptides/$CaCl_2$ decreases from 6/1 to 2/1. However, there are no significant differences between 3/1, 4/1, and 5/1. Considering too much $CaCl_2$ addition could introduce overmuch chloride ion to the chelate, the peptides/$CaCl_2$ is 5/1 in this study. Previous study demonstrated that the calcium-chelate rate increased, with the rising peptides/$CaCl_2$ ratio. When the ratio of peptides/$CaCl_2$ was 5/1, the calcium chelating rate of 75.43% was obtained (Wu et al., 2019). Based on the above results, the optimized preparing conditions are pH 7, temperature 60 ℃, time 60 min, peptides/ $CaCl_2$ 5/1, respectively. Under these process conditions, the calcium-chelating capacity is 42.70 ± 1.09 μg/mg in agreement with previous studies. Cui, Sun, Jiang, Wang, & Lin, (2017) have studied the calcium-chelating capacity of sea cucumber ovum hydrolysate, and the maximum calcium-chelating capacity reached to 53.45 mg/g, when the preparing conditions were as follows: mass ratio of peptides/$CaCl_2$ 3/1, temperature 50 °C, and pH 8.5. (Liao et al., 2020) isolated three novel peptides from tilapia bone collagen hydrolysate, the maximum calcium-chelating capacity reached to 28.4 ± 0.94 mg/g.

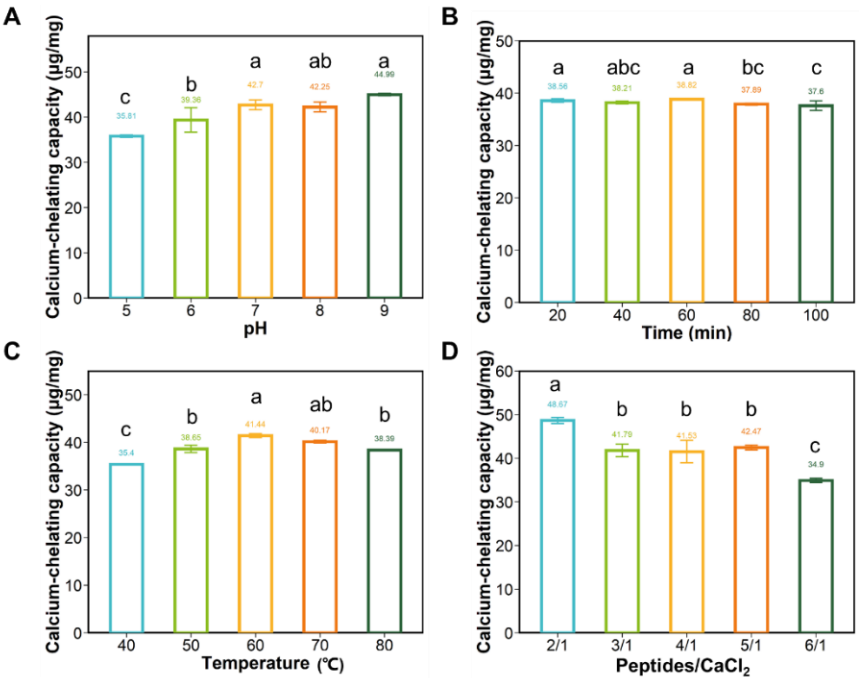

Figure 4-1 Effects of different processing conditions on calcium-binding capacity. (A) pH, (B) time, (C) temperature, (D) mass ratio of peptides/$CaCl_2$ (W/W). Duncan's test was used to evaluate the significant differences between different groups. The different letters mean the significant difference between two groups.

4.3.3. Physicochemical properties of CPs-Ca

The food qualities including physicochemical properties and sensory properties are essential standards for food acceptance, trial, and repurchase intention (Hung & Verbeke, 2018). Thus, the physicochemical properties of CPs and CPs-Ca chelate were evaluated. In Figure 4-2A, after chelating calcium, the moisture content (0.095) and water activity (0.513) of CPs-Ca chelate significantly decrease to 0.061 ($P < 0.05$) and 0.107 ($P < 0.001$), respectively. The main reason may be the fact that the aggregated spatial structure of CPs-Ca is not conducive to moisture retention.

Compared with the particle size distribution of CPs, the particle size distribution of CPs-Ca aggregates on a large size range with two peaks (Figure 4-2B). This is due to the intermolecular forces between calcium ions and peptides resulting in the particle cluster formation. As reported (Sun et al., 2017), calcium facilitated the formation of β-sheet structure and induced structural folding of peptides to form spherical nanoparticles. The results of viscosity and shear rate can demonstrate the information of solute interaction. As Figure 4-2C–D shows, the CPs-Ca sample exhibited pseudoplastic behavior. The viscosity increases with the gradual raise of shear rate. The shear stress and shear viscosity of CPs-Ca samples are higher than those of CPs

at 0–300 shear rat/s. The main reason may be the formation of crosslinking between peptides and calcium ions, resulting in mechanical performance enhancement.

Acidic amino acids (Asp and Glu) have been considered as essential amino acids to chelating calcium ions due to hydroxyl groups (Sun et al., 2020). Many food-derived peptides-calcium chelate has been found to contain Asp or Glu, such as FDHIVY, YQEPVIAPKL, and SSSEE (Liao et al., 2020) To study the potential mechanism of calcium chelating peptides, the amino acid contents of CPs and CPs-Ca were obtained. After chelating calcium, the contents of Asp and Glu increase significantly ($P < 0.05$) (Figure 4-2E). The contents of Ala, Gly, Ile, Leu, Met, Phe, Thr, and Val in CPs-Ca are obviously lower than that in CPs ($P < 0.05$). Among these amino acids, Met and Thr are polar uncharged amino acids, and the other amino acids are nonpolar amino acids. The results indicate nonpolar amino acids and polar neutral amino acids are not helpful to form peptides-calcium chelate. Recent studies reported the amino group of the Lys side chain and the carboxyl of the Glu side chain could be the calcium-binding sites (Hou et al., 2018). The main reason may be the isolated electron pair in the oxygen and nitrogen. However, in the present study, after chelating calcium, the contents of Lys raise weakly ($P > 0.05$). It may be due to the higher calcium-chelating capacity of carboxylate compared with that of amino group. The above results are consistent with previous studies that reported that the hydroxyl groups of Asp and Glu were the major chelating sites for peptides-calcium chelate (Cui et al., 2019).

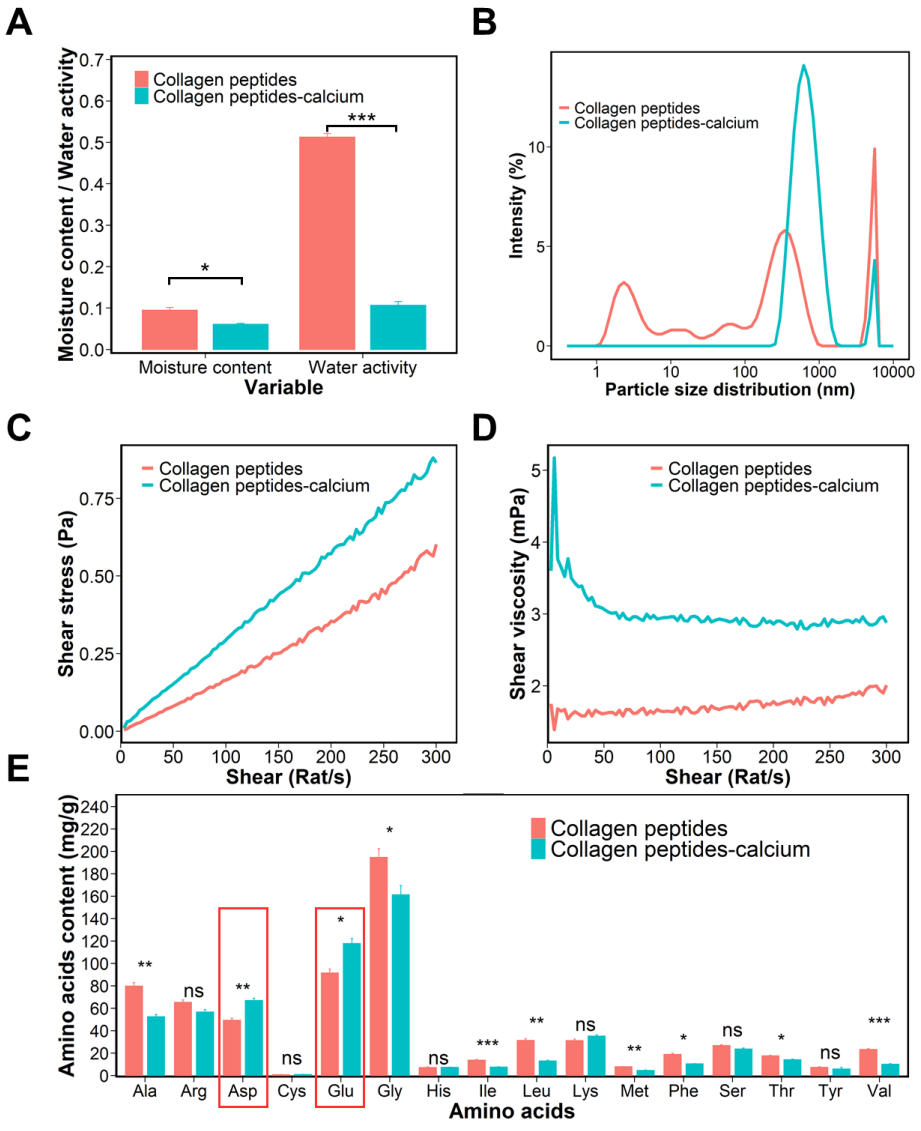

Figure 4-2 Physicochemical properties of CPs-Ca and CPs. (A) moisture content and water activity, (B) particle size distribution, (C) shear stress, (D) shear viscosity (E) amino acids content. The statistical method is t-Test. The symbols indicate statistical significance: ns: P > 0.05, *: P <= 0.05, **: P <= 0.01, ***: P <= 0.001.

4.3.4. Structural characterizations of CPs-Ca

4.3.4.1. Molecular mass distribution analysis

As shown in Figure 4-3A, after chelating calcium, the molecular mass of CPs distributes < 500 Da of CPs decreases from 54.4% to 41.9% ($P < 0.05$). Meanwhile, the molecular mass 500–1000 Da decreases from 24.0 to 18.1% ($P < 0.05$). On the contrary, the molecular masses distribute 2000–3000 Da, 3000–5000 Da, > 5000 Da all raise. The major reason may be the new forming chelate bonds between calcium ions and peptides, which could crosslink peptides to form large molecular mass. This is in agreement with the information of hydrate particle size in Figure 4-2B.

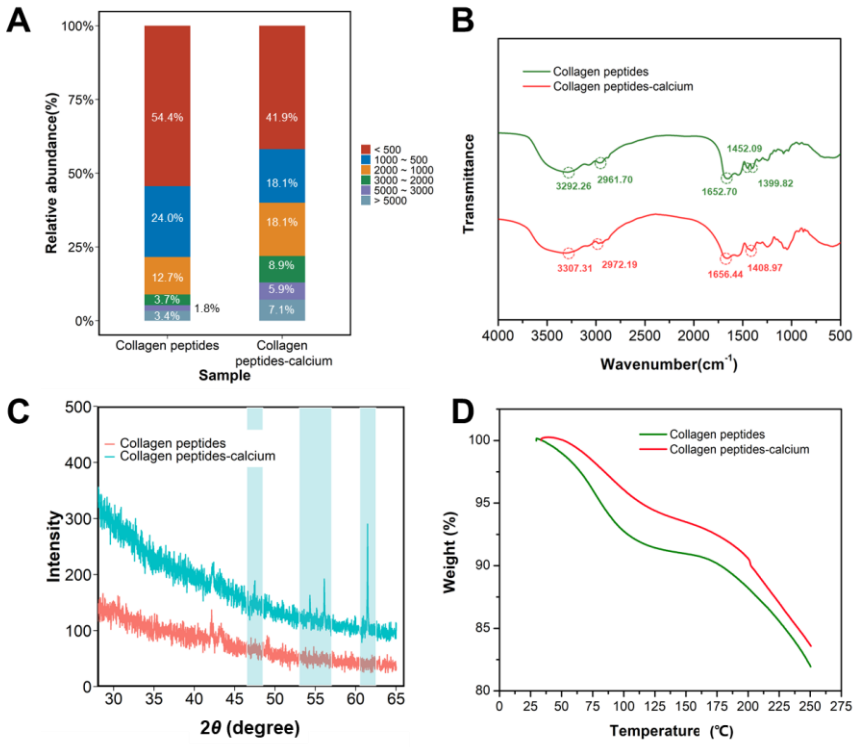

Figure 4-3 Structural characterization of CPs-Ca and CPs. (A) molecular mass distribution, (B) FT-IR spectra in the regions from 4000 to 500 cm^{-1}, (C) XRD spectra, (D) TGA.

4.3.4.2. FT-IR analysis

The characteristic change of FTIR absorption peak is widely used to reflect the chemical structure of sample. Especially, the application in the interactions between metal ions and organic ligand groups in peptides is extensive (Wang et al., 2020; Zhang et al., 2018). As shown in Figure 4-3B, the FTIR spectrum changed after calcium-binding to peptides. The wavenumber shifted from 3292.26 to 3307.31 cm^{-1},

which might be attributed to a stretch and hydrogen bonds replaced in the CPs-Ca, indicating that O-H and N-H also contribute to the formation of the chelate due to dipole field effect or induction effect. The vibrational spectral region of 1700–1500 cm^{-1} corresponds to stretching vibration of amide I (1700–1600 cm^{-1}; C=O) and amide II (1580–1510 cm^{-1}; C-N, N-H) (Chen, Cheng, Li, Yang, & Lin, 2005). In this FTIR spectra, the peak of the amide-I band (C=O stretching vibration) changed from 1652.70 to 1656.44 cm^{-1}, which was relevant with the stretching vibrations of the carbonyl group (C=O) in the amide bond (peptide bond). These results indicated the carboxylate group was involved in the formation of CPs-Ca chelate, corresponding to the results of previous study (Wang et al., 2020). Meanwhile, the vibrational spectral region of 1430–1370 cm^{-1} is related to the stretching vibration of the carboxylate group (-COO-). After chelating calcium, the peak of FTIR spectra changes from 1399.82 to 1408.97 cm^{-1}, suggesting that -COO- might bind calcium, and turn to –COO–Ca (Sun et al., 2020). Based on the above results, it is speculated that the binding sites of peptides with calcium include carboxyl oxygen, hydroxyl oxygen and amino nitrogen atom, which is consistent with previous studies (Wang et al., 2018; Yang et al., 2021).

4.3.4.3. XRD analysis

X-ray spectra can reflect the formation of complexes between organic ligands with metal ions, including the appearance, shifting, and disappearance. This analysis method has been widely applied to indicate the reaction between peptides and calcium. As shown in Figure 4-3C, there is a weak diffraction peak in the X-ray spectroscopy of CPs, suggesting that the CPs present a random amorphous structure. After peptides chelating with calcium, the spectroscopy of CPs-Ca has significantly changed. There are two strong and sharp diffraction peaks, indicating that forming the new ordered crystal structure. This phenomenon demonstrates that the scattering intensity is drastically increased due to chain associations and formation of junction zones. Previous study had similar results that the CPs-Ca was a different substance from CPs with new crystalline structure (L. Wang et al., 2018).

4.3.4.4. TGA analysis

As seen in Figure 4-3D, the weight of CPs declines rapidly with the increasing temperature of 25–125 ℃. In comparison, the weight of CPs-Ca demonstrates a relative gentle decline at the temperature of 25–125 ℃. The result indicates that chelating calcium could enhance the thermal stability of CPs. The main reason may be that the coordinate bonds between CPs and calcium ions, so breaking the chemical bonds needs more energy. These results indicate that CPs-Ca is a more stable substance compared to CPs.

4.3.4.5. Morphology analysis of CPs-Ca

SEM is mainly used to analyze microstructure in materials, such as medical, biology, and food processing, etc. Therefore, SEM was applied to evaluate the microstructure of CPs and CPs-Ca. As shown in Figure 4-4 (A3 and B3), the surface of CPs is smooth. In comparison, the surface of CPs-Ca was rough with many granular aggregates. The major reason could be the changes in internal structure due to coordinate bonds between peptides and calcium ions, resulting in the compact structure of CPs-Ca

(Wang et al., 2020). In addition, the energy dispersive spectrometer (EDS) was used to evaluate the internal element distribution of CPs and CPs-Ca in more detail, as shown in Figure 4-4 (A1 and B1). The EDS spectra of CPs and CPs-Ca show remarkable peaks for carbon, nitrogen, oxygen, sodium, chlorine, sulfur, and calcium. The CPs sample basically does not contain calcium (0.09%), and the Ca signal strength of CPs-Ca (3.86%) is higher than that of CPs, which is consistent with the result of previous studies (Sun et al., 2020; Yang et al., 2021). As Figure 4-4A2 and B2 show the element mapping images of CPs and CPs-Ca, respectively. A weak signal of calcium of CPs, and the image of CPs-Ca shows strong signal strength of calcium. Based on the above results, the SEM analysis demonstrates that CPs-Ca has granular aggregates. The EDS results indicate that the high calcium-chelating capacity between peptides and calcium ions.

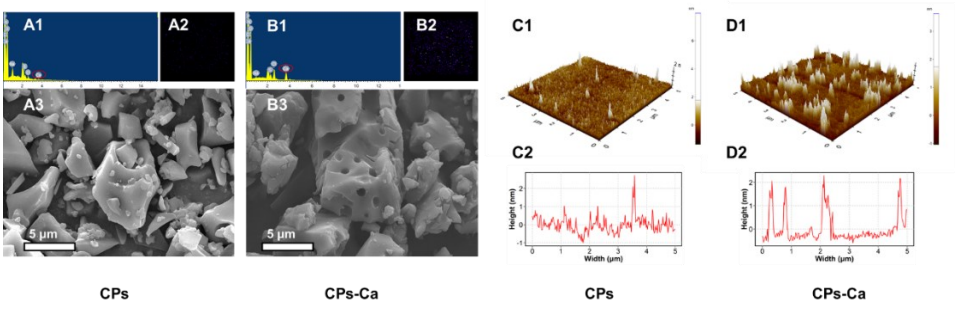

Figure 4-4 Microstructure of CPs-Ca and CPs. (A1, B1) EDS images, (A2, B2) element mapping images, (A3, B3) SEM images, (C1, D1) AFM images, (C2, D2) AFM height distribution curves.

The surface morphology of CPs-Ca and CPs were also evaluated by AFM, as shown in Figure 4-4 (C and D). The AFM image of CPs-Ca shows blocky aggregates, mainly due to the intermolecular aggregation generated by the sulfhydryl group, carboxyl group, and amino group in collagen peptides (Lin et al., 2015). As Figure 4-C1 and C2 shows, the surface peaks of CPs-Ca are clearly larger and denser than those of CPs. As shown in Figure 4-4 (C2 and D2), the height of peaks of CPs-Ca doesn't significantly increase after calcium chelating. However, the curve of CPs-Ca shows obviously several large wave peaks. In comparison, the curve of CPs shows many small wave peaks. These results indicate that the CPs-Ca with a remarkable aggregation in the atomic microstructure.

4.3.5. Stability of CPs-Ca

In the gastrointestinal environment, the unfavorable factors (H+ and protease) could induce calcium release to produce insoluble precipitation and Ca $(OH)_2$, leading to low bioavailability of calcium. Therefore, it is significant to study the stability of CPs-Ca in different environments. In this study, the calcium retention rates of CPs-Ca against the temperature and gastrointestinal environment were studied to assess its

stability. According to Figure 4-5A, with the increase of temperature from 50–80 ℃, there are not a significant difference in different heating treatments, which indicates that CPs-Ca is stable in high temperature. This result is consistent with previous study that the chelate has great resistance against thermal processing (W. Wu et al., 2019).

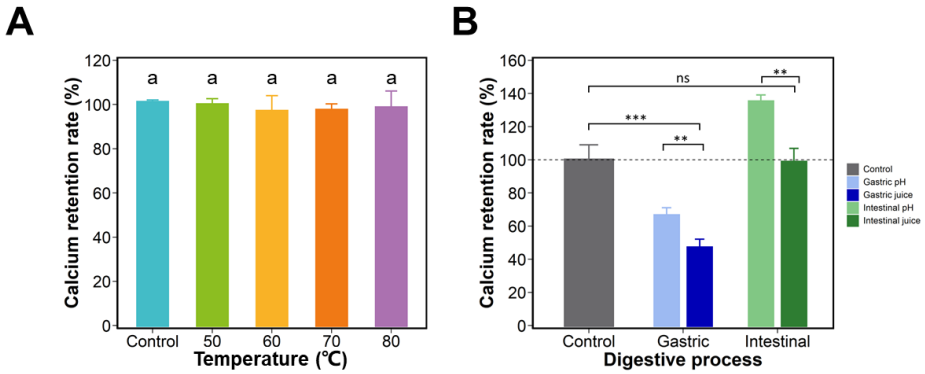

Figure 4-5 Stability of CPs-Ca. (A) stability of chelate at various incubation temperature, (B) stability of chelate at various digestive processes. Duncan's test was used to evaluate the significant differences between different groups in Figure 4-5A. The groups containing the same letter are not significant differences. The statistical method is t-Test in Figure 4-5B. The symbols indicate statistical significance: ns: $P > 0.05$, *: $P <= 0.05$, **: $P <= 0.01$, ***: $P <= 0.001$.

In Figure 4-5B, the stability of CPs-Ca in the gastrointestinal was studied. To study the effect of gastrointestinal pH value on the stability of CPs-Ca, the gastric pH (2.0) and intestinal pH (7.5) were selected as the experimental conditions. The calcium retention rate in intestinal pH shows 2 times that in gastric pH and there is a significant difference ($P < 0.05$). It's worth noting that the calcium retention rate in intestinal pH is higher than that in control (> 100%). These results may be due to that the high H+ concentration in gastric environment could compete with calcium ions for active binding groups, which leads the calcium ion release in the control. However, in the intestinal pH, the alkaline environment not only inhibits the calcium ion release from CPs-Ca, but also promote the rechelation between peptides and Ca^{2+}. Thus, the calcium retention rate in intestinal pH shows higher than that in control (> 100%). After adding protease digestion (pepsin and intestine protease), the calcium retention rates of CPs-Ca in gastric juice and intestinal juice compared with control, decrease to 46.9% ($P < 0.05$) and 98.5% ($P > 0.05$), respectively. Meanwhile, the calcium retention rate of CPs-Ca with gastric juice is lower than that of intestinal juice ($P < 0.05$), which reveals that the gastric environment is the main place for releasing calcium ions. Meanwhile, after adding protease, the calcium retention rates significantly decrease than before adding protease, respectively, which reveals that protease could induce the degradation of chelate. The main reason may be that the protease could hydrolysis polypeptides to release Ca^{2+}, except for the effect of pH. These results are in agreement with the study of (Cui et al., 2019), demonstrated that

the main reason for Ca^{2+} releasing was pH change during *in vitro* simulated gastrointestinal digestion process, and the weak alkaline condition of intestinal environment might cause rechelation of the peptides with calcium ions. Previous study showed the stability of the chelate was weakly affected by pepsin, but it was sensitive to pH (Wu et al., 2019). The results indicated that gastric digestion is the main place causing calcium release. In comparison, the intestinal digestion does not have much effect on the stability, under the coordination action of intestine protease and weak base. The CPs-Ca is stable in the gastrointestinal digestion, which could possibly enhance calcium absorption.

4.4. Conclusions

In this study, the cattle bone collagen peptides were applied to prepare CPs-Ca, and the preparation conditions (pH 7, temperature 60 °C, time 60 min, peptides/$CaCl_2$ 5/1) were optimized by single factor test. The results of physical characteristics indicate that CPs-Ca is obviously different from CPs. The FT-IR analysis demonstrates that chelating sites are carboxyl oxygen, hydroxyl oxygen, and amino nitrogen atom of CPs. The results of XRD spectroscopy, SEM, AFM showed that the structural changes after calcium chelating. Calcium ions cross-link with peptides, resulting in the formation of ordered crystal structure and the aggregation in microstructure. The stability analysis reveals the CPs-Ca is stable during thermal processing and gastrointestinal digestion. In conclusion, those findings demonstrate that the CPs-Ca has the potential function to improve calcium bioavailability as a calcium supplement.

5

Chapter V. Preparation of cattle bone collagen peptides-calcium chelate with ultrasound method and its structural characterization, stability analysis, and bioactivity on MC3T3-E1 cells

Adapt from:

Zhang, H., Qi, L., Wang, X., Guo, Y., Liu, J., Xu, Y., Liu, C., Zhang, C., & Richel, A. (2023). Preparation of a cattle bone collagen peptide–calcium chelate by the ultrasound method and its structural characterization, stability analysis, and bioactivity on MC3T3-E1 cells. Food & Function. https://doi.org/10.1039/D2FO02146C

Abstract: This study was designed to prepare cattle bone-derived collagen peptides-calcium chelate by ultrasound method (CPs-Ca-US), and its structural characterization, stability, and bioactivity on MC3T3-E1 cells were characterized. Single-factor experiments optimized the preparation conditions: ultrasound power 90 W, ultrasound time 40 min, $CaCl_2$/peptides 1/2, pH 7. Under these conditions, the calcium-chelating ability reached 39.48 μg/mg. The result of Fourier transform-infrared spectroscopy indicated that carboxyl oxygen and amino nitrogen atom were chelation sites. Morphological analysis indicated that CPs-Ca-US was characterized by porous surface and large particles. Stability analysis demonstrated that CPs-Ca-US was stable in the thermal environment and intestinal digestion. CPs-Ca-US showed a more stable property in gastric juice than chelate prepared by the hydrothermal method. Cell experiments indicated that CPs-Ca-US increased osteoblast proliferation (proliferation rate 153% at a concentration of 300 μg/mL) and altered the cell cycle. Significantly, CPs-Ca-US enhanced calcium absorption by interacting with calcium-sensing receptor and promoted the mineralization of MC3T3-E1 cells. This study provides the scientific basis for applying the ultrasound method to prepare peptides-calcium chelate and clarifies the positive role of chelate in bone building.

Keywords: Peptides-calcium chelate, Ultrasound, Structural characterization, Stability, MC3T3-E1

5.1. Introduction

Recently, peptides-calcium chelate has attracted widespread interest as a novel carrier to deliver calcium. Peptides could assemble with other molecules to form macromolecular structures via chemical bonds including coordination bonds, hydrophilic, hydrophobic, electrostatic interactions, and ionic bonds (Tomadoni et al., 2020). Chelate could enhance the bioavailability of calcium due to the increased solubility and protection from inhibitors in the digestive tract. Many peptides could resist the degradation in the gastrointestinal and plasmic environment (such as pepsin, trypsin, and plasma protease), and reach integrally their target organs.(Ji et al., 2022; Xu et al., 2019) Therefore, peptides-calcium chelate could enhance calcium bioavailability and exert the bioactivity of peptides (Cui et al., 2018). Many researchers are focusing on food protein-derived peptides-calcium chelate, such as pig bone, chicken foot, milk, and tilapia bone.(Liao et al., 2020; Malison et al., 2021; Wu et al., 2019; Zhao et al., 2014) Cattle is one of the most important livestock resources globally. In 2019, the global production of beef was about 62.9 million tons, and collagen-rich bovine bones, skins, and tendons yield was up to 31.4 million tons (Song et al., 2021). More interestingly, collagen peptides derived from cattle bone have been evidenced to possess anti-osteoporosis function (Chen et al., 2022). From economic, environmental protection, and human health perspectives, the high-value utilization of cattle bone resources is of great significance.

The preparation method of peptides-calcium chelate is usually hydrothermal method. In solution, peptides could aggregate to form amorphous or highly structured amyloid-like fibrils, which may limit the chelating ability of peptides (Zapadka et al., 2017). With the development of innovative food processing technologies, the ultrasound method, one of the innovative technologies, has been more widely concerned (Li et al., 2021; L. Zhang et al., 2018). The ultrasound method is an eco-friendly, effective, safe, and non-toxic technology (ultrasonic waves above 20 kHz). Ultrasound produces powerful forces at the microscopic scale by shock causing chemical changes in the medium (Ulug et al., 2021). Ultrasound could produce cavitation, which can change the protein structure and expose more groups, meaning more chelation sites between peptides and Ca^{2+}. Li et al., (2021) demonstrated that ultrasound treatment could decrease the aggregation of peptides to small and uniform structure. Ultrasound treatment was widely applied to extract proteins and peptides from natural products facilitating higher yields and extraction rates (Kadam et al., 2015). To the best of our knowledge, there are few reports about the application of the ultrasound method in peptides-calcium chelate preparation. The cavitation pressure and high temperature caused from ultrasonic treatment could accelerate the progress of chemical reactions, promote the mutual penetration of molecules and open chemical bonds. At the same time, it can further accelerate the chelation reaction through the absorption of sound, secondary effects caused by the resonance properties of the medium and the container. These, we predicted ultrasound method could be applied for preparing chelate. In particular, the studies related to the effects of hydrothermal method and ultrasound method on the structure of chelate are limited. Current researches mainly focused on the isolation of calcium-binding peptides, structural analysis, and transportation across Caco-2 cells (Malison et al., 2021; Wu et al., 2019). Several studies

demonstrated peptides-calcium chelate could promote intestinal calcium absorption (Cui et al., 2019; Wu et al., 2019). Therefore, based on previous studies, we investigated the bone formation bioactivity of chelate by cell experiment of murine osteoblasts MC3T3-E1.

The primary purpose of the present study was to prepare cattle bone collagen-derived peptides-calcium chelate by ultrasound method. Single-factor experiments optimized the processing conditions. The amino acid composition, Fourier transform-infrared spectroscopy (FT-IR), molecular mass distribution, thermalgravimetric analysis (TGA), stability of CPs-Ca-US, and its biological function on MC3T3-E1 cells were determined.

5.2. Materials and methods

5.2.1. Materials

Cattle bone-derived collagen peptides were provided by Inner Mongolia Peptide (Mengtai) Biological Engineering Co., Ltd (Inner Mongolia province, China). The collagen peptides were isolated by hot-pressure and enzymatic hydrolysis from cattle bone. The protein purity reached 93.2%. The molecular wight was mainly < 500 Da (78.7%). The amino acid composition of collagen peptides was shown in Figure 5-2E in detail. Calcium chloride was purchased from Sigma-Aldrich (St. Louis, MO, USA). Murine osteoblast MC3T3-E1 cells, α-MEM medium, fetal bovine serum, and osteogenic differentiation medium were purchased from Procell Life Science & Technology Co., Ltd.

5.2.2. Preparation experiment of peptides-calcium chelate by ultrasound method

Collagen peptides dissolved in ultrapure water (50 mg/mL), and then $CaCl_2$ was added. The above solution was mixed thoroughly by a vortex mixer for 1min in a 30 mL glass bottle. Then, the preparation of CPs-Ca-US by ultrasound (20–25 kHz) was conducted using an ultrasonic cell disruptor (Scientz-IID, Ningbo Xinzhi Biotechnology Co., Ltd., Ningbo, China). According to previous pre-experiments and literature review, the optimized process parameters included ultrasound power (60–180 W), ultrasound time (20–60 min), the ratio of $CaCl_2$/peptides (1/6–1/2), and pH value (5–9). To exclude the influence of temperature on the chelating process, the glass bottle was placed in an ice-water bath, and the temperature was controlled within a stable range (4.46 ± 0.26 °C) detected by a temperature recorder (L93-1, Hangzhou Loggertech Co., Ltd, Hangzhou, China). After the chelation reaction, 9 times volume ethanol was added to the chelated solution to precipitate collagen peptides-calcium chelate and separate the chelate and calcium ions. Then, the precipitation was washed with 90% ethanol for several times to remove free calcium ions as far as possible. Finally, the above solution was centrifuged at 8000 × g for 15 min. The obtained precipitation was lyophilized and marked as CPs-Ca-US. The schematic diagram is shown in Figure 5-1A.

According to the previous study, the chelate prepared by hydrothermal method was as a control (Zhang et al., 2021). Collagen peptides dissolved in ultrapure water, and then $CaCl_2$ was added ($CaCl_2$/peptides, W/W, 1/5). The solution was stirred at 60 °C for 60 min to obtain peptides-calcium chelate. After the chelation reaction, 9 times volume ethanol was added to the chelated solution to precipitate collagen peptides-calcium chelate and separate the chelate and calcium ions. Then, the precipitation was washed with 90% ethanol for several times to remove free calcium ions as far as possible. Finally, the above solution was centrifuged at 8000 × g for 15 min. The precipitate was collected after lyophilizing and recorded as CPs-Ca-HT. The calcium content of CPs-Ca-HT and CPs-Ca-US was detected to describe the calcium-chelating ability (CCA). The yield of chelate = recycled chelate (g)/added collagen peptides (g).

5.2.3. Molecular weight determination

The molecular weight of sample was determined by an HPLC apparatus (Agilent 1260) equipped with DAWN HELEOS-II (Wyatt Technology Corporation, America) and Optilabr EX (Wyatt Technology Corporation, USA) detectors, and a TSK gel G4000PWxl column (7.8 × 300 mm, TOSOH, Tokyo, Japan). Briefly, the mobile phase included 54.9% of ultrapure water, 0.1% of trifluoroacetic acid, and 45% of acetonitrile. The standard sample was composed of Gly-Sar (146 Da), Gly-Gly-Tyr-Arg (451 Da), bacitracin (1422 Da), aprotinin (6511 Da), and Cytochrome C (12327 Da), purchased from Sigma-Aldrich (St. Louis, MO, USA).

5.2.4. Amino acids analysis

Amino acid contents of CPs, CPs-Ca-HT, and CPs-Ca-US samples were determined by an amino acid automatic analyzer (L-8900, Hitachi LTD, Japan). The sample was hydrolyzed with 6 M HCl at 110 °C for 24 h. Before amino acid analysis, the hydrolysate was filtrated by filter membrane to remove impurities.

5.2.5. Fourier transform-infrared (FT-IR) spectroscopy

FT-IR spectra of CPs, CPs-Ca-HT, and CPs-Ca-US samples was analyzed with an FT-IR spectrometer (Tensor-27, Bruker Company, Germany). The mixture of dried sample powder and KBr powder was thoroughly ground and compressed into a tablet, and KBr powder was applied as the background. The FT-IR spectra was measured in the wavenumber ranging from 4000 to 400 cm^{-1} and the spectral resolution was 4 cm^{-1}.

5.2.6. Circular dichroism (CD) spectroscopy

The secondary structure of CPs, CPs-Ca-HT, and CPs-Ca-US samples was determined by a circular dichroism spectroscopy (Jasco Co., Jasco J-810, Tokyo, Japan) according to the previous study (Sun et al., 2020). Each sample was solubilized in ultrapure water at a 1 mg/mL concentration before detection. CD spectra was determined at 190–260 nm with a 2 nm slit. The percentage composition of the secondary structure was determined by the Spectra Manager Version 2.1.1.1 software (JASCO Co., Tokyo, Japan).

5.2.7. Scanning electron microscope (SEM)

Scanning electron microscope image was obtained to present the microstructure of CPs, CPs-Ca-HT, and CPs-Ca-US by a scanning electron microscope (Zeiss Merlin Compact, Germany) equipped with energy dispersive spectroscopy (EDS) under 10 kV of accelerating voltage. Before obtaining SEM and element mapping images, the sample was sprayed with gold plating film.

5.2.8. Atomic force microscopy (AFM)

Atomic force microscopy image was obtained by atomic force microscopy (AFM, NX-10, Park Systems). The sample solution (20 μL, 10 mg/mL sample) was dropped on the mica sheet. The scanning image was observed under the tapping mode at 15 kV.

5.2.9. Thermalgravimetric analysis (TGA)

The thermal property of CPs, CPs-Ca-HT, and CPs-Ca-US was determined by a thermal gravimetric analyzer (Pyris Diamond TG/DTA, PerkinElmer, USA) from 30 to 500 °C at 10 °C/min under N_2 atmosphere.

5.2.10. Stability analysis

The stability analysis was conducted according to the previous study (Wu et al., 2020). The aqueous solution of CPs-Ca-US (10 mg/mL) was heated to different temperatures (50, 60, 70, 80 °C) and incubated for 1 h (pH 7). After incubation, the heated solution was mixed with ethanol and then centrifuged at 8000 × g for 15 min to obtain chelate. The stability of CPs-Ca-US against gastrointestinal digestion *in vitro* was determined. CPs-Ca-US dissolved in ultrapure water with gastric pH (2.0) and intestinal pH (7.5), respectively. Next, CPs-Ca-US dissolved in simulated human gastric juice (A7920, Solarbio, Beijing, China) and simulated human intestinal juice (A1790, Solarbio, Beijing, China). The above solution was incubated at 37 °C for 1 h. To terminate digestion, the solution was heated at 100 °C for 10 min. The chelate of CPs-Ca-US in control group cereal dissolved in distilled water at 22 °C for 1 h, and the solution was mixed with ethanol and then centrifuged at 8000 × g for 15 min to obtain chelate. The calcium content in chelate was analyzed by an atomic absorption spectrophotometer. The formula of calcium retention rate was as follows:

$$\text{Calcium retention rate (\%)} = \frac{\text{Calcium content in treatment group}}{\text{Calcium content in control group}} \times 100$$

5.2.11. Cell proliferation

MC3T3-E1 cells were cultured in α-MEM medium supplemented with 10% fetal bovine serum. The cells were cultured in a cell incubator at 37 °C and 5% CO_2. The cells were seeded at 5000 cells/well in a 96-well plate. After 24 h of incubation, MC3T3-E1 cells were treated with $CaCl_2$ (9.24 μg/mL), mixture of CP (71.67 μg/mL) and $CaCl_2$ (9.24 μg/mL), CPs-Ca-HT (75 μg/mL), CPs-Ca-US (75 μg/mL, 100 μg/mL, 200 μg/mL, 300 μg/mL) for 72 h. In the mixture of CP and $CaCl_2$, peptides and

calcium content were equal to those in CPs-Ca-US (75 μg/mL). The calcium content in CPs-Ca-US was similar to CPs-Ca-HT. Cells treated with the medium (without sample) were used as the normal group. MTT cell assay (C0009S, Beyotime) kit was applied to detect cell proliferation according to the instruction.

5.2.12. Cell cycle assay

After the culturing of MC3T3-E1 cells exposed to medium with $CaCl_2$ (9.24 μg/mL), mixture of CPs (71.67 μg/mL) and $CaCl_2$ (9.24 μg/mL), CPs-Ca-HT (75 μg/mL), CPs-Ca-US (75 μg/mL, 150 μg/mL, 300 μg/mL) for 72 h and normal medium for 72 h, the cell cycle was analyzed by DNA content quantitation assay (CA1510-20T, Solarbio, Beijing, China) with a Flow cytometer (CytoFLEX, Beckman Coulter, Germany).

5.2.13. Confocal laser scanning microscopy (CLSM)

Intracellular calcium ions of MC3T3-E1 cells were determined by a CLSM (LSM880, ZEISS, Germany). MC3T3-E1 cells were cultured with $CaCl_2$ (36.63 μg/mL), mixture of CPs (286.68 μg/mL) and $CaCl_2$ (36.63 μg/mL), CPs-Ca-HT (300 μg/mL), CPs-Ca-US (300 μg/mL), CPs-Ca-US (300 μg/mL) + R568 (CaSR agonist, 5 μM), and CPs-Ca-US (300 μg/mL) + Calhex231 (CaSR inhibitor, 3 μM) for 24 h. In the mixture of CP and $CaCl_2$, peptides and calcium content were equal to those in chelate. After cultivation, MC3T3-E1 cells were washed with phosphate buffer solution (PBS) and were stained with 5 μM Fluo-4/AM (S1060, Beyotime Biotechnology) for 30 min at 37 °C in the dark. Then, 2 μg of Hoechst 33342 (C1029, Beyotime Biotechnology) was added to stain the living cells culturing at 37 °C for 5 min in the dark. The fluorescence of calcium ions was measured by the CLSM. ImageJ software was used to quantify fluorescence intensity.

5.2.14. Mineralization assay

MC3T3-E1 cells were seeded in a 12-well plate and cultured by osteogenic differentiation medium with $CaCl_2$ (9.24 μg/mL), mixture of CPs (71.67 μg/mL) and $CaCl_2$ (9.24 μg/mL), CPs-Ca-HT (75 μg/mL), CPs-Ca-US (75 μg/mL, 100 μg/mL, 200 μg/mL, 300 μg/mL). The cells of normal group were cultured by osteogenic differentiation medium. In the mixture of CPs and $CaCl_2$, peptides and calcium content were equal to those in chelate. The calcium content in CPs-Ca-US was similar to CPs-Ca-HT. After 21 days of cultivation, the cells were washed twice with PBS. Alizarin Red S (pH 4.2, Beyotime) was used to stain cells for 30 min at 22 ± 4 °C. Then, to remove the unbound dye, cells were washed with distilled water. The mineralization image was observed by an inverted microscope (IX51, Olympus, Japan). To quantify the bound dye, the cells were destained with 10% cetylpyridinium chloride in the dark for 1 h. The concentration of the solubilized Alizarin Red S was measured at 570 nm.

5.2.15. Statistical analyses

R project 4.0 (R Core Team) was used to analyses the data. Analysis of Variance (ANOVA) along with Duncan's multiple comparisons was performed on the obtained data (calcium-chelating ability, secondary structure, cell proliferation, cell cycle, and

intracellular calcium ions). One-way ANOVA was performed on the data of amino acid content and calcium retention rate. *P*-value < 0.05 was considered statistically significant. All data were expressed as the Mean ± SD (standard deviation). *ggplot2* package of R project was used to data visualization.

5.3. Results and discussion

5.3.1. Effect of process conditions on calcium-chelating ability

To optimize the preparation process of peptides-calcium chelate by ultrasound method, the effects of ultrasound power (W), ultrasound time (min), $CaCl_2$/peptides (weight/weight, W/W), and pH value on CCA were evaluated. Except for the experimental variable, the process conditions were selected as follows: pH 7, ultrasound power 120 W, ultrasound time 30 min, $CaCl_2$/peptides 1/2. Ultrasound time and ultrasound power were regarded as the main factors affecting chemical reaction. Meanwhile, our previous study demonstrated that the $CaCl_2$/peptides and pH value also obviously influenced the CCA (Zhang et al., 2021).

In Figure 5-1B, as ultrasound time increased from 20 to 40 min, the CCA reached a peak value of 38.95 μg/g. However, with the ultrasound time was extended to 60 min, the CCA showed a downward trend. The increased ultrasound temperature can accelerate the interaction of peptide molecules and calcium ions to form chelate. However, excessive ultrasound may cause breaks of coordination bonds due to the continuous increase of hydrogen ion concentration in water (Chen & Kalback, 1967). When the ultrasound time exceeded 40 min, the aggregation of collagen peptides played a major role, thereby reducing the solubility of peptides and the ability of peptides to bind calcium. Gülseren et al., (2007) indicated the particle size of bovine serum albumin increased up to 3.4 times after 90 min ultrasound treatment. In Figure 5-1C, as ultrasound power varied from 60 W to 120 W, the CCA reached the maximum value of 38.52 μg/g at 120 W. There was no significant difference among 90–180 W. The CCA increased rapidly under the low ultrasound power (60–120 W), then showed a decreased trend under the high ultrasound power (120–180 W). Under the low ultrasound power, since ultrasound cavitation destroyed noncovalent bonds (hydrophobic interaction, electrostatic interaction, and hydrogen bonding), large peptide clusters became smaller fragments. As the ultrasound power was increased to a certain point, the effect of ultrasound on the chelation reaction reached a balance. When the power was too large, it would destroy the coordination bond between peptides and calcium ions. The ultrasound treatment promoted changes in the secondary structure of collagen peptides producing an intermediary molten globule state, meanwhile denaturation and aggregation are occurred (Abadía-García et al., 2016). The excess radicals caused by ultrasound cavitation effect might enhance the movement of protein molecules and increase the chance of collisions between protein molecules, leading the increase of particle size. The large size particles were not conducive to chelation reaction between collagen peptides and calcium ions. Thus, with the increase of ultrasonic power (> 120 W) and ultrasonic time (> 40 min), the content of insoluble peptides increased, so that the CCA decreased. As shown in

Figure 5-1D, with the increased $CaCl_2$/peptides from 1/6 to 1/2, the CCA significantly increased. The increased calcium ion ratio meant more contact opportunities between peptide molecules and calcium ions. As shown in Figure 5-1E, with the increasing pH from 5 to 10, the CCA increased significantly (pH 5–7) and then appeared no significant change (pH 7–9). In the neutral or alkaline environment, the hydrogen ion concentration decreased, which could improve the coordination between Ca^{2+} with NH^{3+} and $COOH^{-}$.

The optimized preparation conditions of the ultrasound method were ultrasound time 40 min, ultrasound power 90 W, $CaCl_2$/ peptides 1/2, and pH 7, according to the above results. Under these process parameters, the CCA reached 39.48 ± 0.19 μg/mg. Meanwhile, no significant difference was observed between hydrothermal method (44 ± 4%) and ultrasound method (41 ± 6%) in the yield of chelate. Previous studies demonstrated similar results: the CCA of sea cucumber ovum hydrolysate reached 53.45 mg/g, and the CCA of egg white peptides reached 44 mg/g (Cui et al., 2017; Huang et al., 2021). Liao et al., (2020) isolated three peptides from tilapia bone collagen hydrolysate, and the CCA of peptides reached 18.80, 35.73, and 28.4 mg/g, respectively. The CCA of this study was similar to the above-mentioned studies and lower than some studies. The main reason may be that the low-temperature environment (4.46 ± 0.26 °C) in this study was not conducive to the formation of peptides-calcium chelate. The ultrasound process is often accompanied by an increase of temperature, which could promote the chelation reaction. The CCA will show a higher value if cooling is not performed in the ultrasound method.

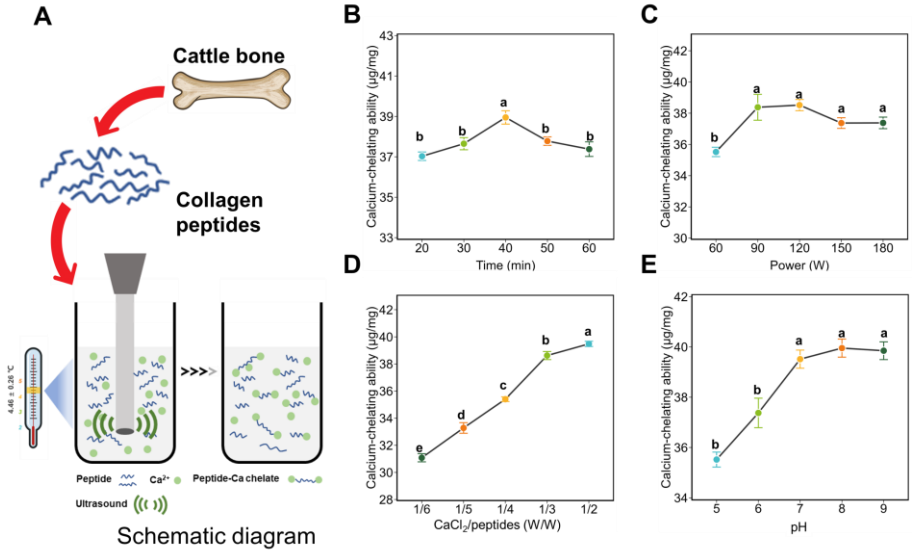

Figure 5-1: (A) Schematic representation of fabricating CPs-Ca-US by ultrasound method, Calcium-chelating ability affected by (B) ultrasound time, (C) ultrasound power, (D) $CaCl_2$/peptides, (E) pH value. Duncan's test was used to evaluate the significant differences between different groups. The different letters mean a significant difference between the two groups.

5.3.2. Structural characterization

5.3.2.1. FT-IR analysis

The characteristic change of FT-IR spectra was used to determine interactions between metal ions and organic groups. As Figure 5-2A shows, after the chelate reaction, the band of CPs (3273.95 cm^{-1}) shifted to 3385.28 cm^{-1} (CPs-Ca-HT) and 3400.74 cm^{-1} (CPs-Ca-US), which may be due to the combination between –NH2 and Ca^{2+} (Yang et al., 2021). Stretching of NH enabled N-Ca to replace hydrogen bonds. The FT-IR spectra indicated that the wavenumber at 1656.00 cm^{-1} (CPs) of the amide I band shifted to 1657.27 cm^{-1} (CPs-Ca-HT) and 1657.36 cm^{-1} (CPs-Ca-US) after peptides bounded to calcium, which is due to the C=O stretching vibrations. The band at 1401.49 cm^{-1} for the −COO− groups in the CPs moved to 1407.44 cm^{-1} (CPs-Ca-HT) and 1408.09 (CPs-Ca-US), indicating that the −COO− groups in Asp and Glu of the peptides might play a crucial role in calcium chelation (Cui et al., 2019). The wavenumber of the amide II band at 1547.55 cm^{-1} (CPs) shifted to 1555.81 cm^{-1} and 1555.26 cm^{-1} after the chelation, which also indicated binding of the −COO– with Ca^{2+} (Malison et al., 2021). No significant difference was observed in FT-IR spectra between CPs-Ca-HT and CPs-Ca-US. These results provided evidence that Ca^{2+} was chelated by CPs to form CPs-Ca-US, and the calcium-binding sites of were the carboxyl oxygen and amino nitrogen atoms of Glu and Asp. These results were consistent with previous studies, such as white carp skin collagen peptides and whey peptides (Yang et al., 2021; L. Zhao et al., 2014)

5.3.2.2. Circular dichroism spectroscopy analysis

Figure 5-2B shows the percentage composition of secondary structure deduced from the CD spectra. It is generally applied to investigate the structure change of proteins/peptides. The results indicated that the secondary structure was composed of α-helix, β-sheet, β-turn, and random coil. After calcium chelation, the α-helix structure for CPs-Ca-HT and CPs-Ca-US significantly decreased accompanied by a significant increase in the content of random coil structure. The result appeared that calcium-induced the structural change of CPs from α-helix to the random coil. CPs-Ca-HT and CPs-Ca-US both showed structural transformation. This was consistent with previous studies that indicated Ca^{2+} favored the decrease of α-helix structure of protein (Sun et al., 2020; Zhang et al., 2012). The secondary structures of CPs-Ca-HT and CPs-Ca-US showed similar results. These results indicated that chelated calcium ions could alter the spatial structure of peptides.

5.3.2.3. Thermalgravimetric analysis

The thermal stability of CPs, CPs-Ca-HT, and CPs-Ca-US was evaluated by the thermogravimetric analysis. As shown in Figure 5-2C, during 25–200 °C, the weight of all samples showed a slight decrease due to the evaporation of moisture. During 200–400 °C, the weight of CPs declined rapidly. Compared with CPs, the weight of CPs-Ca-HT, and CPs-Ca-US indicated a relatively slow decline at 200–400 °C. No significant difference was observed in the thermogravimetric curve between CPs-Ca-HT and CPs-Ca-US. The result indicated that CPs-Ca-US exhibited high stability in the thermal environment. Because of the coordinate bonds between peptides and

calcium ions, the thermal degradation of CPs-Ca-US needed more energy to break chemical bonds.

5.3.2.4. Molecular mass distribution analysis

The molecular mass distribution of CPs, CPs-Ca-HT, and CPs-Ca-US are shown in Figure 5-2D. After the chelate reaction, the molecular mass distribution presented a significant change between CPs and CPs-Ca-US. The proportions of < 500 Da, and 500–1000 Da in CPs-Ca-US decreased significantly ($P < 0.05$), relative to these of CPs. On the contrary, the proportions of 1000–2000 Da, 2000–3000 Da, and 3000–5 000 Da, > 5000 Da increased. CPs-Ca-HT and CPs-Ca-US showed similar results without significant differences. The major reason may be the formation of supramolecular structures through coordination bonds and ionic bonds in CPs-Ca-US, which caused the molecular mass increased.

5.3.2.5. Amino acid component

The amino acid compositions of CPs and CPs-Ca-US are shown in Figure 5-2E. Types of amino acids contribute to the calcium-binding ability of peptides with different efficiency (Qu et al., 2022). In the chelate, the contents of Asp and Glu were significantly increased compared with those in CPs ($P < 0.05$). Previous studies indicated that acidic amino acids were crucial to chelate metal ions due to more active side chain groups, such as hydroxyl groups (Sun et al., 2020; Torres-Fuentes et al., 2012; Zhang et al., 2021). Qu et al., (2022) also found the increased contents of Asp and Glu significantly, and Lys in peptides-iron chelate relative to before chelation. In this study, similar results were obtained that the increased content of Asp and Glu in CPs-Ca-US, but the difference of Lys did not reach a statistically significant level. This result was consistent with FT-IR analysis that the calcium-binding sites were the carboxyl oxygen and amino nitrogen atoms of Glu and Asp. The contents of Ala, Gly, Ile, Leu, Met, Phe, Thr, and Val in CPs-Ca-US decreased signally ($P < 0.05$) indicating that non-polar amino acids and uncharged polar amino acids were not involved in the chelation reaction. Meanwhile, no significant difference was observed in amino acid composition between CPs-Ca-US and CPs-Ca-HT.

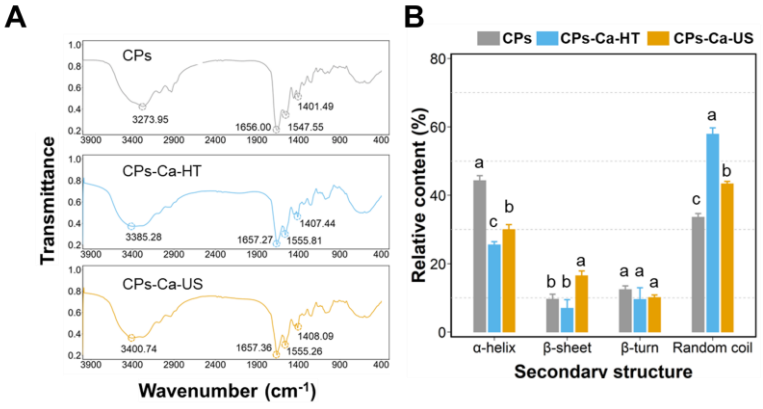

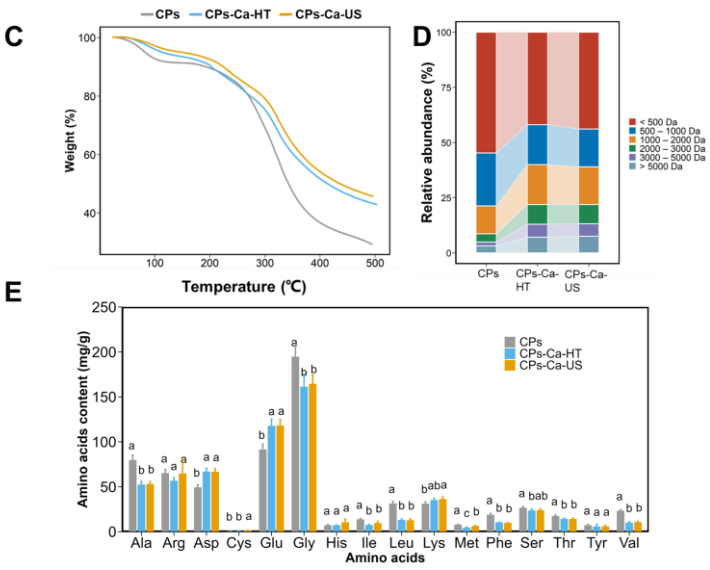

Figure 5-2: Structural characterization properties. (A) FTIR spectra, (B) Secondary structure, (C) Thermalgravimetric analysis, (D) Molecular mass distribution, (E) Amino acid content. CPs: collagen peptides; CPs-Ca-US: collagen peptides-calcium chelate prepared by ultrasound method; CPs-Ca-HT: collagen peptides-calcium chelate prepared by hydrothermal method. Duncan's test was used to evaluate the significant differences between different groups. The different letters mean a significant difference between the two groups.

5.3.2.6. Scanning electron microscope analysis

SEM image was used to examine the microstructure of CPs-Ca-HT and CPs-Ca-US. The SEM is extensively used for microscale material and structure characterization. As shown in Figure 5-3 (A2, B2, C2), collagen peptides presented small partial structure with a smooth surface. After binding with calcium, CPs-Ca-HT and CPs-Ca-US exhibited clusters and large-size particles. These observations agreed with a previous study, indicating that after binding peptide hydrophilic groups, the metal ions can promote aggregation, leading to the formation of compact particles (Zhang et al., 2021). The EDS was used to determine the elemental compositions of CPs and CPs-Ca-US in detail, as shown in Figure 5-3 (A1, B1, C1). There was a clear calcium peak in the CPs-Ca-US, which indicated that calcium ions had interacted with CPs. As Figure 5-3 (A3, B3, C3) show, the element mapping image of CPs indicated a weak signal of calcium, and the intensity of calcium signal was strong in CPs-Ca-US. The element mapping image and EDS results confirmed the successful preparation of peptides-calcium chelate. Meanwhile, no significant difference was observed in SEM image, EDS, and element mapping image between CPs-Ca-HT and CPs-Ca-US. These results demonstrated that chelate reaction could alter the microstructure of peptides, which was in line with the results of FT-IR and molecular mass distribution analysis.

5.3.2.7. Atomic force microscopy analysis

The three-dimensional images of CPs and CPs-Ca-US are shown in Figure 5-3 (A4, B4, C4). The AFM image of CPs-Ca-US showed aggregates with larger particles. It may be due to the combination of calcium ions with the peptides, resulting in the structural change and larger particles formed, which was consistent with a previous study (Qu et al., 2022). Compared with CPs-Ca-HT, the total number of particles of CPs-Ca-US increased, and the particle size decreased. The possible reason may be that ultrasound treatment could decrease the aggregation of peptides to form small and uniform structure (Li et al., 2021).

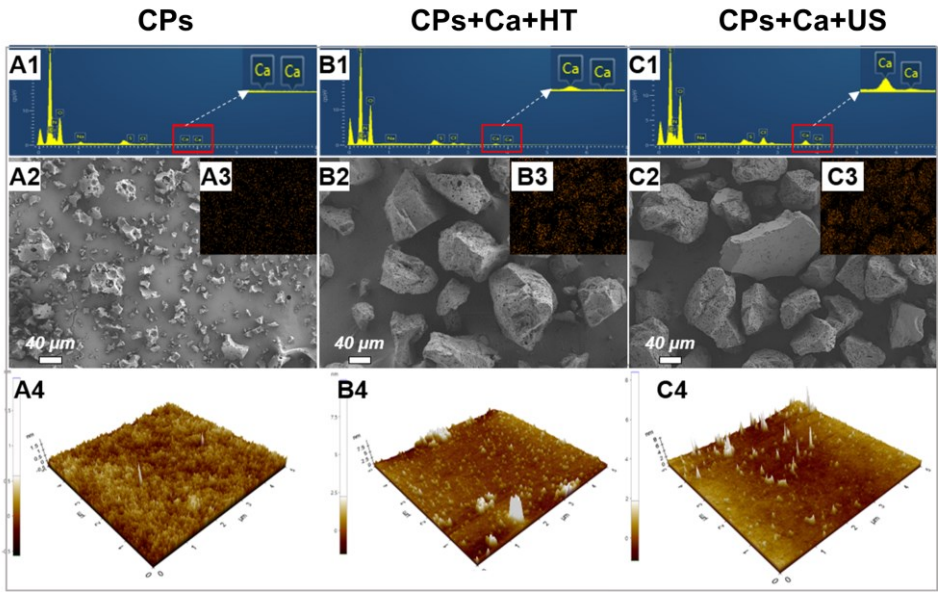

Figure 5-3: Microstructure of CPs-Ca-US. (A1, B1, C1) Energy dispersive spectroscopy, (A2, B2, C2) Scanning electron microscope image, (A3, B3, C3) Element mapping image of calcium, (A4, B4, C4) Atomic force microscopy image. CPs: collagen peptides; CPs-Ca-US: collagen peptides-calcium chelate prepared by ultrasound method; CPs-Ca-HT: collagen peptides-calcium chelate prepared by hydrothermal method.

5.3.2.8. Stability analysis

The stability of the CPs-Ca-US at different temperatures was shown in Figure 5-4A. As the temperature increased from 50 °C to 80 °C, there was no significant effect of temperature on the calcium retention rate. The calcium retention rates of CPs-Ca-US and CPs-Ca-US presented the same results under different treatments. This result was in line with a previous study that peptides-calcium chelate exhibited good thermal stability (Wu et al., 2019). CPs-Ca-US could maintain high thermal stability (retention rate > 95%) in a wide temperature range (50–80 °C).

Dietary supplements are absorbed by the intestinal tract through gastrointestinal digestion, and the biological activity may get undesirable effects due to the

unfavorable factors (H^+ and protease). Therefore, it is crucial to evaluate the digestive stability of CPs-Ca-US in gastrointestinal digestion. To simulate the pH environment of the gastrointestinal tract, CPs-Ca-US dissolved in the gastric pH (2.0) and intestinal pH (7.5) solutions without protease. As shown in Figure 5-4B, the calcium retention rate of CPs-Ca-US decreased significantly under gastric pH and gastric juice conditions ($P < 0.05$). It was speculated that high H^+ concentration under gastric conditions could compete with calcium ions to bind with NH^{3+} and $COOH^-$, which induced the Ca^{2+} release of CPs-Ca-US. This result was consistent with the lower CCA under acidic conditions (pH = 5 and 6). Under the intestinal pH condition, the calcium retention rate of CPs-Ca-US increased significantly compared with that of control. This may be because the alkaline environment did not destroy the stable structure of the chelate and was beneficial to the chelation reaction. Under the gastric juice and intestinal juice, the calcium retention rate of CPs-Ca-US decreased signally ($P < 0.05$), compared with gastric pH and intestinal pH, respectively. It was speculated that peptides might be hydrolyzed by pepsin (gastric juice) and trypsin (intestinal juice) to form smaller peptides or amino acids, accompanied by the dissociation of peptides-calcium chelate. A similar result was reported in a previous study that the re-chelation between peptides and Ca^{2+} was found in a weak alkaline environment (Cui et al., 2019). Wu et al., (2019) indicated that the chelate stability was little affected by pepsin, and was sensitive to the change of pH value, which was consistent with the presented results. The calcium retention rate of CPs-Ca-HT showed the same variation pattern as that of CPs-Ca-US. It was worth noting that the calcium retention rates of CPs-Ca-US increased under gastric juice and intestinal pH relative to that of CPs-Ca-HT ($P < 0.05$). The possible reason may be the formation of more stable coordination bonds by ultrasound method, caused by mechanical agitation and mixing, and the rise in local temperatures and pressures because of cavitation (Chen & Kalback, 1967). In the ultrasound process, not only thermal and mechanical effects but also cavitation effects have a significant effect on chemical reaction. The cavitation effect can change the chemical processes in the system and enhance the rate of the reaction process or initiate new reaction mechanisms by forming various types of free radicals (Kondo & Kano, 1988). According to the high stability of CPs-Ca-US, it was selected to carry out follow-up cell experiments. Previous studies reported peptides-calcium chelate could promote calcium absorption across Caco-2 cell monolayer (Malison et al., 2021; Wu et al., 2019). Asai et al., (2019) demonstrated the food-derived collagen peptides can be found in human blood. The evidence indicated peptides-calcium chelate could be absorbed through the gut. To further study the bioactivity of CPs-Ca-US on bone building, the effect of CPs-Ca-US on the cell proliferation, cell cycle, and mineral deposition on MC3T3-E1 cells were investigated.

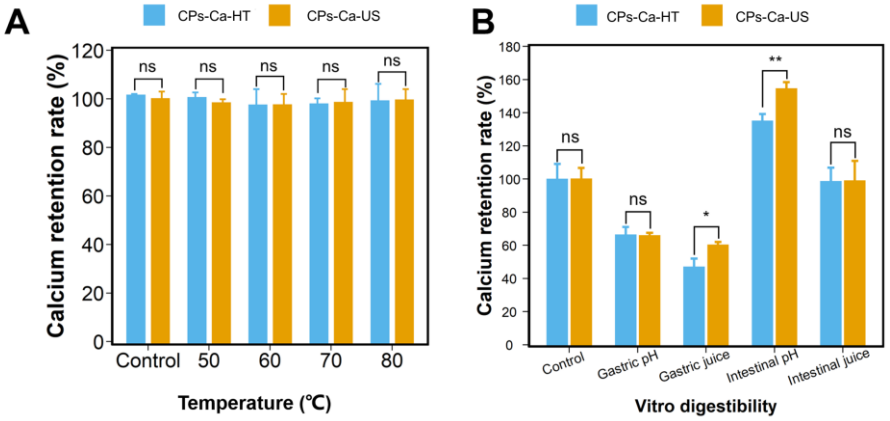

Figure 5-4: Stability of CPs-Ca-US. (A) Stability of chelate at various incubation temperature, (B) Stability of chelate at various digestive process. CPs: collagen peptides; CPs-Ca-US: collagen peptides-calcium chelate prepared by ultrasound method; CPs-Ca-HT: collagen peptides-calcium chelate prepared by hydrothermal method. The statistical method is one-way ANOVA. The symbols indicate statistical significance: ns ($P > 0.05$), * ($P \leq 0.05$), ** ($P \leq 0.01$).

5.3.3. Effects of CPs-Ca-US on MC3T3-E1 cells

5.3.3.1. Cell proliferation assay

As indicated in Figure 5-5B, the proportion of G0/G1 phase of MC3T3-E1cells intervened with CPs-Ca-US (> 75 μg/mL) was lower ($P < 0.05$) than that of the normal cells. There was no significant difference between normal, $CaCl_2$, CPs + $CaCl_2$, CPs-Ca-HT (75), CPs-Ca-US (75) groups. With the increase of concentration of CPs-Ca-US, the percentage of G2/M phase was increased ($P < 0.05$), and the percentage of G0/G1 phase was increased ($P < 0.05$). There suggested that CPs-Ca-US facilitated the transition of the cell cycle from G0/G1 to G2/M phase. The observed cell cycle arrest at the G2/M phase suggested that CPs-Ca-US may play a role in cell proliferation by promoting DNA synthesis. CPs-Ca-US enhances the transfer and absorption of calcium, which could refer to the proliferation of MC3T3-E1 cells. The calcium ion signals affect the changes in different cell cycle phases (Machaca, 2011).

5.3.3.2. Cell cycle alteration

As indicated in Figure 5-5B, the proportion of G0/G1 phase of MC3T3-E1cells intervened with CPs-Ca-US was lower ($P < 0.05$) than that of the control cells. The percentage of G2/M phase was increased ($P < 0.05$), which suggested that CPs-Ca-US facilitated the transition of the cell cycle from G0/G1 to G2/M phase. The observed cell cycle arrest at the G2/M phase suggested that CPs-Ca-US may play a role in cell proliferation by promoting DNA synthesis. CPs-Ca-US enhances the transfer and absorption of calcium (Huang et al., 2021), which could refer to the proliferation of MC3T3-E1 cells. The calcium ion signals affect the changes in different cell cycle phases (Machaca, 2011).

5.3.3.3. Intracellular calcium ions

Calcium-sensing receptor (CaSR) is a class G-protein coupled receptor, which is widespread in prokaryotic and eukaryotic cells, regulating calcium and other metal ion homeostasis. To evaluate the mechanism of CPs-Ca-US on calcium absorption, the effect of CaSR on intracellular calcium ions of MC3T3-E1 cells was studied. In Figure 5-5C, the Fluo-4/AM image in CPs-Ca-US + R568 (CaSR agonist) presented strong green fluorescence, followed by CPs-Ca-US, CPs-Ca-HT, and CPs-Ca-US + Calhex123 (CaSR inhibitor). Then, ImageJ software was applied to quantify the fluorescence intensity. As shown in Figure 5-5D, the fluorescent intensity of calcium ions in the chelates (CPs-Ca-HT and CPs-Ca-US) increased significantly ($P < 0.05$) compared with the normal, $CaCl_2$, and CPs + $CaCl_2$ groups. It suggested that chelates could enhance calcium absorption. No significant difference was observed in CPs-Ca-HT and CPs-Ca-US groups. CPs-Ca-US could interact with the membrane and open calcium channels to influence calcium absorption. After the co-incubation of CPs-Ca-US and R568, the fluorescent intensity of calcium increased significantly ($P < 0.05$) compared with that of the CPs-Ca-US group. This indicated that CPs-Ca-US induced the calcium ions influx may be related with the CaSR. However, after the co-incubation of CPs-Ca-US and Calhex231, the fluorescent intensity did not show a significant difference relative to that of the CPs-Ca-US. The main reason may be that calcium ions were absorbed not only through the CaSR pathway, but also through other pathways, such as TRPV5, TRPV6, and Cav1.3 (Wongdee et al., 2021). The specific calcium absorption mechanism remains to be further studied. These results indicated that CPs-Ca-US enhanced the calcium absorption in MC3T3-E1 cells by interacting with CaSR.

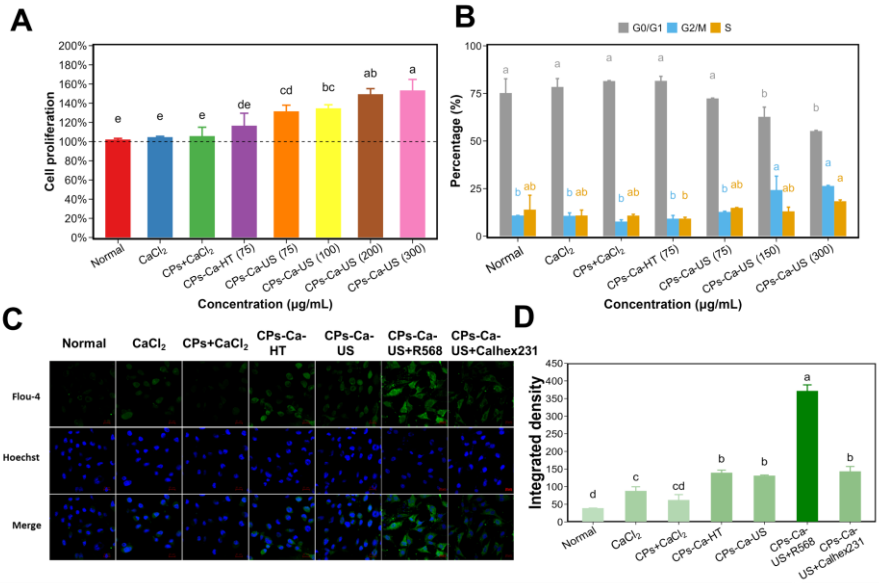

Figure 5-5: (A) Effect of different concentrations of CPs-Ca-US on the proliferation rate of

MC3T3-E1 cells, (B) Effect of different concentrations of CPs-Ca-US on the cell cycle of MC3T3-E1 cells, (C) The intracellular calcium ions stained by Fluo-4/AM, (D) The relative green fluorescent intensity of Fluo-4/AM. CPs: collagen peptides; CPs-Ca-US: collagen peptides-calcium chelate prepared by ultrasound method; CPs-Ca-HT: collagen peptides-calcium chelate prepared by hydrothermal method; R568: CaSR agonist; Calhex231: CaSR inhibitor. The numbers in parentheses represent concentrations (μg/mL). Duncan's test was used to evaluate the significant differences between different groups. The different letters mean the significant difference between the two groups.

5.3.3.4. Mineral deposition

As a marker of osteoblast differentiation and maturation, mineralization is also the main morphological features of osteoblasts performing osteogenic functions. Observing the mineralization level of osteoblasts is a commonly used technique for studying osteoblast differentiation. As shown in Figure 5-6, compared with normal group, the mineralization level in all treated groups was increased. The chelate (CPs-Ca-US and CPs-Ca-HT) showed increased mineralization level compared with $CaCl_2$ and CPs + $CaCl_2$. At the same concentration of 75 μg/mL, the mineralization level in CPs-Ca-US was higher than that in CPs-Ca-HT. This difference may be due to the higher stability of CPs-Ca-US compared with CPs-Ca-US. In the cytoplasm and on the cell surface, cellular proteases may destroy the structure of the chelate (Roessner et al., 2000), and CPs-Ca-US might have high resistance proteases. Meanwhile, with the increase of CPs-Ca-US concentration, the mineralization level gradually elevated. This suggested that the differentiation activity of the CPs-Ca-US for osteoblast cells exhibited a dose-response. However, the difference did not reach a statistically significant level among CPs-Ca-US (75 μg/mL), CPs-Ca-US (100 μg/mL), and CPs-Ca-US (200 μg/mL). CPs-Ca-US could improve calcium absorption by activating calcium/calmodulin mediated calcium/calmodulin-dependent protein kinase (CaMK2), and the increase in intracellular calcium concentration resulted in the activation of numerous targets including CaMK2, which plays a critical role in osteoblast differentiation (Jung et al., 2010). This result was consistent with the above-mentioned results of calcium fluorescence imaging. On the other hand, CPs-Ca-US could provide more calcium ions and a higher-density nucleation sites for minerals formation, which facilitated the mineralization process. The collagen peptides of chelate could significantly increase ($P < 0.05$) the expression of Frizzled-5, β-catenin, Wnt5a, and GSK-3β (Ye, Zhang, Zhu, et al., 2020). The translocation of β-catenin from the cytoplasm to the nucleus functions combined with T cell factor enhancer lymphoid enhancer factor (TCF/LEF) to recruit coactivators, leading to the upregulation expression of target genes, such as Runt-related transcription factor 2 (Runx2) and osteoprotegerin (OPG). Runx2 and OPG are important transcription factors associated with the expression with osteoblast differentiation (Hwang et al., 2009; Wu et al., 2022). The proline in the collagen peptide sequence might also be contribute to the bioactivity of peptides.(Andrushchenko et al., 2006) Proline-rich peptides could promote osteogenic differentiation of MC3T3-E1 cells (Rubert et al., 2011). Wu et al., (2020) also reported a similar result that porcine bone collagen peptides-calcium chelate enhanced the differentiation and mineralization on MC3T3-E1 cells.

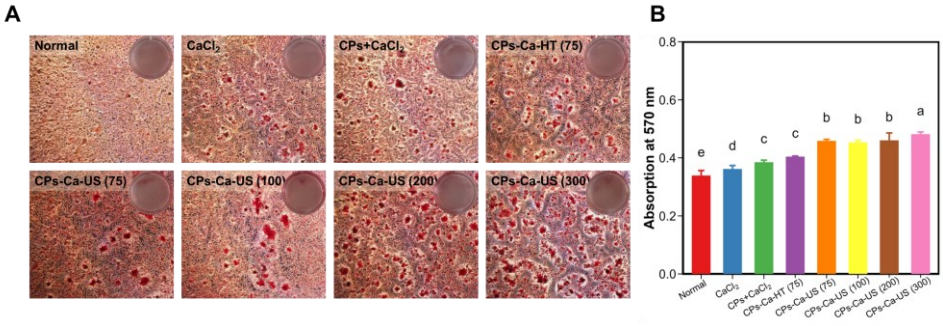

Figure 5-6: (A) Effect of CPs-Ca-US on mineralization of MC3T3-E1 cells, (B) Quantitative analysis of binding of alizarin red dye to MC3T3-E1 cells. CPs-Ca-HT: collagen peptides-calcium chelate prepared by hydrothermal method. CPs-Ca-US: collagen peptides-calcium chelate prepared by ultrasound method. The numbers in parentheses represent concentrations (μg/mL). In CPs+$CaCl_2$, peptides and calcium content were equal to those in CPs-Ca-US (75 μg/mL). In $CaCl_2$, calcium content was equal to that in CPs-Ca-US (75 μg/mL). Duncan's test was used to evaluate the significant differences between different groups. The different letters mean the significant difference between the two groups.

5.4. Conclusions

In summary, cattle bone-derived collagen peptides-calcium chelate prepared by ultrasound method (CPs-Ca-US) was successfully prepared and characterized, and the calcium-chelating ability reached 39.48 μg/mg. Various structure analyses confirmed that chelating sites of CPs-Ca-US were carboxyl oxygen and amino nitrogen. CPs-Ca-US showed porous surface, large particles, high thermal stability, and digestive stability in intestinal digestion. CPs-Ca-US showed a more stable property in gastric juice than chelate prepared by the hydrothermal method. CPs-Ca-US could significantly promote the proliferation and mineralization of MC3T3-E1 cells and promote calcium absorption by interacting with CaSR. CPs-Ca-US is a promising calcium supplement to improve calcium bioactivity. Further studies will be focused on peptides-calcium chelate absorption and transport mechanism.

6

Chapter VI. Cattle bone collagen peptides-calcium chelate relieves osteoporosis by modulating gut microbiota in ovariectomized rat

Abstract: In this study, cattle bone collagen peptides-peptide chelate (CPs-Ca) was prepared to evaluate its anti-osteoporosis effect *in vivo* by ovariectomized rat. Results showed that CPs-Ca improved the bone mineral density and microstructure of femur, as well as modulated the bone turnover markers level in serum. CPs-Ca dietary intervention increased the SCFs contents in feces. In addition, CPs-Ca treatment increased the *Bifidobacterium*, *Escherichia-Shigella*, and *Allobaculum*, while decreased *Firmicutes*, and the *Firmicutes*/*Bacteroidetes* ratio at phylum level along with some specific gut microbiota community changes at genus level. CPs-Ca could be a potential dietary supplement to alleviate the osteoporosis by modulating gut microbiota. This study provides the scientific basis for applying CPs-Ca as the food supplement on osteoporosis treatment.

Keywords: Collagen peptides-calcium chelate, Anti-osteoporosis, Gut microbiota

6.1. Introduction

Osteoporosis (OP) is common metabolic bone diseases charactered with decreased bone mass, destruction of bone tissue microarchitecture, resulting in an increased risk of bone fracture. Simultaneously, osteoporosis caused a heavy economic burden worldwide. The cost of preventing and managing osteoporosis in the European Union is estimated at 37 billion euros, which could increase by 25% until 2025 (Svedbom et al., 2013). Multiple factors can induce osteoporosis, such as age, gender, race, genetics, dietary, and physical activity. Insufficient calcium intake causes mobilization of bone and leads sooner or later to osteoporosis (Nordin, 1997). Therefore, health professionals have paid much attention to both safety and economical food-derived calcium supplement to enhance intestinal calcium absorption, especially the peptides-calcium chelate. It as a new method of delivering calcium has attracted significant attention.

The gut microbiota (GM) has been proposed to play a critical role in the mechanisms and biological processes underlying human health and diseases. Gut microbiota has become a recent topic of interest in the role of many diseases, such as bone health. Gut microbiota could regulate bone mass via the effects on the immune system, which in turn regulates osteoclastogenesis (Ohlsson & Sjögren, 2015). The composition of the GM is modulated by many environmental factors including diet and antibiotic treatments. Gut microbiota-derived metabolites short-chain fatty acids (SCFAs) can improve bone mineral density (BMD) by the reduction of osteoclast differentiation and the inhibition bone resorption (Lucas et al., 2018). Alterations in the microbiome or metabolites affect bone growth and health. McCabe et al., (2015) demonstrated that gut microbiota could modulate bone mass by decreasing intestinal inflammation and changing intestinal calcium absorption in mice. A number of studies indicated that food-derived peptides could modulated gut microbiota, such as collagen peptides (Guo et al., 2021; Wang et al., 2020), whey peptides (Y. Li et al., 2016), and soy bioactive peptides (Ashaolu, 2020). Calcium is the essential mineral element that can be absorbed from the gut for bone mechanical strength. Collagen peptide-calcium chelate (CPs-Ca) could enhance osteoblast proliferation, differentiation, and mineralization (H. Zhang et al., 2023). A novel calcium-binding peptide from cattle bone collagen hydrolysate could possess good calcium transport activity and bioavailability (Qi et al., 2023). Therefore, based on the activity of CPs-Ca *in vitro* and its limited study for osteoporosis (H. Zhang et al., 2023), it is necessary to investigate the effect of CPs-Ca on osteoporosis *in vivo*. In our previous study, yak bone collagen peptides intervention relieve osteoporosis via the regulation of the amino acid metabolism and lipid metabolism (Ye et al., 2020). The obvious role of gut microbiota in the pathogenesis of OP supports the potentially reliable concept of modulating gut microbiota for the treatment of OP. The treatment of CPs-Ca in the diet against osteoporosis and how that would modulate the gut microbiota remains unclear.

In this study, the main purpose was to investigate the anti-osteoporosis effects of cattle bone derived CPs-Ca. The OP rat model was established by bilateral ovariectomy to simulate the OP caused by estrogen deficiency in postmenopausal women. Parameters including micro-CT, bone turnover markers in serum, gut

microbiota and SCFAs in feces were investigated.

6.2. Materials and Methods

6.2.1. Materials

Cattle bone-derived collagen peptides were provided by Inner Mongolia Peptide (Mengtai) Biological Engineering Co., Ltd (Inner Mongolia province, China). Calcium chloride was purchased from Sigma-Aldrich (St. Louis, MO, USA).

6.2.2. Preparation experiment of CPs-Ca

According to the previous study, the chelate was prepared (hydrothermal method) (Zhang et al., 2021). CPs was dissolved in ultrapure water, and then $CaCl_2$ was added ($CaCl_2$/peptides, W/W, 1/5). The solution was stirred at 60 ℃ for 60 min to obtain peptides-calcium chelate. Then, ethanol was added to the above solution. To obtain precipitation, the reacted solution was centrifuged at 8000 × g for 15 min. The precipitate was collected after lyophilizing at –38 ℃ for 48 h and recorded as CPs-Ca.

6.2.3. Animal experiments

Eight-month-old female Sprague Dawley rats (Bodyweight 392.02 ± 34.01 g) were prepared from Weitong Lihua Laboratory Animal Technology Co., Ltd (Beijing, China). The rats were housed in a suitable environment at 25 ± 2 ℃ and 55 ± 5% of relative humidity. After acclimatization (1 week), OP rat mode was established by ovariectomy. This model is widely applied for studying OP that are relevant to postmenopausal bone loss. After recovery from surgery of rats (4 weeks), the OP rats were randomly divided into four groups (n = 6 per group). Before dietary intervention, the serum estrogen content was determined to certificate the success of the ovariectomy operation. The detailed diets of the different groups were as follows: (1) the Sham operation group (Sham group): oral gavage of physiological saline (1 mL/100 g/day); (2) the CPs group: oral gavage of collagen peptides (483 mg/kg/day, the content of Collagen peptides was equal with that of CPs-Ca group); (3) the CPs-Ca group: oral gavage of collagen peptides-calcium chelate (500 mg/kg/day); (4) the $CaCO_3$ group: oral gavage of calcium carbonate (41.9 mg/kg/day, the content of Ca^{2+} was equal with that of CPs-Ca group); (5) the OP group: oral gavage of physiological saline (1 mL/100 g/day). All rats were allowed free access to pelleted AIN-93 (calcium content 1.0%–1.8%) diet and deionized water. The dietary intervention continued for 12 weeks. Detail time nodes of the animal experiment was shown in Figure 6-1A. Meanwhile, in our previous studies, ovariectomized rats were treated with 17β-estradiol (100 μg/kg/day) rats as the drug control group (Shen et al., 2021; Zhang et al., 2020). The osteoporosis treatment of 17β-estradiol was better than CPs, CPs-Ca, and $CaCO_3$.

6.2.4. Sample collection

The feces samples were collected at the 12th week of the dietary intervention, the

feces samples were collected individually and stored at 80 ℃ to determine the gut microbiota. After rat sacrifice, blood was collected, and serum was obtained by the centrifugation of the blood at 2000 g for 15 min. The right femurs and visceral tissues (heart, liver, lung, kidney, and spleen) were stored in 4% paraformaldehyde for further analysis.

6.2.5. Bone turnover markers analysis

The bone turnover markers (BTMs) in the serum including the alkaline phosphatase (BAP), osteocalcin (OCN), procollagen type I Npeptide (PINP), tartrate-resistant acid phosphatase (TRACP), serum C-terminal telopeptide of type I collagen (S.CTX), receptor activator of nuclear factor-κB ligand (RANKL) were determined using ELISA kits (Beijing Donggeboye Biotechnology Co., Ltd., Beijing, China) according to the manufacturers.

6.2.6. Micro-CT scanning

The Micro-CT imaging was performed using the Micro-CT scan (Inveon Micro-PET/CT, Siemens, Germany) according to the manufacturer's instructions. The region of interest was set at 200 slices off an offset slice at the end of epiphyseal growth plate. The software of CTAN (version 1.17.7.2) and CTvox (version 3.30) was used to reconstruct X-ray images. Bone mineral density (BMD), bone volume fraction (BV/TV), trabecular number (Tb.N), trabecular thickness (Tb.Th), trabecular separation (Tb.Sp), and bone cortical thickness (Cw.T) were calculated.

6.2.7. Histological analysis

Samples were stored in 4% paraformaldehyde for 24 h, and then embedded in paraffin and serially sliced. The sections were stained with hematoxylin and eosin (H&E), and observed under a microscope (Olympus Inc., Tokyo, Japan). The area of the ileum villi was calculated using the Image J software (Rawak Software Inc., Stuttgart, Germany).

6.2.8. Sequencing of 16S rRNA of Gut Microbiota

The microbial total genomic DNA was extracted based on a previous study (Zhang et al., 2021). 1% agarose gel electrophoresis was used to test the DNA concentration and quality. The hypervariable region (V3-V4) of the bacterial 16S rRNA gene was amplified by PCR (ABI GeneAmp® 9700, USA) using the forward primer 338F (5′ACTCCTACGGGAGGCAGCAG-3′) and the reverse primer 806R (5′-GGACTACHVGGGTWTCTAAT-3′). The amplicons were extracted and further purified using the AxyPrep DNA Gel Extraction Kit (Axygen Biosciences, Union City, CA, USA) and quantified with a QuantiFluor™ST (Promega, USA).

After sequencing, raw fastq files were demultiplexed and quality-filtered by QIIME software package (version 1.9.1). Operational taxonomic units (OTUs) were clustered at 97% similarity using UPARSE (version 7.0.1090 http://drive5.com/uparse/). Then the clean reads were obtained by removing the chimeric reads, which was conducted using UCHIME software (version 8.1). Taxonomic annotation of OTUs was performed with RDP Classifier against the SILVA database v. 128.

6.2.9. Short chain fatty acids in feces

The fecal samples were dispersed in 75% aqueous ethanol (100 mg/mL) and mixed well. Then, the mixture was incubated in 40 ℃ water bath for 30 min and centrifuged (10000 r/min for 5 min at 4 ℃). The collected supernatant was carried out to detect short chain fatty acid contents by a gas chromatograph (Agilent 8890 B) equipped with a hydrogen flame ionization detector and an elastic quartz capillary column (30 m × 0.25 mm × 0.25 μm, DB-1, Agilent, USA). The standard including acetic acid, butyric acid, isobutyric acid, isovaleric acid, pentanoic acid, and propionic acid (> 99%) for gas chromatograph analysis were purchased from ANPEL laboratory technologies Inc (Shanghai, China).

6.2.10. Statistical analysis

Data from all measurements were presented as means ± standard deviation (SD). t-Test and Duncan's test were performed to determine statistically significant using the statistical programming language R (R Core Team, 2016). $P < 0.05$ was considered as statistically significant. *ggplot2* package of R project was applied to data visualization.

6.3. Results

6.3.1. Physical parameters

As shown in Figure 6-1B, OP group rats showed the highest body weights among all groups, and Sham group rats had the lowest body weights. The estrogen decline in OP group rats could induced weight gain (Roudebush et al., 1993). The body weights of the CPs, CPs-Ca, and $CaCO_3$ groups rat decreased during week 3 to week 12, compared with that of OP groups rats. It was speculated that collagen peptides could inhibit the weight increase caused by estrogen decline. One study discovered that food-derived active peptides could modulate the structure of the gut microbiota (Mu et al., 2022), which was one of one principal regulator of circulating estrogens (Baker et al., 2017).

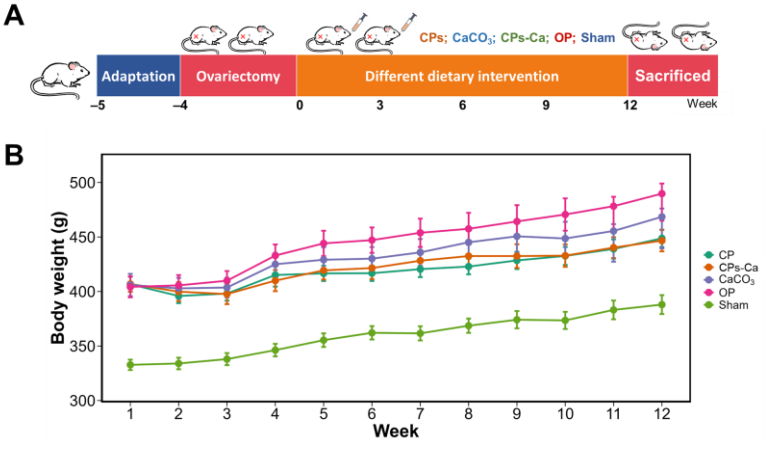

Figure 6-1: (A) Detail time nodes of the animal experiment; (B) The body weight change of rats during the experimental period. CPs: Collagen peptides group; OP: osteoporosis group; CPs-Ca: Collagen peptides-calcium chelate group; Sham: Sham operation group

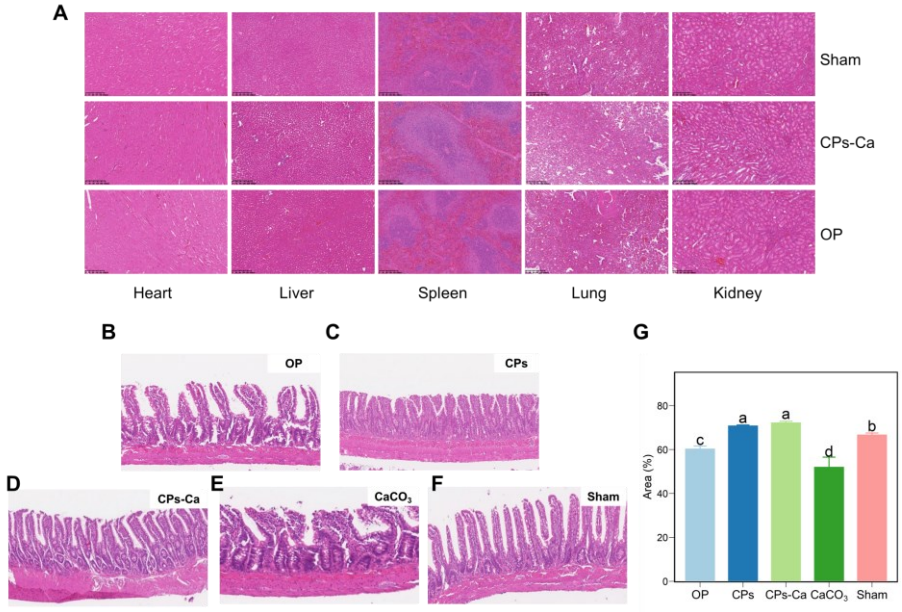

Figure 6-2: Histopathological analysis of viscera and small intestine. (A) Histopathological analysis of viscera tissues in different groups; (B–F) Histological observations of ileum villi in OP, CPs, CPs-Ca, $CaCO_3$, and Sham groups, respectively; (G) Relative area of ileum villi in different groups. Duncan's test was used to evaluate the significant differences between different groups. The different letters mean the significant difference between the two groups. CPs: Collagen peptides group; OP: osteoporosis group; CPs-Ca: Collagen peptides-calcium chelate group; Sham: Sham operation group.

6.3.2. Histopathology

In Figure 6-2A, the histopathological structure results of heart, liver, spleen, lung, and kidney did not show significant difference in all groups. This indicated that ovariectomy did not result in tissue lesion and CPs-Ca was a kind of healthy and reliable calcium supplement. To evaluate the effect of CPs-Ca on small intestine, the histological structure of ileum villi was observed by H&E stain.

The effects of dietary interventions on intestinal histological properties were determined in Figure 6-2 (B–F). The distance between adjacent ileum villi in the OP group was relatively increased than that in the Sham group. The long-term calcium deficiency might trigger the response mechanism of abnormal growth of ileum villi (Vavrusova & Skibsted, 2014). The $CaCO_3$ group showed the biggest villi spacing in all groups. The ileum villi of CPs and CPs-Ca groups exhibited tight structure. The main reason may be that $CaCO_3$ had some damages to the regularity and fullness of

villi, which was the limitations of traditional inorganic calcium supplements. Collagen peptides could prevent intestinal barrier disruption following burn injury, due to its protective effects on intestinal tight junction integrity (Chen et al., 2019). In Figure 6-2G, the relative area of villi was calculated according to the histological images. The relative area of villi in CPs and CPs-Ca groups were significantly higher than that in $CaCO_3$ and OP groups. These results indicated that CPs-Ca was a kind of calcium supplement without side effects. Further research will be carried out to confirm this.

6.3.3. Bone turnover markers

Bone turnover markers have been widely used to study the changes in bone remodeling in osteoporosis. BTMs can provide useful information for the management of osteoporosis patients, including the initial clinical assessment, guiding, and monitoring of treatment (Naylor & Eastell, 2012). Serum Ca, P, BAP, OCN, PINP, S.CTX, PINP, DPD, and TRAP are the important bone turnover markers to evaluate bone formation and resorption (Baker et al., 2017). Serum Ca, P, BAP, OCN and PINP are the bone formation markers, while TRAP, S.CTX and DPD are the bone resorption markers. The changes in these BTMs were shown in Figure 6-3. Results recorded no difference in the serum P content among all the groups. Whereas there was a significant decrease of serum Ca content in the OP group, compared with the Sham CPs, and CPs-Ca group. Meanwhile, BAP, OCN, and PINP levels in the OP group decreased significantly compared with those in the Sham group, while S.CTX, DPD, and TRAP levels increased significantly. Several studies found similar results in the osteoporosis model (Ye et al., 2018). This indicated the OP rat mode was successfully established. Compared with OP rats, CPs-Ca increased bone formation markers and decreased bone resorption markers in serum, which was consistent with anti-osteoporosis ingredients including collagen peptides (Ye et al., 2020), chondroitin sulfate calcium complex (Shen et al., 2021), and polysaccharides (Mei et al., 2021). Meanwhile, the CPs, and $CaCO_3$ groups showed varying degrees of influence to the BTMs. These changes of BTMs were induced by the dietary intervention of CPs, CPs-Ca, and $CaCO_3$, and the CPs-Ca group showed the best treatment effect.

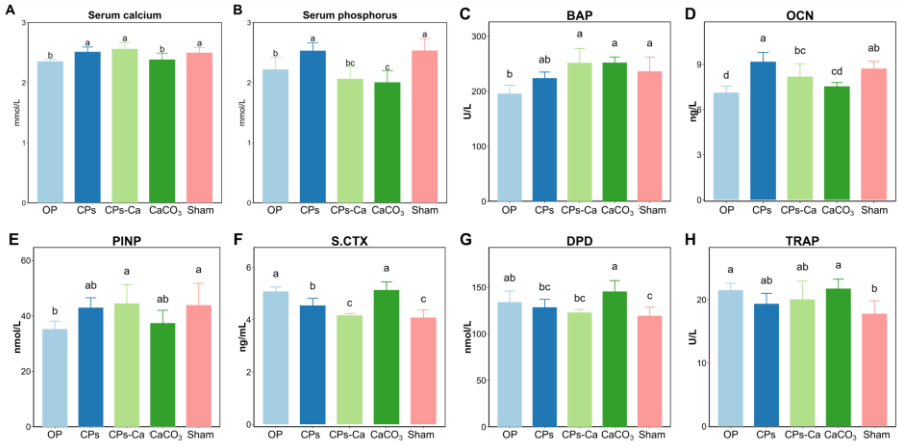

Figure: 6-3: Biochemical parameters in the serum. (A) Serum calcium; (B) Serum phosphorus; (C) Bone alkaline phosphatase (BAP); (D) Osteocalcin (OCN); (E) Procollagen type I N-peptide (PINP); (F) Serum C-terminal telopeptide of type I collagen (S.CTX); (G) Deoxypyridinoline (DPD); (H) Tartrate-resistant acid phosphatase (TRAP). Different letters mean significant differences compared with the other fraction at $P < 0.05$. CPs: Collagen peptides group; OP: osteoporosis group; CPs-Ca: Collagen peptides-calcium chelate group; Sham: Sham operation group.

6.3.4. Micro-CT analysis

The vertical and segmented micrographs of micro-CT in different groups were shown in Figure 6-4A, respectively. Compared with the Sham group, the trabeculae in the OP group was sparse and with large gaps. This indicated that the OP mode was established successfully. After CPs, $CaCO_3$, and CPs-Ca intervention, the bone structures of groups was significant improved with different degrees, compared with the OP group. According to the scanning images, the quantitative morphometry was obtained including BMD, BV.TV, Cw.T, Tb.Th, Tb.Sp, and Tb.N. Bone mineral density is the gold index for the diagnosis of OP.

As shown in Figure 6-4A, compared with the OP group, the parameters of BMD, BT.TV, and Tb.N of CPs-Ca group was increased significantly ($P < 0.05$). The CPs and $CaCO_3$ groups also showed the increased trend, and the difference did not reach a significant level. No difference of Cw.T was observed among all groups. In terms of Tb.Th, there was no difference among the OP, CPs, CPs-Ca and $CaCO_3$ groups.

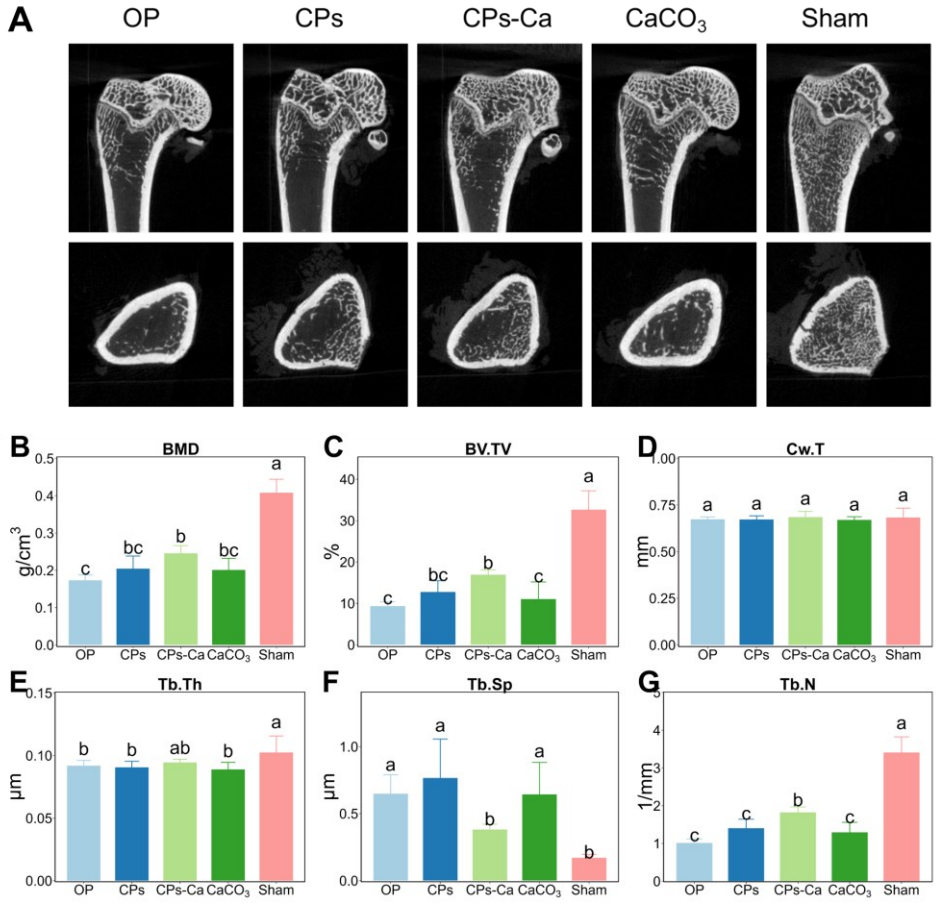

Figure 6-4: Effects of CPs-Ca on the microarchitecture femur of the OP rats. (A) Representative micro-CT images of the trabecular bone microarchitecture in the right femurs. (B) Bone mineral density (BMD). (C) Bone volume fraction (BV/TV). (D) Bone cortical thickness (Cw·T). (E) Trabecular thickness (Tb·Th). (F) Trabecular separation (Tb·Sp). (G) Trabecular number (Tb·N). The different letters mean the significant difference between the two groups ($P < 0.05$). CPs: Collagen peptides group; OP: osteoporosis group; CPs-Ca: Collagen peptides-calcium chelate group; Sham: Sham operation group.

6.3.5. Gut microbiota community

A number of studies have demonstrated that the gut microbiota is a pivotal role in bone metabolism and the pathogenesis of osteoporosis (Mei et al., 2021). Therefore, we investigated the effect of CPs-Ca on modulating gut microbiota community by 16S rRNA gene sequencing and evaluated the potential bacterial functionality using Tax4Fun analysis. Tax4Fun is a software package that predicts the functional capabilities of microbial communities based on 16S rRNA datasets.

According to the sequencing results, the total number of OTUs in the OP and CPs-Ca groups was 812 and 845, respectively. There were 24 specific OTUs in the OP group and 47 specific OTUs in the CPs-Ca group (Figure 6-5A and Figure 6-5B). Shannon index, Simpson index, Chao1 index, and Abundance-based coverage Estimator (ACE) index were applied to evaluate the gut microbial diversity in Figure 6-5C and Figure 6-5D. There was no significant difference in microbial diversity between the OP and CPs-Ca groups, indicating that CPs-Ca intervention cannot influence the gut microbiota richness and alpha diversity. To evaluate the beta diversity of gut microbiota, principal components analysis (PCA) and partial least squares discriminant analysis (PLS-DA) were performed for microbiome samples. As shown in Figure 6-5E, the samples showed two separated clusters, indicating a distinct microbial structure between the OP and CPs-Ca groups. The samples of Sham and CPs-Ca groups had high overlap. The main two PCA components accounted for 26.6% and 20.5%, respectively. As shown in Figure 6-5F, PLS-DA1 and PLS-DA2 explained 26% and 17% of the total variance, respectively. The results of PCA and PLS-DA indicated significant changes in the gut microbial profile after CPs-Ca supplementation.

The treatment of CPs-Ca could shift the structure of the gut microbiota toward that of the Sham group. Notably, the OP group had been kept away from both the CPs-Ca and Sham groups, suggesting that CPs-Ca could modulate the imbalance of OP gut microbiota back to a healthy state. In Figure 6-6 (A-C), at the phylum level, *Bacteroidetes* and *Firmicutes* were the two most abundant bacteria among all the groups, and the relative abundance displayed significant changes between the OP group and CPs-Ca group, including *Firmicutes* (92.4% in OP versus 84.9% in CPs-Ca) ($P < 0.01$) and *Bacteroidetes* (5.0% in OP versus 9.0% in CPs-Ca) ($P < 0.05$). The ratio of *Firmicutes*/*Bacteroidetes* of the CPs-Ca group (11.7%) was significantly decreased compared to that of the OP group (19.2%). The relative abundances of *Firmicutes*, *Bacteroidetes* and the ratio of *Firmicutes*/*Bacteroidetes* in the CPs-Ca group were similar to those in the Sham group. At the genus level, the microbial communities with significant differences between the OP group and CPs-Ca were shown in Figure 6-6D. The relative abundance of *Bifidobacterium*, *Escherichia-Shigella*, *Lactobacillus*, and *Allobaculum* showed a significant increase ($P < 0.05$). Linear discriminant analysis Effect Size (LEfSe) was performed to identify the characteristic bacteria (LDA score > 4.0) of the OP and CPs-Ca groups (Figure 6-6E). Our results indicated that a total of 10 different bacteria were screened, and there were 5 significant differences in the OP and CPs-Ca groups, respectively. As shown in Figure 6-6F, the functional contribution of the bacteria in the CPs-Ca group was predicted by Tax4Fun. On the KEGG pathway level I, the functional contributions of the CPs-Ca group were enriched in Environmental information processing, Genetic information processing, and Metabolism.

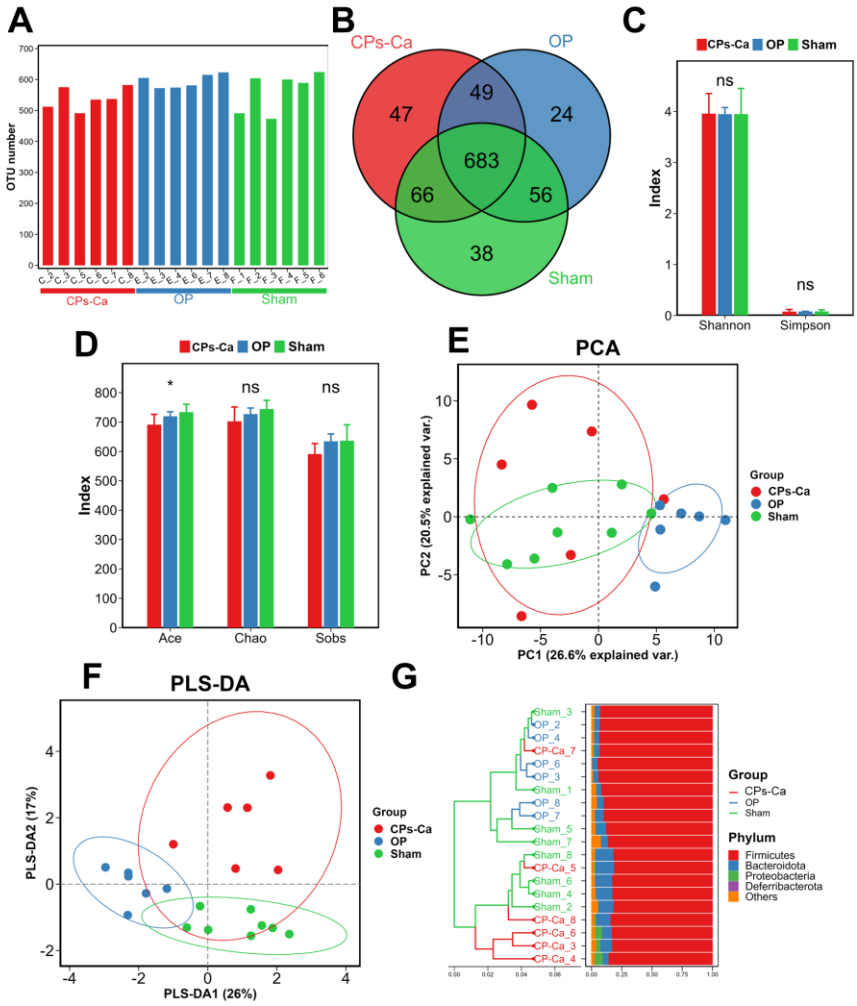

Figure 6-5: Effect of CP-Ca on the gut microbial community composition. (A) Individual OUT number. (B) Venn diagram. (C) and (D) Alpha diversity of gut microbiota. (E) Principal components analysis. (F) Partial least squares discriminant analysis. (G) Clustering analysis of the gut microbiota among samples (at order level). CPs: Collagen peptides group; OP: osteoporosis group; CPs-Ca: Collagen peptides-calcium chelate group; Sham: Sham operation group.

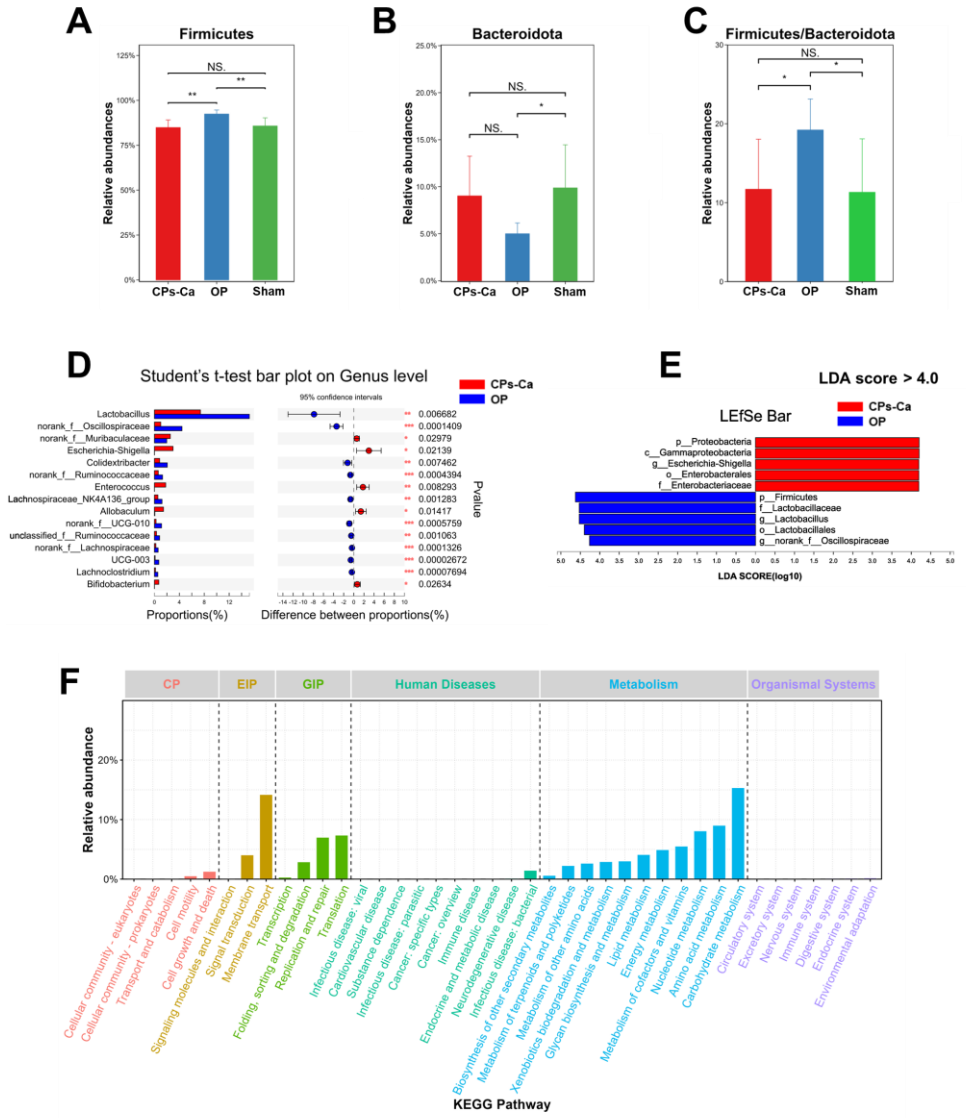

.

Figure 6-6: The significant different bacterial taxa analysis in CPs-Ca and OP groups. (A) The relative abundance of *Firmicutes* at phylum level. (B) The relative abundance of *Bacteroidota* at phylum level. (C) The ratio of *Firmicutes*/*Bacteroidota* on phylum level. (D) Student's t-test at genus level. (E) Linear discriminant analysis effect size. (F) Predictive gut microbiota functional profile in CPs-Ca group. CPs: Collagen peptides group; OP: osteoporosis group; CPs-Ca: Collagen peptides-calcium chelate group; Sham: Sham operation group.

6.3.6. Short chain fatty acids of feces

The gut microbiota is thought to modulate the bone metabolism by inducing or producing metabolites and fermentative substrates such as short chain fatty acids (SCFAs) (Koh et al., 2016). To investigate the effect of CPs-Ca diet on SCFAs, the SCFAs content in feces was determined, including acetic acid, propionic acid, butyric acid, isobutyric acid, pentanoic acid, and isovaleric acid. As shown in Figure 6-7, all the concentrations of SCFAs in CPs-Ca group were higher than that in OP group. The concentrations of butyric acid and propionic acid showed significant difference ($P < 0.05$), and the difference the acetic acid, isobutyric acid, isovaleric acid, pentanoic acid did not reach a statistically significant level.

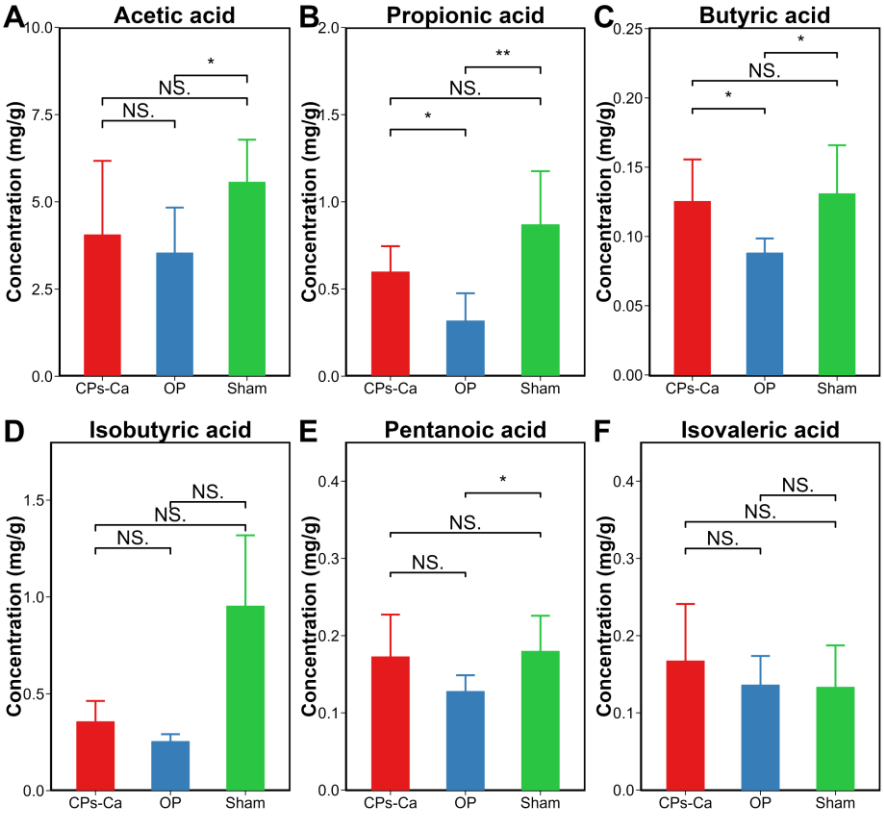

Figure 6-7: Effects of CPs-Ca on the short chain fatty acids in the feces. (A) Acetic acid content. (B) Propionic acid (C) Butyric acid. (D) Isobutyric acid. (E) Pentanoic acid. (F) Isovaleric acid. The symbols indicate statistical significance: ns ($P > 0.05$), * ($P \leq 0.05$), ** ($P \leq 0.01$), *** ($P \leq 0.001$). CPs: collagen peptides group; CPs-Ca: collagen peptides-calcium chelate group; Sham: Sham operation group.

6.4. Discussion

Osteoporosis is a kind of metabolic bone disease associated with bone metabolism, which is imbalanced by the bone formation and resorption (Mei et al., 2020). It is estimated that 50% women and 20% men will suffer an osteoporotic fracture (IOF Fracture Working Group et al., 2013). Due to the side-effects of various drugs, natural productions have attracted an increasing attention for experimental research and clinical trials in osteoporosis and other bone-related diseases. Pacific cod bone derived collagen peptides-calcium chelate could improve bioavailability of Ca and prevent Ca deficiency (Peng et al., 2017). However, the effects of collagen peptides-chelate on estrogen deficiency-induced osteoporosis are still not clear.

It is well known that bone turnover comprises two processes: the removal of old bone (resorption) and the laying down of new bone (formation) (Mei et al., 2021). Bone turnover markers can provide information that is useful for the management of patients with osteoporosis, for both the initial clinical assessment and for guiding and monitoring of treatment (Naylor & Eastell, 2012), In this study, the emerging data in the animal model of ovariectomy-induced osteoporosis indicated that exposure to CPs-Ca was advantageous to bone metabolism by increasing the bone density and the modulation of BTMs. CPs-Ca treatment increased the serum bone formation markers PINP, BAP, and OCN, which was consistent with our previous studies (Shen et al., 2021; Ye et al., 2020b). Our analysis of the serum levels of bone turnover markers demonstrated that CPs-Ca could improve bone formation and prevented bone absorption in OP rats.

Further analysis with micro-CT scanning results indicated that CPs-Ca intervention could ameliorate the ovariectomy-induced the bone microarchitecture depreciation, according to the increase of BMD, BV/TV and Tb· N and the reduction of Tb· Sp. Overall, CPs, CPs-Ca, and $CaCO_3$ treatments could improve anti-osteoporosis in ovariectomized rats, and the CPs-Ca treatment showed the best treatment. The component peptide and calcium of CPs-Ca could alleviate osteoporosis. CPs-Ca reflected the advantage of collagen peptides and calcium co-supplementation. Peptides-calcium could improve bioavailability of calcium and prevent calcium precipitation in the intestinal tract.

It is well known that the gut microbiota plays a critical role in the regulation of important biological processes and the mechanisms underlying numerous complex diseases. In the present study, the results of 16S rDNA high-throughput sequencing indicated that that the ovariectomy-induced OP could significantly promote rat bone loss and change the gut microbiota profile, inducing a totally different bacteria transfer compared with that in the Sham group. The CPs-Ca treatment could promote the bone formation in ovariectomized rats by affecting the gut microbiota and restore the gut microbiota profile to Sham group.

CPs-Ca could not influence the gut microbiota richness (alpha diversity). At the phylum level, the relative abundance of the gut microbiota displayed significant changes in the CPs-Ca group versus OP group. The relative abundances of *Firmicutes* and *Bacteroidetes*, and the ratio of *Firmicutes*/*Bacteroidetes* in CPs-Ca group were similar with Sham group. Previous study demonstrated that *Firmicutes* could activate

osteoclasts and increase inflammation (Yatsonsky et al., 2019). The ratio of *Firmicutes*/*Bacteroidetes* significantly increased in type 1 patients with upregulated TLR4, which activate the inflammation reaction by participating in the TLR4/NF-κB signaling pathway (Shen et al., 2020). It was speculated that CPs-Ca showed anti-osteoporosis by regulating inflammation reaction. Our previous study demonstrated dietary type II Collagen peptides could decrease inflammation cytokine levels in osteoarthritis rats.

Additionally, at genus level, compared with OP group, the relative content of *Bifidobacterium* and *Allobaculum* significantly increased. As many health benefits had been reported for *Allobaculum*, which related to the regulation of obesity (Zhang et al., 2021). *Bifidobacterium* longum as a probiotic could increase bone mass density in rats with bone loss after ovariectomy. Taken together, CPs-Ca intervention indicated the gut microbiota community alterations instead of CPs and were probably involved in anti-osteoporosis activity. Fecal microbiota transplantation should be used to confirm the influences of these gut microbiota communities on osteoporosis in the further study. A number of studies confirmed that *Allobaculum* linked to the butyrate content *in vivo* (Han et al., 2018; Mei et al., 2020). Thus, the content of *Allobaculum* was calculated, and it was significantly increased in CPs-Ca group (1.27%), compared with OP group (0.15%).

In our study, after CPs-Ca intervention, SCFAs level showed increase compared with that of OP group. Short chain fatty acids could directly intervene osteoclast differentiation, bone formation, and affect mineral absorption. Xiao et al., (2016) indicated that dietary mannitol increased the absorption of Ca and Mg by modifying SCFAs. Lucas et al., (2018) demonstrated that treatment of mice with SCFA significantly increases bone mass and prevents postmenopausal and inflammation-induced bone loss. Propionate and butyrate downregulate important osteoclast genes such as TRAF6 and NFATc1 (Lucas et al., 2018).

6.5. Conclusions

Our results indicated that dietary CPs-Ca can alleviate the estrogen deficiency-induced osteoporosis, which involved the gut microbiota change in the feces. For the OP rats, CPs-Ca dietary intervention increases the BMD and improves the microstructure and changes the bone formation-related or bone resorption-related BTMs level in serum. CPs-Ca dietary intervention increased the SCFs contents in feces. In addition, CPs-Ca intervention altered the gut microbiota structure in osteoporosis rat. Our results provide fundamental basis for further preclinical studies and the eventual development of CPs-Ca as a functional food to treat OP.

7

Chapter VII. General discussion, conclusions, and perspectives

7.1. General discussion

The main objective of this study was to extract collagen peptides (CPs) from cattle bones and investigate the potential anti-osteoporosis activity of collagen peptides-calcium chelate (CPs-Ca). Cattle bones, which are rich in collagen, are typically discarded during meat processing. However, the extraction of CPs usually involves the use of alkali and other chemicals, which can lead to effluent during conventional industrial production methods and cause environmental pollution. CPs-Ca, which was prepared through the chelating reaction between $CaCl_2$ and collagen peptides, has been suggested as a potential calcium supplement that can improve calcium bioavailability. Nonetheless, the *in vivo* activity of CPs-Ca on osteoporosis has been little reported and remains to be investigated. To achieve the goals of this study, the following strategies will be employed in accordance with the stated objectives.

- Cattle bones were collected to evaluate the composition (protein content, fat content, minerals content). Meanwhile, the discrimination model for the discrimination of geographical origins and species was established.
- Steam explosion technology could liquefy cattle bone for CPs preparation.
- Hydrothermal method and ultrasound method could be used to prepare CPs-Ca, which had osteogenic activity *in vitro* (MC3T3-E1 cells).
- CPs-Ca, as the calcium supplementary, alleviates the osteoporosis and modulate the gut microbiota *in vivo* (ovariectomized rat).

Each point is further discussed to better understand the preparation of CPs from cattle bone and the bone health activity of CPs-Ca as the calcium supplementary.

7.1.1. Determination of the composition of cattle bone from different regions of China

Cattle is absolutely a very important livestock sector worldwide. Bone is an important part of livestock carcass. The mass of cattle bone accounts for 20–30% of the cattle body, which is rich in protein, fat, and minerals content. Meanwhile, there is the difference of protein content and bioactivity of nutrient ingredient among cattle bone from difference geographical origin and species. Yak bone is considered as Tibetan Medicine in China. The difference in quality leads the difference price of cattle bones from difference geographical origin and species in market. The price of yak bone is roughly twice as high as that of other cattle bones available in the Chinese market, leading to incidents of food fraud, adulteration, and mislabeling.

To comprehensively evaluate the composition of cattle bone, we determined the protein content, fat content, and 50 element contents of a total of 143 cattle bone samples from eight producing regions and two species in China. The protein content in cattle bones varied from 16.67 to 24.85 g/100 g, and the fat content of cattle bone was 7.9–29.97 g/100 g. The protein content of cattle bone was not significantly affected by geographical origin and species, while the sampling site had a significant impact. In comparison, yak bone had a higher fat content than yellow cattle bone. Additionally, the sampling site had a significant effect on both protein and fat content

of cattle bone. Multivariate data analysis techniques, such as Hierarchical cluster analysis (HCA) and Linear discriminant analysis (LDA), were employed to use element contents as chemical indicators to discriminate the species and geographical origins of cattle bone samples. To avoid overfitting of the model, the K-fold cross validation was conducted. And the accuracy for species and geographical origin discrimination was 99.3% and 94.5%, respectively. The content and availability of mineral elements in soils are influenced by different factors, such as humidity, pH, and clay-humus complex. The elemental composition of vegetation reflects the differences in element concentrations in the soils where the plants are cultivated. This, in turn, determines the multi-element composition of animals that consume that vegetation.

7.1.2. Study of the effect of steam explosion on collagen peptides extraction from cattle bone

It is well known that 90% of the organic component of bone is collagen type I (Ferraro et al., 2017). Collagen is widely used in food field and medical field (Cherim et al., 2019; Irastorza et al., 2021; Zheng et al., 2022). Bioactivities of collagen peptides attracts widespread attention, such as skin health, antioxidant, antidiabetic, and bone health (Fu et al., 2019). After refining, a percentage of this waste is typically recycled as meat and bone meal for animal feed, fertilizer, and bulk pet food components. Unfortunately, this leaded to a low-value utilization of cattle bone. Chemical hydrolysis (acid and alkali hydrolysis), enzymatic hydrolysis and fermentation are the most common methods for extracting bioactive peptides. These methods have the limits of high cost, long time-consuming, and environmental pollution. The high toughness and rigidity of cattle bone lead to difficulties in collagen peptides extraction. Steam explosion is a thermophysico-chemical process used for biomass treatment. It offers advantages such as lower costs, reduced energy requirements, greater mechanical efficacy, and greater environmental friendliness.

To achieve the environment-friendly preparation of CPs, we propose using steam explosion to treat cattle bones. Here, we found that steam explosion could partially liquefy cattle bone under the given conditions of pressure and reaction time. With the increase of pressure and reaction time, the protein recovery rate and mineral release rate increased. During the SE process, cattle bone was exposed to high-pressure, saturated steam, which caused the structure of the biomass to be destroyed and decomposed through mechanical shearing and pressure. This process was effective at extracting collagen peptides and mineral releasing from the bone. However, the color of the liquid also turned brown under 2.5 MPa. The main reason may be the presence of chromophores from the aromatic amino acids including tryptophan, tyrosine, and phenylalanine (Smith, 1995). The Maillard reaction induced by SE might lead to brown-colored melanoidins. Under 2.5 MPa–30 min, the protein recovery rate reached to 62.5%. Previous studies have used variable methods to extract protein from animal bones. The protein recovery rate from chicken bone was 80.25% by hot-pressure method (130 ± 0.5 °C for 120 min), and the relative content of < 2000 Da was lower than 20% (Dong et al., 2014). Young, (1976) reported the yield of 11–17% from total protein content in animal bone. The protein recovery rate of chicken cartilage was

92.69% by the combine of hot-pressure (120 °C for 1.5 h) and enzymatic method (Shen et al., 2019). Compared to the studies above, the steam explosion method did not show an advantage in terms of protein recovery rate, but the protein extracted by steam explosion had a smaller molecular weight. In addition, steam explosion significantly decreased the molecular weight determination of collagen peptides ($P < 0.05$). The main reason for this was that steam explosion can break down peptide bonds, which leaded to a significant number of peptides and free amino acids being dissolved in water. The results of scanning electron microscope (SEM) and particle size analysis indicated that the residual solid exhibited microstructural damage and a decrease in particle size. This was caused by the mechanical sheer force of steam explosion. Amino acid analysis indicated that SE could not change the amino acid composition of collagen peptides. In summary, steam explosion could be a potential method to extract CPs from cattle bones without using chemical reagent.

7.1.3. Preparation of CPs-Ca and its bioactivity in vitro

In recent times, the use of peptides-calcium chelate as a new method of delivering calcium has garnered considerable attention. Peptides can combine with various other molecules and create larger structures through a variety of chemical bonds, such as coordination bonds, hydrophilic and hydrophobic interactions, electrostatic interactions, as well as ionic bonds. The use of chelate can improve the bioavailability of calcium by increasing its solubility and shielding it from inhibitors in the digestive tract. As a result, peptides-calcium chelate can boost calcium bioavailability and enable the bioactivity of peptides to take effect.

The hydrothermal method is a common method to collagen prepare collagen peptides-calcium chelate. In solution, peptides could aggregate to form amorphous or highly structured amyloid-like fibrils, which may limit the chelating ability of peptides. With the development of innovative food processing technologies, the ultrasound method, one of the innovative technologies, has been more widely concerned. Ultrasound can create strong forces on a microscopic level, inducing shock waves that cause chemical changes in the medium. These properties can be used to prepare peptides-calcium chelate. There is a limited amount of research on the impact of the hydrothermal and ultrasound methods on the properties of chelates.

The results presented in Chapters IV&V indicated that the chelating sites of CPs and Ca^{2+} are carboxyl oxygen, hydroxyl oxygen, and amino nitrogen atom of CPs. The results of X-ray diffraction (XRD) spectroscopy, SEM, and atomic force microscopy (AFM) showed that the structural changes after calcium chelating. Calcium ions cross-linked with peptides, resulting in the formation of ordered crystal structure and aggregation in microstructure. The stability analysis revealed the CPs-Ca was stable during thermal processing and was partially degraded in gastric environment. It had been speculated that the high concentration of H^+ under gastric conditions could compete with calcium ions for binding sites on $NH3^+$ and $COOH^-$, which may lead to the release of Ca^{2+} from CPs-Ca. The above structural properties did not show significant difference between CPs-Ca-HT (hydrothermal method) and CPs-Ca-US (ultrasound method)). CPs-Ca-US showed a more stable property in

gastric juice than CPs-Ca-HT. One possible explanation was that the ultrasound method may result in the formation of more stable coordination bonds due to mechanical agitation and mixing, as well as increased local temperatures and pressures resulting from cavitation. In cell experiments (Osteoblast, MC3T3-E1 cells), CPs-Ca could significantly improve the proliferation and mineralization of MC3T3-E1 cells and promote calcium absorption by interacting with Calcium-sensing receptor (CaSR). The osteogenic activity of CPs-Ca-US was better than that of CPs-Ca-HT, although the difference was not significant.

7.1.4. The anti-osteoporosis activity of CPs-Ca on the ovariectomized rats

Osteoporosis is a common metabolic bone disease that is characterized by reduced bone mass and the destruction of bone tissue microarchitecture, ultimately leading to an increased risk of bone fractures. Insufficient calcium intake may result in bone mobilization and ultimately lead to osteoporosis. Our previous study showed the osteogenic activity of CPs-Ca by cell experiment (in Chapter V). However, there is only a limited number of animal experiments supporting these claims.

To investigate the anti-osteoporosis activity of CPs-Ca *in vivo*, the female Sprague Dawley rat was subjected to bilateral ovariectomy to establish the osteoporosis model stimulating estrogen deficiency osteoporosis in postmenopausal women. After the 12-week dietary intervention of CPs-Ca, the bone mineral density of ovariectomized rats was improved and the number of trabeculae was increased, indicating that CPs-Ca has good anti-osteoporosis activity. Meanwhile, CPs-Ca showed better anti-osteoporosis activity than CPs. The serum levels of bone formation markers were increased, and bone resorption markers were decreased by dietary CPs-Ca. We found that CPs-Ca intervention altered the gut microbiota at the phylum and genus level of osteoporosis rats. CPs-Ca treatment resulted in increased levels of *Bifidobacterium*, *Escherichia-Shigella*, and *Allobaculum*, while simultaneously reducing levels of *Firmicutes*, as well as the *Firmicutes*/*Bacteroidetes* ratio at the phylum level. One hypothesis suggested that the anti-osteoporotic effect of CPs-Ca is achieved by modulating the inflammatory response via the gut microbiota. Meanwhile, CPs-Ca dietary intervention resulted in an elevated level of SCFAs in fecal. They have been shown to enhance calcium absorption by promoting growth of intestinal cells and increasing the absorption area (Wang et al., 2022). Our results confirmed that CPs-Ca, as a dietary supplement, had an anti-osteoporosis activity, which probably involved modulation of gut microbiota.

7.2. Conclusions

In this thesis, the protein content, fat content, and mineral content of cattle bones were determined, and its geographical origin and species were discriminated by the LDA. The effects of effect of steam explosion on collagen peptides extraction were studied. Collagen peptides-calcium chelate was prepared by hydrothermal method and ultrasound method. And its structural characteristics and anti-osteoporosis *in vivo* were investigated.

7.2.1. Determination of the composition of cattle bone from different regions of China

The protein and fat content of cattle bone were both affected by the sampling site, whereas geographical origin and species did not have a significant impact. Compared to yellow cattle bone, yak bone had a higher fat content. The geographical origin and species of yellow cattle bone and yak bone can be discriminated by the bone elemental profiles. The combined use of multi-element analysis and LDA was well-suited for the distinction of the geographic origin and species (yellow cattle vs. yak), with K-cross validation accuracies of 94.5% and 99.3%, respectively.

7.2.2. Study of the effect of steam explosion on collagen peptides extraction from cattle bone

The collagen peptides were extracted from cattle bone by steam explosion method. With the increase of pressure and reaction time, the protein recovery rate and calcium/phosphorus release increased. When exposed to 2.5 MPa for 30 minutes, the protein recovery rate of cattle bone reached 62.5%. However, steam explosion had destruction effects on the powder, reducing its average particle size and damaging its microstructure. Moreover, as pressure and reaction time increased, the degree of bone destruction also gradually increased. In addition to these effects, steam explosion under high pressure (2.5 MPa) induced undesirable color changes. The determination of molecular weight for collagen peptides was significantly reduced as a result of steam explosion.

7.2.3. Preparation of cattle bone collagen peptides-calcium chelate

The cattle bone collagen peptides were applied to prepare CPs-Ca by hydrothermal method, and the preparation conditions (pH 7, temperature 60 ℃, time 60 min, peptides/$CaCl_2$ 5/1) were optimized by single factor test, and the calcium-chelating ability reached 42.70 μg/mg. The chelating sites are carboxyl oxygen, hydroxyl oxygen, and amino nitrogen atom of CPs. After calcium chelating, the structure changed. CPs-Ca formatted ordered crystal structure and aggregated in microstructure. CPs-Ca is stable during thermal processing. The gastric digestion environment could lead to partial dissociation of CPs-Ca.

We also prepared collagen peptides-calcium chelate by ultrasound method (CPs-Ca-US), and the calcium-chelating ability reached 39.48 μg/mg. CPs-Ca-US showed the similar structural properties compared with CPs-Ca-HT. However, CPs-Ca-US showed a more stable property in gastric juice than CPs-Ca-HT. CPs-Ca-US could significantly improve the proliferation and mineralization of MC3T3-E1 cells and promote calcium absorption by interacting with CaSR.

7.2.4. Cattle bone collagen peptides-calcium chelate relieves osteoporosis by modulating gut microbiota in ovariectomized rat

Animal experiment indicated that dietary CPs-Ca could alleviate the estrogen

deficiency-induced OP in rats. For the OP rats, CPs-Ca dietary intervention increased BMD and improved the microstructure and changed the bone formation-related or bone resorption-related BTMs level in serum. CPs-Ca dietary intervention increased the SCFs contents in feces. Furthermore, intervention with CPs-Ca caused changes in the gut microbiota structure of osteoporosis rats. These results provided a fundamental basis for further preclinical studies and the eventual development of CPs-Ca as a functional food to treat OP.

7.3. Perspectives

Our results showed that the combination of bone elemental profiles and multi-element analyses can be used to discriminate the geographical origin and species of China's cattle bones. The geographical origins included eight provinces in China: Inner Mongolia, Shandong, Gansu, Henan, Shaanxi, Tibet, Sichuan, and Jilin. Sample species included yellow cattle and yak. However, the effect of sex and age was not included in this study. Due to the limited sample size of only 143 samples, there is a possibility of errors in the obtained results. This study only considered the discrimination of two species, more samples and species should be considered. The availability of the developed method in case of adulteration needs to be investigated in future studies.

Steam explosion pre-treatment can be used to produce collagen peptides. Part of cattle bone can be liquefied by the steam explosion at relatively high pressure and temperature, but the color of the liquefaction fluid becomes brown, which means that the chemical reaction of components such as proteins (peptides) or carbohydrates in the raw material has occurred. Meanwhile, the recovery rate of collagen peptides is not desired (62.5%). Thus, the process parameters for extracting the collagen peptides need to be further optimized for improving the recovery rate of collagen peptides and avoiding or reducing unpleasant color. Of course, before large-scale production, pilot-scale production must be tested in a factory.

The hydrothermal method and ultrasound method can be used to prepare the CPs-Ca. There are no obvious structural differences between CPs-Ca prepared with the two methods. However, CPs-Ca-US showed a more stable property in gastric juice than chelate prepared by the hydrothermal method. Is there a difference in anti-osteoporotic bioactivity between the two methods? This needs to be investigated *in vivo*.

As for the bioactivity of CPs-Ca, it has shown efficacy in calcium absorption by cell experiments. However, its anti-osteoporosis activity is poorly reported in animal experiments and clinical experiments. Therefore, we investigated bioactivity properties of CPs-Ca in cell experiments and animal experiments, such as cell proliferation, BTMs, and micro-CT. CPs-Ca can be used as a dietary supplement for bone care to improve bone mineral density and BTMs. However, the mechanism of CPs-Ca against osteoporosis is not clear. it is necessary to carry out a more comprehensive study of cellular pathways. On the other hand, CPs-Ca could relieve osteoporosis and modulate gut microbiota in ovariectomized rats. However, further investigations including the faecal bacteria transplantation experiments are necessary

to confirm the effect of gut microbiota caused by CPs-Ca. Additionally, before using it in the clinic, more animal experiments should be conducted to evaluate its efficacy and side effects more accurately. Based on our current animal results, CPs-Ca as a dietary supplement has a prospect for application against osteoporosis caused by estrogen deficiency.

References

Abadía-García, L., Castaño-Tostado, E., Ozimek, L., Romero-Gómez, S., Ozuna, C., & Amaya-Llano, S. L. (2016). Impact of ultrasound pretreatment on whey protein hydrolysis by vegetable proteases. *Innovative Food Science & Emerging Technologies*, *37*, 84–90. https://doi.org/10.1016/j.ifset.2016.08.010

Andrushchenko, V., Vogel, H., & Prenner, E. (2006). Solvent-dependent structure of two tryptophan-rich antimicrobial peptides and their analogs studied by FTIR and CD spectroscopy. *Biochimica et Biophysica Acta (BBA) - Biomembranes*, *1758*(10), 1596–1608. https://doi.org/10.1016/j.bbamem.2006.07.013

Asai, T., Takahashi, A., Ito, K., Uetake, T., Matsumura, Y., Ikeda, K., Inagaki, N., Nakata, M., Imanishi, Y., & Sato, K. (2019). Amount of collagen in the meat contained in japanese daily dishes and the collagen peptide content in human blood after ingestion of cooked fish meat. *Journal of Agricultural and Food Chemistry*, *67*(10), 2831–2838. https://doi.org/10.1021/acs.jafc.8b06896

Ashaolu, T. J. (2020). Soy bioactive peptides and the gut microbiota modulation. *Applied Microbiology and Biotechnology*, *104*(21), 9009–9017. https://doi.org/10.1007/s00253-020-10799-2

Baghurst, K., Record, S., & Leppard, P. (2001). Red meat consumption in australia: intakes, nutrient contribution and changes over time. *Australian Journal of Nutrition & Dietetics*, *57*, 3–36.

Baker, J. M., Al-Nakkash, L., & Herbst-Kralovetz, M. M. (2017). Estrogen–gut microbiome axis: physiological and clinical implications. *Maturitas*, *103*, 45–53. https://doi.org/10.1016/j.maturitas.2017.06.025

Balk, E. M., Adam, G. P., Langberg, V. N., Earley, A., Clark, P., Ebeling, P. R., Mithal, A., Rizzoli, R., Zerbini, C. A. F., Pierroz, D. D., Dawson-Hughes, B., & for the International Osteoporosis Foundation Calcium Steering Committee. (2017). Global dietary calcium intake among adults: a systematic review. *Osteoporosis International*, *28*(12), 3315–3324. https://doi.org/10.1007/s00198-017-4230-x

Barakat, N. A. M., Khil, M. S., Omran, A. M., Sheikh, F. A., & Kim, H. Y. (2009). Extraction of pure natural hydroxyapatite from the bovine bones bio waste by three different methods. *Journal of Materials Processing Technology*, *209*(7), 3408–3415. https://doi.org/10.1016/j.jmatprotec.2008.07.040

Barbosa, R. M., Batista, B. L., Varrique, R. M., Coelho, V. A., Campiglia, A. D., & Barbosa, F. (2014). The use of advanced chemometric techniques and trace element levels for controlling the authenticity of organic coffee. *Food Research International*, *61*, 246–251. https://doi.org/10.1016/j.foodres.2013.07.060

Barboza, G. D. de, Guizzardi, S., & Talamoni, N. T. de. (2015). Molecular aspects of intestinal calcium absorption. *World Journal of Gastroenterology*, *21*(23), 7142–7154. https://doi.org/10.3748/wjg.v21.i23.7142

Bartl, R., Frisch, B., & Bartl, C. (2009). *Osteoporosis: diagnosis, prevention, therapy* (2nd rev. ed). Springer.

Behkami, S., Zain, S. M., Gholami, M., & Bakirdere, S. (2017). Isotopic ratio analysis

of cattle tail hair: a potential tool in building the database for cow milk geographical traceability. *Food Chem*, *217*, 438–444. https://doi.org/10.1016/j.foodchem.2016.08.130

Bello, A. E., & Oesser, S. (2006). Collagen hydrolysate for the treatment of osteoarthritis and other joint disorders:a review of the literature. *Current Medical Research and Opinion*, *22*(11), 2221–2232. https://doi.org/10.1185/030079906X148373

Bonadio, T. G. M., Sato, F., Medina, A. N., Weinand, W. R., Baesso, M. L., & Lima, W. M. (2013). Bioactivity and structural properties of nanostructured bulk composites containing Nb2O5 and natural hydroxyapatite. *Journal of Applied Physics*, *113*(22), 223505. https://doi.org/10.1063/1.4809653

Brown, C. (2017). Staying strong. *Nature*, *550*(7674), 15–17. https://doi.org/10.1038/550S15a

Cabrera, M. C., Ramos, A. L. L. D. P., Saadoun, A., & Brito, G. (2010). Selenium, copper, zinc, iron and manganese content of seven meat cuts from hereford and braford steers fed pasture in uruguay. *Meat Science*, *84*(3), 518–528. https://doi.org/10.1016/j.meatsci.2009.10.007

Caetano-Silva, M. E., Netto, F. M., Bertoldo-Pacheco, M. T., Alegría, A., & Cilla, A. (2021). Peptide-metal complexes: obtention and role in increasing bioavailability and decreasing the pro-oxidant effect of minerals. *Critical Reviews in Food Science and Nutrition*, *61*(9), 1470–1489. https://doi.org/10.1080/10408398.2020.1761770

Cantarella, M., Cantarella, L., Gallifuoco, A., Spera, A., & Alfani, F. (2004). Comparison of different detoxification methods for steam-exploded poplar wood as a substrate for the bioproduction of ethanol in SHF and SSF. *Process Biochemistry*, *39*(11), 1533–1542. https://doi.org/10.1016/S0032-9592(03)00285-1

Cao, C., Xiao, Z., Ge, C., & Wu, Y. (2021). Animal by-products collagen and derived peptide, as important components of innovative sustainable food systems—a comprehensive review. *Critical Reviews in Food Science and Nutrition*, *0*(0), 1–25. https://doi.org/10.1080/10408398.2021.1931807

Chang, M., Chen, Y., Lian, Y., Chang, B., Huang, C., Huang, W., Pan, Y., & Jeng, J. (2018). Butyrate Stimulates Histone H3 Acetylation, 8-Isoprostane Production, RANKL Expression, and Regulated Osteoprotegerin Expression/Secretion in MG-63 Osteoblastic Cells. *International Journal of Molecular Sciences*, *19*(12), 4071. https://doi.org/10.3390/ijms19124071

Chen, C., & Chi, Y. (2012). Antioxidant, ace inhibitory activities and functional properties of egg white protein hydrolysate: biological activities and functional properties. *Journal of Food Biochemistry*, *36*(4), 383–394. https://doi.org/10.1111/j.1745-4514.2011.00555.x

Chen, J. W., & Kalback, W. M. (1967). Effect of ultrasound on chemical reaction rate. *Industrial & Engineering Chemistry Fundamentals*, *6*(2), 175–178. https://doi.org/10.1021/i160022a003

Chen, M., Ji, H., Zhang, Z., Zeng, X., Su, W., & Liu, S. (2019). A novel calcium-chelating peptide purified from auxis thazard protien hydrolysate and its binding properties with calcium. *Journal of Functional Foods*, *60*, 103447. https://doi.org/10.1016/j.jff.2019.103447

Chen, Q., Gao, X., Zhang, H., Li, B., Yu, G., & Li, B. (2019). Collagen peptides administration in early enteral nutrition intervention attenuates burn-induced intestinal barrier disruption: effects on tight junction structure. *Journal of Functional Foods*, *55*, 167–174. https://doi.org/10.1016/j.jff.2019.02.028

Chen, Y., Greenbaum, J., Shen, H., & Deng, H. (2017). Association between gut microbiota and bone health: potential mechanisms and prospective. *The Journal of Clinical Endocrinology & Metabolism*, *102*(10), 3635–3646. https://doi.org/10.1210/jc.2017-00513

Chen, Y., Guo, Y., Liu, Y., Zhang, C., Huang, F., & Chen, L. (2022). Identification of Di/Tripeptide(s) With Osteoblasts Proliferation Stimulation Abilities of Yak Bone Collagen by in silico Screening and Molecular Docking. *Frontiers in Nutrition*, *9*. https://www.frontiersin.org/articles/10.3389/fnut.2022.874259

Cherim, M., Mustafa, A., Cadar, E., Lupașcu, N., Paris, S., & Sirbu, R. (2019). Collagen Sources and Areas of Use. *European Journal of Medicine and Natural Sciences*, *2*(2), 8–13. https://doi.org/10.26417/ejis.v4i1.p122-128

Conde-Mejía, C., Jiménez-Gutiérrez, A., & El-Halwagi, M. (2012). A comparison of pretreatment methods for bioethanol production from lignocellulosic materials. *Process Safety and Environmental Protection*, *90*(3), 189–202. https://doi.org/10.1016/j.psep.2011.08.004

Cui, P., Lin, S., Han, W., Jiang, P., Zhu, B., & Sun, N. (2019). Calcium delivery system assembled by a nanostructured peptide derived from the sea cucumber ovum. *Journal of Agricultural and Food Chemistry*, *67*(44), 12283–12292. https://doi.org/10.1021/acs.jafc.9b04522

Cui, P., Lin, S., Jin, Z., Zhu, B., Song, L., & Sun, N. (2018). In vitro digestion profile and calcium absorption studies of a sea cucumber ovum derived heptapeptide–calcium complex. *Food & Function*, *9*(9), 4582–4592. https://doi.org/10.1039/C8FO00910D

Cui, P., Sun, N., Jiang, P., Wang, D., & Lin, S. (2017). Optimised condition for preparing sea cucumber ovum hydrolysate–calcium complex and its structural analysis. *International Journal of Food Science & Technology*, *52*(8), 1914–1922. https://doi.org/10.1111/ijfs.13468

Cui, Y., Yang, L., Lu, W., Yang, H., Zhang, Y., Zhou, X., Ma, Y., Feng, J., & Shen, Q. (2021). Effect of steam explosion pretreatment on the production of microscale tuna bone power by ultra-speed pulverization. *Food Chemistry*, *347*, 129011. https://doi.org/10.1016/j.foodchem.2021.129011

D'Amelio, P., & Sassi, F. (2018). Gut microbiota, immune system, and bone. *Calcified Tissue International*, *102*(4), 415–425. https://doi.org/10.1007/s00223-017-0331-y

Damodaran, S., & Wang, S. (2017). Ice crystal growth inhibition by peptides from fish gelatin hydrolysate. *Food Hydrocolloids*, *70*, 46–56. https://doi.org/10.1016/j.foodhyd.2017.03.029

Ding, L., Wang, L., Zhang, Y., & Liu, J. (2015). Transport of antihypertensive peptide RVPSL, ovotransferrin 328–332, in human intestinal caco-2 cell monolayers. *Journal of Agricultural and Food Chemistry*, *63*(37), 8143–8150. https://doi.org/10.1021/acs.jafc.5b01824

do Amaral, E. S., Vieira Silva, D., Dos Anjos, L., Schilling, A. C., Dalmolin, Â. C., & Mielke, M. S. (2019). Relationships between reflectance and absorbance chlorophyll indices with RGB (red, green, blue) image components in seedlings of tropical tree species at nursery stage. *New Forests*, *50*(3), 377–388. https://doi.org/10.1007/s11056-018-9662-4

Dong, X., Li, X., Zhang, C., Wang, J., Tang, C., Sun, H., Jia, W., Li, Y., & Chen, L. (2014). Development of a novel method for hot-pressure extraction of protein from chicken bone and the effect of enzymatic hydrolysis on the extracts. *Food Chemistry*, *157*, 339–346. https://doi.org/10.1016/j.foodchem.2014.02.043

Dong, Z. Y., Li, M. Y., Tian, G., Zhang, T. H., Ren, H., & Quek, S. Y. (2019). Effects of ultrasonic pretreatment on the structure and functionality of chicken bone protein prepared by enzymatic method. *Food Chemistry*, *299*, 125103. https://doi.org/10.1016/j.foodchem.2019.125103

Doyle, B. B., Bendit, E. G., & Blout, E. R. (1975). Infrared spectroscopy of collagen and collagen-like polypeptides. *Biopolymers*, *14*(5), 937–957. https://doi.org/10.1002/bip.1975.360140505

Drivelos, S. A., & Georgiou, C. A. (2012). Multi-element and multi-isotope-ratio analysis to determine the geographical origin of foods in the european union. *Trac Trends in Analytical Chemistry*, *40*, 38–51. https://doi.org/10.1016/j.trac.2012.08.003

Eastridge, M. L. (2006). Major advances in applied dairy cattle nutrition. *Journal of Dairy Science*, *89*(4), 1318–1323. https://doi.org/10.3168/jds.S0022-0302(06)72199-3

Epova, E. N., Bérail, S., Séby, F., Barre, J. P. G., Vacchina, V., Médina, B., Sarthou, L., & Donard, O. F. X. (2020). Potential of lead elemental and isotopic signatures for authenticity and geographical origin of bordeaux wines. *Food Chemistry*, *303*, 125277. https://doi.org/10.1016/j.foodchem.2019.125277

Fantuz, F., Salimei, E., & Papademas, P. (2016). *Macro- and micronutrients in non-cow milk and products and their impact on human health* (Vol. 9).

Ferraro, V., Gaillard-Martinie, B., Sayd, T., Chambon, C., Anton, M., & Santé-Lhoutellier, V. (2017). Collagen type I from bovine bone. effect of animal age, bone anatomy and drying methodology on extraction yield, self-assembly, thermal behaviour and electrokinetic potential. *International Journal of Biological Macromolecules*, *97*, 55–66. https://doi.org/10.1016/j.ijbiomac.2016.12.068

Fu, Y., Therkildsen, M., Aluko, R. E., & Lametsch, R. (2019). Exploration of collagen recovered from animal by-products as a precursor of bioactive peptides: successes

and challenges. *Critical Reviews in Food Science and Nutrition*, *59*(13), 2011–2027. https://doi.org/10.1080/10408398.2018.1436038

Gemede, H. F. (2014). Antinutritional factors in plant foods: potential health benefits and adverse effects. *International Journal of Nutrition and Food Sciences*, *3*(4), 284. https://doi.org/10.11648/j.ijnfs.20140304.18

Gülseren, İ., Güzey, D., Bruce, B. D., & Weiss, J. (2007). Structural and functional changes in ultrasonicated bovine serum albumin solutions. *Ultrasonics Sonochemistry*, *14*(2), 173–183. https://doi.org/10.1016/j.ultsonch.2005.07.006

Guo, D., Liu, W., Zhang, X., Zhao, M., Zhu, B., Hou, T., & He, H. (2019). Duck egg white–derived peptide VSEE (val-ser-glu-glu) regulates bone and lipid metabolisms by wnt/β-catenin signaling pathway and intestinal microbiota. *Molecular Nutrition & Food Research*, *63*(24), 1900525. https://doi.org/10.1002/mnfr.201900525

Guo, D., Zhao, M., Xu, W., He, H., Li, B., & Hou, T. (2021). Dietary interventions for better management of osteoporosis: an overview. *Critical Reviews in Food Science and Nutrition*, 1–20. https://doi.org/10.1080/10408398.2021.1944975

Guo, J., Ding, Y., Zhu, K., Sun, X., Peng, W., & Zhou, H. (2015). Effect of steam flash explosion pretreatment on phytate degradation of wheat bran. *Food and Bioprocess Technology*, *8*(7), 1552–1560. https://doi.org/10.1007/s11947-015-1517-9

Guo, Z., Liu, C., Hu, B., Zhu, L., Yang, Y., Liu, F., Gu, Z., Xin, Y., & Zhang, L. (2021). Simulated gastrointestinal digestion of yak bone collagen hydrolysates and insights into its effects on gut microbiota composition in mice. *Food Bioscience*, *44*, 101463. https://doi.org/10.1016/j.fbio.2021.101463

Han, K., Jin, W., Mao, Z., Dong, S., Zhang, Q., Yang, Y., Chen, B., Wu, H., & Zeng, M. (2018). Microbiome and butyrate production are altered in the gut of rats fed a glycated fish protein diet. *Journal of Functional Foods*, *47*, 423–433. https://doi.org/10.1016/j.jff.2018.06.007

Harper, B. A., Barbut, S., Lim, L.-T., & Marcone, M. F. (2012). Microstructural and textural investigation of various manufactured collagen sausage casings. *Food Research International*, *49*(1), 494–500. https://doi.org/10.1016/j.foodres.2012.07.043

Hong, H., Fan, H., Chalamaiah, M., & Wu, J. (2019). Preparation of low-molecular-weight, collagen hydrolysates (peptides): current progress, challenges, and future perspectives. *Food Chemistry*, *301*, 125222. https://doi.org/10.1016/j.foodchem.2019.125222

Hong, H., Roy, B. C., Chalamaiah, M., Bruce, H. L., & Wu, J. (2018). Pretreatment with formic acid enhances the production of small peptides from highly cross-linked collagen of spent hens. *Food Chemistry*, *258*, 174–180. https://doi.org/10.1016/j.foodchem.2018.03.036

Hou, H., Li, B., Zhao, X., Zhang, Z., & Li, P. (2011). Optimization of enzymatic hydrolysis of alaska pollock frame for preparing protein hydrolysates with low-

bitterness. *LWT - Food Science and Technology*, *44*(2), 421–428. https://doi.org/10.1016/j.lwt.2010.09.009

Hou, H., Wang, S., Zhu, X., Li, Q., Fan, Y., Cheng, D., & Li, B. (2018). A novel calcium-binding peptide from antarctic krill protein hydrolysates and identification of binding sites of calcium-peptide complex. *Food Chemistry*, *243*, 389–395. https://doi.org/10.1016/j.foodchem.2017.09.152

Hou, T., Liu, Y., Guo, D., Li, B., & He, H. (2017). Collagen peptides from crucian skin improve calcium bioavailability and structural characterization by HPLC–ESI-MS/MS. *Journal of Agricultural and Food Chemistry*, *65*(40), 8847–8854. https://doi.org/10.1021/acs.jafc.7b03059

Hou, T., Wang, C., Ma, Z., Shi, W., Weiwei, L., & He, H. (2015). Desalted duck egg white peptides: promotion of calcium uptake and structure characterization. *Journal of Agricultural and Food Chemistry*, *63*(37), 8170–8176. https://doi.org/10.1021/acs.jafc.5b03097

Hu, C. H., Yao, C. H., Chan, T. M., Huang, T. L., Sen, Y., Huang, C. Y., & Ho, C. Y. (2016). Effects of Different Concentrations of Collagenous Peptide from Fish Scales on Osteoblast Proliferation and Osteoclast Resorption. *The Chinese Journal of Physiology*, *59*(4), 191–201. https://doi.org/10.4077/CJP.2016.BAE398

Hu, R., Chen, G., & Li, Y. (2020). Production and characterization of antioxidative hydrolysates and peptides from corn gluten meal using papain, ficin, and bromelain. *Molecules*, *25*(18), 4091. https://doi.org/10.3390/molecules25184091

Huang, S., Zhao, L., Cai, X., Wang, S., Bao, Y., Hong, J., & Rao, P. (2015). Purification and characterisation of a glutamic acid-containing peptide with calcium-binding capacity from whey protein hydrolysate. *Journal of Dairy Research*, *82*(1), 29–35. https://doi.org/10.1017/S0022029914000715

Huang, W., Lan, Y., Liao, W., Lin, L., Liu, G., Xu, H., Xue, J., Guo, B., Cao, Y., & Miao, J. (2021). Preparation, characterization and biological activities of egg white peptides-calcium chelate. *LWT-Food Science and Technology*, *149*, 112035. https://doi.org/10.1016/j.lwt.2021.112035

Hwang, I., Seo, E., & Ha, H. (2009). Wnt/β-catenin signaling: a novel target for therapeutic intervention of fibrotic kidney disease. *Archives of Pharmacal Research*, *32*(12), 1653–1662. https://doi.org/10.1007/s12272-009-2200-3

IOF Fracture Working Group, Åkesson, K., Marsh, D., Mitchell, P. J., McLellan, A. R., Stenmark, J., Pierroz, D. D., Kyer, C., & Cooper, C. (2013). Capture the fracture: a best practice framework and global campaign to break the fragility fracture cycle. *Osteoporosis International*, *24*(8), 2135–2152. https://doi.org/10.1007/s00198-013-2348-z

Irastorza, A., Zarandona, I., Andonegi, M., Guerrero, P., & de la Caba, K. (2021). The versatility of collagen and chitosan: From food to biomedical applications. *Food Hydrocolloids*, *116*, 106633. https://doi.org/10.1016/j.foodhyd.2021.106633

Jacquet, N., Maniet, G., Vanderghem, C., Delvigne, F., & Richel, A. (2015). Application of steam explosion as pretreatment on lignocellulosic material: a review. *Industrial & Engineering Chemistry Research*, *54*(10), 2593–2598.

https://doi.org/10.1021/ie503151g

Jacquet, N., Quiévy, N., Vanderghem, C., Janas, S., Blecker, C., Wathelet, B., Devaux, J., & Paquot, M. (2011). Influence of steam explosion on the thermal stability of cellulose fibres. *Polymer Degradation and Stability*, *96*(9), 1582–1588. https://doi.org/10.1016/j.polymdegradstab.2011.05.021

Ji, H., Zhao, W., & Yu, Z. (2022). Interaction mechanism of three egg protein derived ACE inhibitory tri-peptides and DPPC membrane using FS, FTIR, and DSC studies. *Food Chemistry: X*, *15*, 100366. https://doi.org/10.1016/j.fochx.2022.100366

Jia, W., Liu, W., Mi, S., Zhang, C., Li, X., Wu, T., & Yu, Q. (2017). Comparison of six methylation methods for fatty acid determination in yak bone using gas chromatography. *Food Analytical Methods*, *10*, 3496–3507. https://doi.org/10.1007/s12161-017-0881-7

Jung, G., Park, Y., & Han, J. (2010). Effects of HA released calcium ion on osteoblast differentiation. *Journal of Materials Science: Materials in Medicine*, *21*(5), 1649–1654. https://doi.org/10.1007/s10856-010-4011-y

Kadam, S. U., Tiwari, B. K., Álvarez, C., & O'Donnell, C. P. (2015). Ultrasound applications for the extraction, identification and delivery of food proteins and bioactive peptides. *Trends in Food Science & Technology*, *46*(1), 60–67. https://doi.org/10.1016/j.tifs.2015.07.012

Karabagias, I. K., Louppis, A. P., Karabournioti, S., Kontakos, S., Papastephanou, C., & Kontominas, M. G. (2017). Characterization and geographical discrimination of commercial citrus spp. honeys produced in different mediterranean countries based on minerals, volatile compounds and physicochemical parameters, using chemometrics. *Food Chemistry*, *217*, 445–455. https://doi.org/10.1016/j.foodchem.2016.08.124

Karami, Z., & Akbari-adergani, B. (2019). Bioactive food derived peptides: a review on correlation between structure of bioactive peptides and their functional properties. *Journal of Food Science and Technology*, *56*(2), 535–547. https://doi.org/10.1007/s13197-018-3549-4

Kelly, S. D., Heaton, K., & Hoogewerff, J. (2005). Tracing the geographical origin of food: the application of multi-element and multi-isotope analysis. *Trends in Food Science and Technology*, *16*(12), 555–567. https://doi.org/10.1016/j.tifs.2005.08.008

Khosla, S., & Hofbauer, L. C. (2017). Osteoporosis treatment: recent developments and ongoing challenges. *The Lancet Diabetes & Endocrinology*, *5*(11), 898–907. https://doi.org/10.1016/S2213-8587(17)30188-2

Kim, J. S., Hwang, I. M., Lee, G. H., Park, Y. M., Choi, J. Y., Jamila, N., Khan, N., & Kim, K. S. (2017). Geographical origin authentication of pork using multi-element and multivariate data analyses. *Meat Science*, *123*, 13–20. https://doi.org/10.1016/j.meatsci.2016.08.011

Kim, K., & Thornton, I. (1993). Influence of ordovician uraniferous black shales on

the trace element composition of soils and food crops, korea. *Applied Geochemistry*, *8*, 249–255. https://doi.org/10.1016/S0883-2927(09)80045-0

Koh, A., De Vadder, F., Kovatcheva-Datchary, P., & Bäckhed, F. (2016). From dietary fiber to host physiology: short-chain fatty acids as key bacterial metabolites. *Cell*, *165*(6), 1332–1345. https://doi.org/10.1016/j.cell.2016.05.041

Kondo, T., & Kano, E. (1988). Effect of free radicals induced by ultrasonic cavitation on cell killing. *International Journal of Radiation Biology*, *54*(3), 475–486. https://doi.org/10.1080/09553008814551841

Kong, F., Zeng, Q., Li, Y., Di, X., Ding, Y., & Guo, X. (2022). Effect of steam explosion on nutritional components, physicochemical and rheological properties of brown rice powder. *Frontiers in Nutrition*, *9*, 954654. https://doi.org/10.3389/fnut.2022.954654

Lama-Muñoz, A., Rubio-Senent, F., Bermúdez-Oria, A., Fernández-Bolaños, J., Prior, Á. F., & Rodríguez-Gutiérrez, G. (2019). The use of industrial thermal techniques to improve the bioactive compounds extraction and the olive oil solid waste utilization. *Innovative Food Science & Emerging Technologies*, *55*, 11–17. https://doi.org/10.1016/j.ifset.2019.05.009

León-López, A., Morales-Peñaloza, A., Martínez-Juárez, V. M., Vargas-Torres, A., Zeugolis, D. I., & Aguirre-Álvarez, G. (2019). Hydrolyzed collagen—sources and applications. *Molecules*, *24*(22), 4031. https://doi.org/10.3390/molecules24224031

Li, B., Yang, W., Nie, Y., Kang, F., Goff, H. D., & Cui, S. W. (2019). Effect of steam explosion on dietary fiber, polysaccharide, protein and physicochemical properties of okara. *Food Hydrocolloids*, *94*, 48–56. https://doi.org/10.1016/j.foodhyd.2019.02.042

Li, H., Hu, Y., Zhao, X., Wan, W., Du, X., Kong, B., & Xia, X. (2021). Effects of different ultrasound powers on the structure and stability of protein from sea cucumber gonad. *LWT- Food Science and Technology*, *137*, 110403. https://doi.org/10.1016/j.lwt.2020.110403

Li, L., & Wang, Z. (2018). Ovarian aging and osteoporosis. In Z. Wang (Ed.), *Aging and Aging-Related Diseases: Mechanisms and Interventions* (pp. 199–215). Springer. https://doi.org/10.1007/978-981-13-1117-8_13

Li, Y., Amorim, M., Marques, C., Calhau, C., & Pintado, M. (2016). Effects of whey peptide extract on the growth of probiotics and gut microbiota. *Journal of Functional Foods*, *21*, 507–516. https://doi.org/10.1016/j.jff.2015.10.035

Liao, W., Chen, H., Jin, W., Yang, Z., Cao, Y., & Miao, J. (2020). Three newly isolated calcium-chelating peptides from tilapia bone collagen hydrolysate enhance calcium absorption activity in intestinal caco-2 cells. *Journal of Agricultural and Food Chemistry*, *68*(7), 2091–2098. https://doi.org/10.1021/acs.jafc.9b07602

Lima, C. M., Fernandes, D. D. S., Pereira, G. E., Gomes, A. A., Araujo, M. C. U., & Diniz, P. (2020). Digital image-based tracing of geographic origin, winemaker, and grape type for red wine authentication. *Food Chem*, *312*, 126–136.

https://doi.org/10.1016/j.foodchem.2019.126060

Lin, J., Cai, X., Tang, M., & Wang, S. (2015). Preparation and evaluation of the chelating nanocomposite fabricated with marine algae schizochytrium sp. protein hydrolysate and calcium. *Journal of Agricultural and Food Chemistry*, *63*(44), 9704–9714. https://doi.org/10.1021/acs.jafc.5b04001

Long, C. G., Braswell, E., Zhu, D., Apigo, J., Baum, J., & Brodsky, B. (1993). Characterization of collagen-like peptides containing interruptions in the repeating gly-X-Y sequence. *Biochemistry*, *32*(43), 11688–11695. https://doi.org/10.1021/bi00094a027

Lucas, S., Omata, Y., Hofmann, J., Böttcher, M., Iljazovic, A., Sarter, K., Albrecht, O., Schulz, O., Krishnacoumar, B., Krönke, G., Herrmann, M., Mougiakakos, D., Strowig, T., Schett, G., & Zaiss, M. M. (2018). Short-chain fatty acids regulate systemic bone mass and protect from pathological bone loss. *Nature Communications*, *9*(1). https://doi.org/10.1038/s41467-017-02490-4

Macfarlane, S., & Macfarlane, G. T. (2003). Regulation of short-chain fatty acid production. *Proceedings of the Nutrition Society*, *62*(1), 67–72. https://doi.org/10.1079/PNS2002207

Magdas, D. A., Feher, I., Cristea, G., Voica, C., Tabaran, A., Mihaiu, M., Cordea, D. V., Balteanu, V. A., & Dan, S. D. (2019). Geographical origin and species differentiation of transylvanian cheese. comparative study of isotopic and elemental profiling vs. DNA results. *Food Chem*, *277*, 307–313. https://doi.org/10.1016/j.foodchem.2018.10.103

Malison, A., Arpanutud, P., & Keeratipibul, S. (2021). Chicken foot broth byproduct: a new source for highly effective peptide-calcium chelate. *Food Chemistry*, *345*, 128713. https://doi.org/10.1016/j.foodchem.2020.128713

Maniet, G., Schmetz, Q., Jacquet, N., Temmerman, M., Gofflot, S., & Richel, A. (2017). Effect of steam explosion treatment on chemical composition and characteristic of organosolv fescue lignin. *Industrial Crops and Products*, *99*, 79–85. https://doi.org/10.1016/j.indcrop.2017.01.015

Marciniak, A., Suwal, S., Naderi, N., Pouliot, Y., & Doyen, A. (2018). Enhancing enzymatic hydrolysis of food proteins and production of bioactive peptides using high hydrostatic pressure technology. *Trends in Food Science & Technology*, *80*, 187–198. https://doi.org/10.1016/j.tifs.2018.08.013

Markiewicz, B., Sajnóg, A., Lorenc, W., Hanć, A., Komorowicz, I., Suliburska, J., Kocyłowski, R., & Barałkiewicz, D. (2017). Multielemental analysis of 18 essential and toxic elements in amniotic fluid samples by ICP-MS: full procedure validation and estimation of measurement uncertainty. *Talanta*, *174*, 122–130. https://doi.org/10.1016/j.talanta.2017.05.078

Matsumura, N., Fujii, M., Takeda, Y., Sugita, K., & Shimizu, T. (1993). Angiotensin I-converting enzyme inhibitory peptides derived from bonito bowels autolysate. *Bioscience, Biotechnology, and Biochemistry*, *57*(5), 695–697. https://doi.org/10.1271/bbb.57.695

McCabe, L., Britton, R. A., & Parameswaran, N. (2015). Prebiotic and probiotic regulation of bone health: role of the intestine and its microbiome. *Current Osteoporosis Reports*, *13*(6), 363–371. https://doi.org/10.1007/s11914-015-0292-x

Mei, F., Duan, Z., Chen, M., Lu, J., Zhao, M., Li, L., Shen, X., Xia, G., & Chen, S. (2020). Effect of a high-collagen peptide diet on the gut microbiota and short-chain fatty acid metabolism. *Journal of Functional Foods*, *75*, 104278. https://doi.org/10.1016/j.jff.2020.104278

Mei, F., Meng, K., Gu, Z., Yun, Y., Zhang, W., Zhang, C., Zhong, Q., Pan, F., Shen, X., Xia, G., & Chen, H. (2021). Arecanut (*areca catechu* L.) seed polyphenol-ameliorated osteoporosis by altering gut microbiome via LYZ and the immune system in estrogen-deficient rats. *Journal of Agricultural and Food Chemistry*, *69*(1), 246–258. https://doi.org/10.1021/acs.jafc.0c06671

Melton III, L. J., Johnell, O., Lau, E., Mautalen, C. A., & Seeman, E. (2004). Osteoporosis and the global competition for health care resources. *Journal of Bone and Mineral Research*, *19*(7), 1055–1058. https://doi.org/10.1359/JBMR.040316

Mi, S., Shang, K., Jia, W., Zhang, C., & Fan, Y. (2019). Characterization and authentication of taihe black-boned silky fowl (gallus gallus domesticus brisson) muscles based on mineral profiling using ICP-MS. *Microchemical Journal*, *144*, 26–32. https://doi.org/10.1016/j.microc.2018.08.027

Mu, J., Lin, Q., & Liang, Y. (2022). An update on the effects of food-derived active peptides on the intestinal microecology. *Critical Reviews in Food Science and Nutrition*, 1–15. https://doi.org/10.1080/10408398.2022.2094889

Naylor, K., & Eastell, R. (2012). Bone turnover markers: use in osteoporosis. *Nature Reviews Rheumatology*, *8*(7), 379–389. https://doi.org/10.1038/nrrheum.2012.86

Nguyen, C. T., Yuan, M., Yu, J. S., Ye, T., Cao, H., & Xu, F. (2018). Isolation of ice structuring collagen peptide by ice affinity adsorption, its ice-binding mechanism and breadmaking performance in frozen dough. *Journal of Food Biochemistry*, *42*(3), e12506. https://doi.org/10.1111/jfbc.12506

Nie, J., Shao, S., Xia, W., Liu, Z., Yu, C., Li, R., Wang, W., Li, J., Yuan, Y., & Rogers, K. M. (2020). Stable isotopes verify geographical origin of yak meat from qinghai-tibet plateau. *Meat Science*, *165*, 108–113. https://doi.org/10.1016/j.meatsci.2020.108113

Nijhuis, W. H., Eastwood, D. M., Allgrove, J., Hvid, I., Weinans, H. H., Bank, R. A., & Sakkers, R. J. (2019). Current concepts in osteogenesis imperfecta: bone structure, biomechanics and medical management. *Journal of Children's Orthopaedics*, *13*(1), 1–11. https://doi.org/10.1302/1863-2548.13.180190

Nordin, B. E. C. (1997). Calcium and osteoporosis. *Nutrition*, *13*(7), 664–686. https://doi.org/10.1016/S0899-9007(97)83011-0

Nordin, B. E. C., Need, A. G., Steurer, T., Morris, H. A., Chatterton, B. E., & Horowitz, M. (1998). Nutrition, osteoporosis, and aging. *Annals of the New York Academy of Sciences*, *854*(1), 336–351. https://doi.org/10.1111/j.1749-6632.1998.tb09914.x

Ohlsson, C., & Sjögren, K. (2015). Effects of the gut microbiota on bone mass. *Trends in Endocrinology & Metabolism*, *26*(2), 69–74. https://doi.org/10.1016/j.tem.2014.11.004

Olszta, M. J., Cheng, X., Jee, S. S., Kumar, R., Kim, Y.-Y., Kaufman, M. J., Douglas, E. P., & Gower, L. B. (2007). Bone structure and formation: a new perspective. *Materials Science and Engineering: R: Reports*, *58*(3), 77–116. https://doi.org/10.1016/j.mser.2007.05.001

Ortea, I., & Gallardo, J. M. (2015). Investigation of production method, geographical origin and species authentication in commercially relevant shrimps using stable isotope ratio and/or multi-element analyses combined with chemometrics: an exploratory analysis. *Food Chemistry*, *170*, 145–153. https://doi.org/10.1016/j.foodchem.2014.08.049

Osborne, C. G., McTyre, R. B., Dudek, J., Roche, K. E., Scheuplein, R., Silverstein, B., Weinberg, M. S., & Salkeld, A. A. (2009). Evidence for the relationship of calcium to blood pressure. *Nutrition Reviews*, *54*(12), 365–381. https://doi.org/10.1111/j.1753-4887.1996.tb03850.x

Oxlund, H., Sekilde, Li., & Ørtoft, G. (1996). Reduced concentration of collagen reducible cross links in human trabecular bone with respect to age and osteoporosis. *Bone*, *19*(5), 479–484. https://doi.org/10.1016/S8756-3282(96)00283-9

Peacock, M. (2010). Calcium metabolism in health and disease. *Clinical Journal of the American Society of Nephrology*, *5*(1), 23–30. https://doi.org/10.2215/CJN.05910809

Peng, Z., Hou, H., Zhang, K., & Li, B. (2017). Effect of calcium-binding peptide from pacific cod (gadus macrocephalus) bone on calcium bioavailability in rats. *Food Chemistry*, *221*, 373–378. https://doi.org/10.1016/j.foodchem.2016.10.078

Prakash, K. H., Kumar, R., Ooi, C. P., Cheang, P., & Khor, K. A. (2006). Apparent solubility of hydroxyapatite in aqueous medium and its influence on the morphology of nanocrystallites with precipitation temperature. *Langmuir*, *22*(26), 11002–11008. https://doi.org/10.1021/la0621665

Proksch, E., Schunck, M., Zague, V., Segger, D., Degwert, J., & Oesser, S. (2014). Oral intake of specific bioactive collagen peptides reduces skin wrinkles and increases dermal matrix synthesis. *Skin Pharmacology and Physiology*, *27*(3), 113–119. https://doi.org/10.1159/000355523

Qi, L., Zhang, H., Guo, Y., Zhang, C., & Xu, Y. (2023). A novel calcium-binding peptide from bovine bone collagen hydrolysate and chelation mechanism and calcium absorption activity of peptide-calcium chelate. *Food Chemistry*, *410*, 135387. https://doi.org/10.1016/j.foodchem.2023.135387

Qin, X., Shen, Q., Guo, Y., Liu, J., Zhang, H., Jia, W., Xu, X., & Zhang, C. (2021). An advanced strategy for efficient recycling of bovine bone: preparing high-valued bone powder via instant catapult steam-explosion. *Food Chemistry*, 131614. https://doi.org/10.1016/j.foodchem.2021.131614

Qin, X., Xu, X., Guo, Y., Shen, Q., Liu, J., Yang, C., Scott, E., Bitter, H., & Zhang,

C. (2022). A sustainable and efficient recycling strategy of feather waste into keratin peptides with antimicrobial activity. *Waste Management*, *144*, 421–430. https://doi.org/10.1016/j.wasman.2022.04.017

Qu, W., Feng, Y., Xiong, T., Li, Y., Wahia, H., & Ma, H. (2022). Preparation of corn ACE inhibitory peptide-ferrous chelate by dual-frequency ultrasound and its structure and stability analyses. *Ultrasonics Sonochemistry*, *83*, 105937. https://doi.org/10.1016/j.ultsonch.2022.105937

Quach, D., & Britton, R. A. (2017). Gut microbiota and bone health. In L. R. McCabe & N. Parameswaran (Eds.), *Understanding the Gut-Bone Signaling Axis* (Vol. 1033, pp. 47–58). Springer International Publishing. http://link.springer.com/10.1007/978-3-319-66653-2_4

Raisz, L. G., & Rodan, G. A. (2003). Pathogenesis of osteoporosis. *Endocrinology and Metabolism Clinics of North America*, *32*(1), 15–24. https://doi.org/10.1016/S0889-8529(02)00055-5

Rivas-Vela, C. I., Amaya-Llano, S. L., Castaño-Tostado, E., & Castillo-Herrera, G. A. (2021). Protein hydrolysis by subcritical water: a new perspective on obtaining bioactive peptides. *Molecules*, *26*(21), 6655. https://doi.org/10.3390/molecules26216655

Roessner, A., Krüger, S., & Kido, A. (2000). Cellular proteases and invasion. *Verhandlungen Der Deutschen Gesellschaft Fur Pathologie*, *84*, 69–76.

Roudebush, R. E., Magee, D. E., Benslay, D. N., Bendele, A. M., & Bryant, H. U. (1993). Effect of weight manipulation on bone loss due to ovariectomy and the protective effects of estrogen in the rat. *Calcified Tissue International*, *53*(1), 61–64. https://doi.org/10.1007/BF01352016

Rubert, M., Ramis, J. M., Vondrasek, J., Gayà, A., Lyngstadaas, S. P., & Monjo, M. (2011). Synthetic peptides analogue to enamel proteins promote osteogenic differentiation of MC3T3-e1 and mesenchymal stem cells. *Journal of Biomaterials and Tissue Engineering*, *1*(2), 198–209. https://doi.org/10.1166/jbt.2011.1018

Sager, M., Lucke, A., Ghareeb, K., Allymehr, M., Zebeli, Q., & Bohm, J. (2018). Dietary deoxynivalenol does not affect mineral element accumulation in breast and thigh muscles of broiler chicken. *Mycotoxin Research*, *34*(2), 117–121. https://doi.org/10.1007/s12550-017-0306-x

Serpen, A., & Gökmen, V. (2009). Evaluation of the maillard reaction in potato crisps by acrylamide, antioxidant capacity and color. *Journal of Food Composition and Analysis*, *22*(6), 589–595. https://doi.org/10.1016/j.jfca.2008.11.003

Shen, Q., Zhang, C., Jia, W., Qin, X., Cui, Z., Mo, H., & Richel, A. (2019). Co-production of chondroitin sulfate and peptide from liquefied chicken sternal cartilage by hot-pressure. *Carbohydrate Polymers*, *222*, 115015. https://doi.org/10.1016/j.carbpol.2019.115015

Shen, Q., Zhang, C., Jia, W., Qin, X., Xu, X., Ye, M., Mo, H., & Richel, A. (2019). Liquefaction of chicken sternal cartilage by steam explosion to isolate chondroitin sulfate. *Carbohydrate Polymers*, *215*, 73–81. https://doi.org/10.1016/j.carbpol.2019.03.032

Shen Q., Zhang C., Qin X., Zhang H., Zhang Z., & Richel A. (2021). Modulation of gut microbiota by chondroitin sulfate calcium complex during alleviation of osteoporosis in ovariectomized rats. *Carbohydrate Polymers*, 118099. https://doi.org/10.1016/j.carbpol.2021.118099

Shen, Z., Yang, C., Zhu, P., Tian, C., & Liang, A. (2020). Protective effects of syringin against oxidative stress and inflammation in diabetic pregnant rats via TLR4/MyD88/NF-κB signaling pathway. *Biomedicine & Pharmacotherapy*, *131*, 110681. https://doi.org/10.1016/j.biopha.2020.110681

Singh, B. P., Vij, S., & Hati, S. (2014). Functional significance of bioactive peptides derived from soybean. *Peptides*, *54*, 171–179. https://doi.org/10.1016/j.peptides.2014.01.022

Song, R., Zhang, K., & Wei, R. (2016). In vitro antioxidative activities of squid (ommastrephes bartrami) viscera autolysates and identification of active peptides. *Process Biochemistry*, *51*(10), 1674–1682. https://doi.org/10.1016/j.procbio.2016.06.015

Song, Y., Fu, Y., Huang, S., Liao, L., Wu, Q., Wang, Y., Ge, F., & Fang, B. (2021). Identification and antioxidant activity of bovine bone collagen-derived novel peptides prepared by recombinant collagenase from bacillus cereus. *Food Chemistry*, *349*, 129143. https://doi.org/10.1016/j.foodchem.2021.129143

Soriano-Romaní, L., Nieto, J. A., & García-Benlloch, S. (2022). Immunomodulatory role of edible bone collagen peptides on macrophage and lymphocyte cell cultures. *Food and Agricultural Immunology*, *33*(1), 546–562. https://doi.org/10.1080/09540105.2022.2098936

Sorushanova, A., Delgado, L. M., Wu, Z., Shologu, N., Kshirsagar, A., Raghunath, R., Mullen, A. M., Bayon, Y., Pandit, A., Raghunath, M., & Zeugolis, D. I. (2019). The collagen suprafamily: from biosynthesis to advanced biomaterial development. *Advanced Materials*, *31*(1), 1801651. https://doi.org/10.1002/adma.201801651

Spink, J., & Moyer, D. C. (2011). Defining the public health threat of food fraud. *Journal of Food Science*, *76*(9), 157–163. https://doi.org/10.1111/j.1750-3841.2011.02417.x

Steelman, J., & Zeitler, P. (2001). Osteoporosis in pediatrics. *Pediatrics in Review*, *22*(2), 56–66. https://doi.org/10.1542/pir.22.2.56

Sui, W., & Chen, H. (2014). Extraction enhancing mechanism of steam exploded radix astragali. *Process Biochemistry*, *49*(12), 2181–2190. https://doi.org/10.1016/j.procbio.2014.08.010

Sui, W., Xiao, Y., Liu, R., Wu, T., & Zhang, M. (2019). Steam explosion modification on tea waste to enhance bioactive compounds' extractability and antioxidant capacity of extracts. *Journal of Food Engineering*, *261*, 51–59. https://doi.org/10.1016/j.jfoodeng.2019.03.015

Sun, N., Cui, P., Lin, S., Yu, C., Tang, Y., Wei, Y., Xiong, Y., & Wu, H. (2017). Characterization of sea cucumber (stichopus japonicus) ovum hydrolysates: calcium chelation, solubility and absorption into intestinal epithelial cells. *Journal*

of the Science of Food and Agriculture, *97*(13), 4604–4611. https://doi.org/10.1002/jsfa.8330

Sun, N., Wang, Y., Bao, Z., Cui, P., Wang, S., & Lin, S. (2020). Calcium binding to herring egg phosphopeptides: binding characteristics, conformational structure and intermolecular forces. *Food Chemistry*, *310*, 125867. https://doi.org/10.1016/j.foodchem.2019.125867

Sun, N., Wu, H., Du, M., Tang, Y., Liu, H., Fu, Y., & Zhu, B. (2016). Food protein-derived calcium chelating peptides: a review. *Trends in Food Science & Technology*, *58*, 140–148. https://doi.org/10.1016/j.tifs.2016.10.004

Svedbom, A., Hernlund, E., Ivergård, M., Compston, J., Cooper, C., Stenmark, J., McCloskey, E. V., Jönsson, B., Kanis, J. A., & EU Review Panel of IOF. (2013). Osteoporosis in the european union: a compendium of country-specific reports. *Archives of Osteoporosis*, *8*, 137. https://doi.org/10.1007/s11657-013-0137-0

Termine, J. D., Kleinman, H. K., Whitson, S. W., Conn, K. M., McGarvey, M. L., & Martin, G. R. (1981). Osteonectin, a bone-specific protein linking mineral to collagen. *Cell*, *26*(1), 99–105. https://doi.org/10.1016/0092-8674(81)90037-4

Tokalioglu, S. (2012). Determination of trace elements in commonly consumed medicinal herbs by ICP-MS and multivariate analysis. *Food Chemistry*, *134*(4), 2504–2508. https://doi.org/10.1016/j.foodchem.2012.04.093

Tokalıoğlu, Ş., Çiçek, B., İnanç, N., Zararsız, G., & Öztürk, A. (2018). Multivariate statistical analysis of data and ICP-MS determination of heavy metals in different brands of spices consumed in kayseri, turkey. *Food Analytical Methods*, *11*, 2407–2418. https://doi.org/10.1007/s12161-018-1209-y

Tomadoni, B., Capello, C., Valencia, G. A., & Gutiérrez, T. J. (2020). Self-assembled proteins for food applications: a review. *Trends in Food Science & Technology*, *101*, 1–16. https://doi.org/10.1016/j.tifs.2020.04.015

Tonin, C., Zoccola, M., Aluigi, A., Varesano, A., Montarsolo, A., Vineis, C., & Zimbardi, F. (2006). Study on the conversion of wool keratin by steam explosion. *Biomacromolecules*, *7*(12), 3499–3504. https://doi.org/10.1021/bm060597w

Torres-Fuentes, C., Alaiz, M., & Vioque, J. (2012). Iron-chelating activity of chickpea protein hydrolysate peptides. *Food Chemistry*, *134*(3), 1585–1588. https://doi.org/10.1016/j.foodchem.2012.03.112

Treloar, A. E. (1981). Menstrual cyclicity and the pre-menopause. *Maturitas*, *3*(3), 249–264. https://doi.org/10.1016/0378-5122(81)90032-3

Trueman, C. N., & Tuross, N. (2002). Trace elements in recent and fossil bone apatite. *Reviews in Mineralogy & Geochemistry*, *48*, 489–521. https://doi.org/10.2138/rmg.2002.48.13

Ulug, S. K., Jahandideh, F., & Wu, J. (2021). Novel technologies for the production of bioactive peptides. *Trends in Food Science & Technology*, *108*, 27–39. https://doi.org/10.1016/j.tifs.2020.12.002

Vannucci, L., Fossi, C., Quattrini, S., Guasti, L., Pampaloni, B., Gronchi, G., Giusti, F., Romagnoli, C., Cianferotti, L., Marcucci, G., & Brandi, M. L. (2018). Calcium intake in bone health: a focus on calcium-rich mineral waters. *Nutrients*, *10*(12),

1930. https://doi.org/10.3390/nu10121930

Vavrusova, M., & Skibsted, L. H. (2014). Calcium nutrition. bioavailability and fortification. *LWT - Food Science and Technology*, *59*(2, Part 2), 1198–1204. https://doi.org/10.1016/j.lwt.2014.04.034

Viguet-Carrin, S., Garnero, P., & Delmas, P. D. (2006). The role of collagen in bone strength. *Osteoporosis International*, *17*(3), 319–336. https://doi.org/10.1007/s00198-005-2035-9

Wan, F., Feng, C., Luo, K., Cui, W., Xia, Z., & Cheng, A. (2022). Effect of steam explosion on phenolics and antioxidant activity in plants: a review. *Trends in Food Science & Technology*, *124*, 13–24. https://doi.org/10.1016/j.tifs.2022.04.003

Wang, B., Wang, Y., Chi, C., Luo, H., Deng, S., & Ma, J. (2013). Isolation and characterization of collagen and antioxidant collagen peptides from scales of croceine croaker (pseudosciaena crocea). *Marine Drugs*, *11*(11), 4641–4661. https://doi.org/10.3390/md11114641

Wang, J., Wu, S., Zhang, Y., Yang, J., & Hu, Z. (2022). Gut microbiota and calcium balance. *Frontiers in Microbiology*, *13*, 1033933. https://doi.org/10.3389/fmicb.2022.1033933

Wang, J., Zhang, B., Lu, W., Liu, J., Zhang, W., Wang, Y., Ma, M., Cao, X., & Guo, Y. (2020). Cell proliferation stimulation ability and osteogenic activity of low molecular weight peptides derived from bovine gelatin hydrolysates. *Journal of Agricultural and Food Chemistry*, *68*(29), 7630–7640. https://doi.org/10.1021/acs.jafc.0c02717

Wang, L., Ding, Y., Zhang, X., Li, Y., Wang, R., Luo, X., Li, Y., Li, J., & Chen, Z. (2018). Isolation of a novel calcium-binding peptide from wheat germ protein hydrolysates and the prediction for its mechanism of combination. *Food Chemistry*, *239*, 416–426. https://doi.org/10.1016/j.foodchem.2017.06.090

Wang, S., Lv, Z., Zhao, W., Wang, L., & He, N. (2020). Collagen peptide from walleye pollock skin attenuated obesity and modulated gut microbiota in high-fat diet-fed mice. *Journal of Functional Foods*, *74*, 104194. https://doi.org/10.1016/j.jff.2020.104194

Wang, W., Yang, B., Li, W., Zhou, Q., Liu, C., & Zheng, C. (2021). Effects of steam explosion pretreatment on the bioactive components and characteristics of rapeseed and rapeseed products. *LWT - Food Science and Technology*, *143*, 111172. https://doi.org/10.1016/j.lwt.2021.111172

Wang, X., Zhang, Z., Xu, H., Li, X., & Hao, X. (2020). Preparation of sheep bone collagen peptide–calcium chelate using enzymolysis-fermentation methodology and its structural characterization and stability analysis. *RSC Advances*, *10*(20), 11624–11633. https://doi.org/10.1039/D0RA00425A

Watanabe-Kamiyama, M., Shimizu, M., Kamiyama, S., Taguchi, Y., Sone, H., Morimatsu, F., Shirakawa, H., Furukawa, Y., & Komai, M. (2010). Absorption and effectiveness of orally administered low molecular weight collagen hydrolysate in rats. *Journal of Agricultural and Food Chemistry*, *58*(2), 835–841.

https://doi.org/10.1021/jf9031487

Weaver, C. M. (2015). Diet, gut microbiome, and bone health. *Current Osteoporosis Reports*, *13*(2), 125–130. https://doi.org/10.1007/s11914-015-0257-0

Wongdee, K., Chanpaisaeng, K., Teerapornpuntakit, J., & Charoenphandhu, N. (2021). Intestinal calcium absorption. In R. Terjung (Ed.), *Comprehensive Physiology* (1st ed., pp. 2047–2073). Wiley. https://onlinelibrary.wiley.com/doi/10.1002/cphy.c200014

Wu, W., He, L., Li, C., Zhao, S., Liang, Y., Yang, F., Zhang, M., Jin, G., & Ma, M. (2020). Phosphorylation of porcine bone collagen peptide to improve its calcium chelating capacity and its effect on promoting the proliferation, differentiation and mineralization of osteoblastic MC3T3-e1 cells. *Journal of Functional Foods*, *64*, 103701. https://doi.org/10.1016/j.jff.2019.103701

Wu, W., He, L., Liang, Y., Yue, L., Peng, W., Jin, G., & Ma, M. (2019). Preparation process optimization of pig bone collagen peptide-calcium chelate using response surface methodology and its structural characterization and stability analysis. *Food Chemistry*, *284*, 80–89. https://doi.org/10.1016/j.foodchem.2019.01.103

Wu, X., Wang, F., Cai, X., & Wang, S. (2022). Characteristics and osteogenic mechanism of glycosylated peptides-calcium chelate. *Current Research in Food Science*, *5*, 1965–1975. https://doi.org/10.1016/j.crfs.2022.10.008

Xiao, J., Sakaguchi, E., Min, X., & Kawasaki, K. (2016). Dietary mannitol increased the absorption of calcium and magnesium in rats. *Journal of Animal Physiology and Animal Nutrition*, *100*(4), 715–722. https://doi.org/10.1111/jpn.12435

Xu, Q., Hong, H., Wu, J., & Yan, X. (2019). Bioavailability of bioactive peptides derived from food proteins across the intestinal epithelial membrane: a review. *Trends in Food Science & Technology*, *86*, 399–411. https://doi.org/10.1016/j.tifs.2019.02.050

Yan, J., Liu, J., Xiong, Y., Qin, W., & Tang, C. (2015). Identification of the geographical origins of pomelos using multielement fingerprinting. *Journal of Food Science*, *80*(2), 228–232. https://doi.org/10.1111/1750-3841.12746

Yang, X., Yu, X., Yagoub, A.-GasimA., Chen, L., Wahia, H., Osae, R., & Zhou, C. (2021). Structure and stability of low molecular weight collagen peptide (prepared from white carp skin) -calcium complex. *LWT- Food Science and Technology*, *136*, 110335. https://doi.org/10.1016/j.lwt.2020.110335

Yatsonsky, D., Pan, K., Shendge, V. B., Liu, J., & Ebraheim, N. A. (2019). Linkage of microbiota and osteoporosis: a mini literature review. *World Journal of Orthopedics*, *10*(3), 123–127. https://doi.org/10.5312/wjo.v10.i3.123

Ye, M., Jia, W., Zhang, C., Shen, Q., Zhu, L., & Wang, L. (2019). Preparation, identification and molecular docking study of novel osteoblast proliferation-promoting peptides from yak (bos grunniens) bones. *RSC Advances*, *9*(26), 14627–14637. https://doi.org/10.1039/c9ra00945k

Ye, M., Zhang, C., Jia, W., Shen, Q., Qin, X., Zhang, H., & Zhu, L. (2020). Metabolomics strategy reveals the osteogenic mechanism of yak (bos grunniens) bone collagen peptides on ovariectomy-induced osteoporosis in rats. *Food &*

Function, *11*(2), 1498–1512. https://doi.org/10.1039/c9fo01944h

Ye, M., Zhang, C., Zhu, L., Jia, W., & Shen, Q. (2020). Yak (bos grunniens) bones collagen-derived peptides stimulate osteoblastic proliferation and differentiation via the activation of wnt/β-catenin signaling pathway. *Journal of the Science of Food and Agriculture*, *100*(6), 2600–2609. https://doi.org/10.1002/jsfa.10286

Young, L. L. (1976). Composition and Properties of an Animal Protein Isolate Prepared from Bone Residue. *Journal of Food Science*, *41*(3), 606–608. https://doi.org/10.1111/j.1365-2621.1976.tb00680.x

Yu, H., Hsu, J., Chang, C., & Tan, F. (2017). Antioxidant properties of porcine liver proteins hydrolyzed using Monascus purpureus. *Food Science and Biotechnology*, *26*(5), 1217–1225. https://doi.org/10.1007/s10068-017-0166-3

Yue, J., Wang, J., Zhang, C., Jia, W., Li, X., & Sun, Z. (2017). Effects of hot-pressure extraction time on composition and gelatin properties of chicken bone extracts. *Journal of Food Science*, *82*(5), 1066–1075. https://doi.org/10.1111/1750-3841.13687

Zaiss, M. M., Jones, R. M., Schett, G., & Pacifici, R. (2019). The gut-bone axis: how bacterial metabolites bridge the distance. *The Journal of Clinical Investigation*, *129*(8), 3018–3028. https://doi.org/10.1172/JCI128521

Zambrowicz, A., Timmer, M., Polanowski, A., Lubec, G., & Trziszka, T. (2013). Manufacturing of peptides exhibiting biological activity. *Amino Acids*, *44*(2), 315–320. https://doi.org/10.1007/s00726-012-1379-7

Zapadka, K. L., Becher, F. J., Gomes dos Santos, A. L., & Jackson, S. E. (2017). Factors affecting the physical stability (aggregation) of peptide therapeutics. *Interface Focus*, *7*(6), 20170030. https://doi.org/10.1098/rsfs.2017.0030

Zhang, H., Qi, L., Shen, Q., Wang, R., Guo, Y., Zhang, C., & Richel, A. (2022). Comparative analysis of the bioactive compounds in chicken cartilage: protective effects of chondroitin sulfate and type II collagen peptides against osteoarthritis involve gut microbiota. *Frontiers in Nutrition*, *9*. https://www.frontiersin.org/article/10.3389/fnut.2022.843360

Zhang, H., Qi, L., Wang, X., Guo, Y., Liu, J., Xu, Y., Liu, C., Zhang, C., & Richel, A. (2023). Preparation of a cattle bone collagen peptide–calcium chelate by the ultrasound method and its structural characterization, stability analysis, and bioactivity on MC3T3-e1 cells. *Food & Function*, *14*(2), 978–989. https://doi.org/10.1039/D2FO02146C

Zhang, H., Zhao, L., Shen, Q., Qi, L., & Richel, A. (2021). Preparation of cattle bone collagen peptides-calcium chelate and its structural characterization and stability. *LWT- Food Science and Technology*, *144*(12), 111264. https://doi.org/10.1016/j.lwt.2021.111264

Zhang, J., Liang, L., Tian, Z., Chen, L., & Subirade, M. (2012). Preparation and in vitro evaluation of calcium-induced soy protein isolate nanoparticles and their formation mechanism study. *Food Chemistry*, *133*(2), 390–399. https://doi.org/10.1016/j.foodchem.2012.01.049

Zhang, K., Li, B., Chen, Q., Zhang, Z., Zhao, X., & Hou, H. (2018). Functional calcium binding peptides from pacific cod (gadus macrocephalus) bone: calcium bioavailability enhancing activity and anti-osteoporosis effects in the ovariectomy-induced osteoporosis rat model. *Nutrients*, *10*(9), 1325. https://doi.org/10.3390/nu10091325

Zhang, K., Li, J., Hou, H., Zhang, H., & Li, B. (2019). Purification and characterization of a novel calcium-biding decapeptide from pacific cod (gadus macrocephalus) bone: molecular properties and calcium chelating modes. *Journal of Functional Foods*, *52*, 670–679. https://doi.org/10.1016/j.jff.2018.11.042

Zhang, L., Zhao, S., Lai, S., Chen, F., & Yang, H. (2018). Combined effects of ultrasound and calcium on the chelate-soluble pectin and quality of strawberries during storage. *Carbohydrate Polymers*, *200*, 427–435. https://doi.org/10.1016/j.carbpol.2018.08.013

Zhang, M., Zhang, X., Zhu, J., Zhao, D.-G., Ma, Y.-Y., Li, D., Ho, C.-T., & Huang, Q. (2021). Bidirectional interaction of nobiletin and gut microbiota in mice fed with a high-fat diet. *Food & Function*, *12*(8), 3516–3526. https://doi.org/10.1039/D1FO00126D

Zhang, S., Liu, S., & Ma, P. (2020). Effect of steam explosion on physicochemical characteristics of bovine bone. *Food Science*, *41*(19), 140–145. https://doi.org/10.7506/spkx1002-6630-20190903-043

Zhang, Y., Yang, R., & Zhao, W. (2014). Improving digestibility of feather meal by steam flash explosion. *Journal of Agricultural and Food Chemistry*, *62*(13), 2745–2751. https://doi.org/10.1021/jf405498k

Zhao, J., & Chen, H. (2013). Correlation of porous structure, mass transfer and enzymatic hydrolysis of steam exploded corn stover. *Chemical Engineering Science*, *104*, 1036–1044. https://doi.org/10.1016/j.ces.2013.10.022

Zhao, L., Huang, S., Cai, X., Hong, J., & Wang, S. (2014). A specific peptide with calcium chelating capacity isolated from whey protein hydrolysate. *Journal of Functional Foods*, *10*, 46–53. https://doi.org/10.1016/j.jff.2014.05.013

Zhao, W., Yang, R., Zhang, Y., & Wu, L. (2012). Sustainable and practical utilization of feather keratin by an innovative physicochemical pretreatment: high density steam flash-explosion. *Green Chemistry*, *14*(12), 3352–3360. https://doi.org/10.1039/C2GC36243K

Zhao, Y., Zhang, B., Chen, G., Chen, A., Yang, S., & Ye, Z. (2013). Tracing the geographic origin of beef in China on the basis of the combination of stable isotopes and multielement analysis. *Journal of Agricultural and Food Chemistry*, *61*(29), 7055–7060. https://doi.org/10.1021/jf400947y

Zheng, M., Wang, X., Chen, Y., Yue, O., Bai, Z., Cui, B., Jiang, H., & Liu, X. (2022). A Review of Recent Progress on Collagen-Based Biomaterials. *Advanced Healthcare Materials*, 2202042. https://doi.org/10.1002/adhm.202202042

Zhu, L., Xie, Y., Wen, B., Ye, M., Liu, Y., Imam, K. M. S. U., Cai, H., Zhang, C., Wang, F., & Xin, F. (2020). Porcine bone collagen peptides promote osteoblast proliferation and differentiation by activating the PI3K/akt signaling pathway.

Journal of Functional Foods, *64*, 103697. https://doi.org/10.1016/j.jff.2019.103697

Appendix-publications

1. Articles

(1) **Zhang, H.**, Liu, W., Shen, Q., Zhao, L., Zhang, C., & Richel, A. (2021). Discrimination of geographical origin and species of China's cattle bones based on multi-element analyses by inductively coupled plasma mass spectrometry. *Food Chemistry*, 356, 129619. https://doi.org/10.1016/j.foodchem.2021.129619 (Chapter II)

(2) **Zhang, H.**, Liu, H., Qi, L., Xv, X., Li, X., Guo, Y., Jia, W., Zhang, C., & Richel, A. (2021). Application of steam explosion treatment on the collagen peptides extraction from cattle bone. *Innovative Food Science and Emerging Technologies*, (Chapter III) (Accept)

(3) **Zhang, H.,** Zhao, L., Shen, Q., Qi, L., & Richel, A. (2021). Preparation of cattle bone collagen peptides-calcium chelate and its structural characterization and stability. *LWT- Food Science and Technology*, *144*(12), 111264. https://doi.org/10.1016/j.lwt.2021.111264 (Chapter IV)

(4) **Zhang, H.,** Qi, L., W, X., G, Y., L, J., Zhang, C., Richel, A. Preparation of cattle bone collagen peptides-calcium chelate with ultrasound method and its structural characterization, stability analysis, and bioactivity on MC3T3-E1 cells. *Food & Function*. https://doi.org/10.1039/D2FO02146C (Chapter V)

(5) **Zhang, H.,** Qi, L., G, Y., Zhang, C., Richel, A. Cattle bone collagen peptides-calcium chelate relieves osteoporosis by modulating gut microbiota and metabolomics in ovariectomized rat (Chapter VI) (Complete the manuscript)

(6) **Zhang, H.,** Qi, L., Shen, Q., Wang, R., Guo, Y., Zhang, C., & Richel, A. (2022). Comparative analysis of the bioactive compounds in chicken cartilage: protective effects of chondroitin sulfate and type II collagen peptides against osteoarthritis involve gut microbiota. *Frontiers in Nutrition*, 9. https://doi.org/10.3389/fnut.2022.843360

(7) Zhao, L., **Zhang, H*.,** Huang, F., Liu, H., Wang, T., Zhang, C. (2023). Authenticating Tibetan pork in China by tracing the species and geographical features based on stable isotopic and multi-elemental fingerprints. *Food Control*, 145, 109411. https://doi.org/10.1016/j.foodcont.2022.109411

2. Patents

(1) Zhang C. H**.**, Qin X. J**.**, **Zhang H. R.**, Jia W**.**, Li X**.**, Zheng Q. K**.**, Mi. S**.**, & Wang. H. Liquefaction equipment for hard bone and co-production of collagen peptides and ultrafine bone. CN109007235B.

3. Flash presentations and posters

(1) 26TH National Symposium for Applied Biological Sciences: **Poster Presentation** of own project, **1st author** (BELGIUM) entitled "Discrimination of

geographical origin and species of China's cattle bones based on multi-element analyses by inductively coupled plasma mass spectrometry" and **the author** was invited to present a flash presentation. 08/07/2022.

(2) 2021–2022 ASIA–Pacific Congress of Meat Science and Technology: **Poster Presentation** of own project, **1st author** (CHINA) entitled "Preparation of cattle bone collagen peptides-calcium chelate and its structural characterization and stability" and **the author** was invited to present a flash presentation. 31/01/2022.